STUDIES ON THE PHYSICAL ARRANGEMENT AND STRUCTURE OF THE *ESCHERICHIA COLI* NUCLEOID: IMPLICATIONS FOR SYNTHETIC GENOME DESIGN

A Dissertation

Presented to the Faculty of the Graduate School

of Cornell University

In Partial Fulfillment of the Requirements for the Degree of

Doctor of Philosophy

by

Patricia Lynn Echtenkamp

May 2009

STUDIES ON THE PHYSICAL ARRANGEMENT AND STRUCTURE OF THE *ESCHERICHIA COLI* NUCLEOID: IMPLICATIONS FOR SYNTHETIC GENOME DESIGN

Patricia Lynn Echtenkamp, Ph. D.

Cornell University 2009

A goal in synthetic biology is the design and construction of an artificial bacterial cell - a functional organism capable of completing some pre-defined task, such as producing therapeutics or decontaminating waste streams. There are several factors that must be considered in synthetic organism design for biotechnological applications, namely: a resilient cell structure, robust cell reproduction, and low mutability. *Escherichia coli* possess many of these characteristics and could serve as a useful model organism for the design and construction of a synthetic organism.

To investigate whether gene organization affects gene expression during the cell cycle, transcript levels of 58 genes in *E. coli* B/r A were determined at five times during the cell division cycle. Approximately 17% of the transcript levels were cell cycle dependent. These genes were divided into two classes: genes displaying increased transcript concentrations following gene replication and genes displaying an increased transcript concentration prior to replication initiation. Transcripts levels for *hns*, *uspA*, and *zwf* were affected by the cell division cycle, but did not fit well into either class. These results indicated that transcription of a significant fraction of the genome was affected by replication cycle progression. Therefore, gene position, with regard to the C period, and gene function are important factors to incorporate into design criteria for synthetic bacterial genomes.

The shape and compaction of the bacterial nucleoid may affect gene accessibility to transcriptional machinery in natural and synthetic systems. The nature and contribution of RNA- and protein-based forces to nucleoid compaction in *Escherichia coli* were investigated. The results indicated that removal of RNA from the bacterial nucleoid affected nucleoid compaction by altering the branching density of the nucleoid macromolecular structure. Brij 58 served as a macromolecular crowding agent in nucleoid isolations and RNA-free nucleoids adopted a compact structure similar in size to exponential-phase nucleoids when the Brij 58 concentration was increased. In addition, control and protein-free nucleoids behaved similarly in solutions containing a macromolecular crowding agent, indicating that the contribution to DNA compaction by nucleoid-associated proteins was small when compared to macromolecular crowding effects.

BIOGRAPHICAL SKETCH

Patricia Lynn Echtenkamp was born in O'Neill, Nebraska in September 1980. She and her family moved to Cairo, Nebraska soon after, where she spent her childhood with her parents Lee and Shirley; her older sister Carol; and her five younger brothers, Matt, Will, Tim, Joe and Mike. Patricia attended the University of Nebraska in Lincoln, Nebraska, and completed an undergraduate thesis under the guidance of S. Madhavan. She graduated in 2003 with a Bachelor of Science in Biochemistry and a Bachelor of Science in Biological Systems Engineering. In August 2003, Patricia began her studies in the School of Chemical and Biomolecular Engineering at Cornell University.

To my early mentors, Robert Meyer and S. Madhavan

ACKNOWLEDGMENTS

The past five years have been quite a journey, during which I've become a better scientist and a better person. For that, I'm grateful to a number of people. Firstly, I'd like to thank my thesis advisor, Michael Shuler for providing advice, encouragement and an environment that fostered individual thought. I'd also like to thank my committee members Kelvin Lee and David Wilson for providing useful advice and suggestions along the way, and especially for helping to think through experimental problems that I encountered. I thank Al Center and Dave Putnam for helping me to develop as a teacher as well as a student.

I'd like to thank my family for their love and support throughout the years. My father was probably the first person to tell me that I'm 'no dummy', and he's never stopped, even during my moody teenage years. My mother is the hardest working person I've ever met, and showed me that you can always try a little harder. Thank you to my sister, Carol, for always making time for her little sister; I know finding a few minutes to talk between your work and your three kids can be challenging. And thank you to my brothers Matt, Will, Tim, Joe and Mike for tirelessly listening to all of my unsolicited advice for them and never getting too tired of my inquiries about their personal lives.

Without my friends at Cornell, I never would have made it though the long, Ithaca winters. Alejandro Becerra-Arteaga was always willing to listen to my problems, whether they were research-related or personal. Sara Yazdi and Dave Chen were always around to make the long days at work a little brighter, and to make sure we all kept at least a smidgen of sanity at all times. Jordan Atlas was my partner in the Minimal Cell project, and turned out to be a good friend and colleague. Jeff Fox and Ashlee McCaskill were always warm and welcoming, and were always great

reminders of ‘home’. I’d like to thank all of the Shuler Research Group members, especially Alejandro and Jordan, Iman El Gheriany, Hui Xu, Jay Sung, Gretchen Mahler, Mandy Esch and Rishard Chen for their camaraderie and unending encouragement. I’m grateful to Bonnie Sisco and Paula Miller for making research possible in the Shuler Group.

Finally, I’d like to that Conor Foley for making my years in Ithaca the happiest years of my life.

This work was supported in part by the National Science Foundation Graduate Research Fellowship Program, and funds from the New York State Office of Science, Technology and Academic Research to Michael L. Shuler. Parts of this work made use of the Cornell Center for Materials Research Facilities supported by the National Science Foundation under Award Number DMR-0520404.

TABLE OF CONTENTS

Biographical Sketch..... iii

Dedication.....iv

Acknowledgements v

Table of Contents vii

List of Figures.....x

List of Tables xv

1 Considerations for the Design and Construction of a Synthetic Platform Cell for Biotechnological Applications.....1

1.1 Introduction 1

1.2 Defining a Hypothetical Minimal Cell 2

1.3 Experimental Approaches to De-constructing Existing Microbes 5

1.4 A Minimal Modern Cell versus a Biotechnology Platform Cell 7

1.4.1 Cellular Growth and Reproduction 7

1.4.2 Enhanced Metabolic Control and Expanded Synthetic Capabilities 9

1.4.3 Reduced Genetic Drift in a Synthetic Organism 11

1.4.4 Mathematical Model of a Synthetic Cell.....13

1.5 *E. coli* as a Model for Synthetic Cell Design 14

1.5.1 Cell Division in *E. coli* 15

1.5.2 *E. coli* Genome Structure 19

1.6 Preview of Subsequent Chapters 20

References 23

2 Cell Cycle Progression in *Escherichia Coli* B/r Affects Transcription of Certain Genes: Implications for Synthetic Genome Design....31
2.1 Abstract....31
2.2 Introduction....32
2.3 Materials and Methods....34
2.3.1 Bacterial Strain, Growth Conditions and Synchronization....34
2.3.2 Microarray Sample Preparation and Hybridization....35
2.3.3 Oligonuceotide Microarray Design and Analysis....37
2.4 Results....46
2.4.1 *E. coli* Synchronous Cultures and Transcript Level Changes....46
2.4.2 Changes in Transcript Levels are Related to the C-Period....48
2.4.3 Transcript Level Increases Following Gene Replication for Some Genes....52
2.4.4 Additional Transcriptional Mechanisms Exist for *zwf, hns* and *uspA*....53
2.4.5 Transcript Level for Nucleotide Biosynthesis Genes Increase near Replication Initiation....53
2.5 Discussion....54
References....60

3 Macromolecular Crowding can Account for RNase-Sensitive Constraint of Bacterial Nucleoid Structure....63
3.1 Abstract....63
3.2 Introduction....63
3.3 Materials and Methods....68
3.3.1 Bacterial Strain and Growth Conditions....68

3.3.2 Nucleoid Preparations for Fluorescence Microscopy.....69
3.3.3 Fragmented *E. coli* Chromosomal DNA Preparations 69
3.3.4 Nucleoid Isolations for Electron Microscopy.....70
3.3.5 Electron Microscopy of Isolated Nucleoids 71
3.4 Results 71
3.4.1 Brij 58 Serves as Macromolecular Crowding Agent in Nucleoid Preparations 71
3.4.2 Compaction of RNA-free Nucleoids Requires High Levels of Brij 58 75
3.4.3 Protein-free Nucleoids and Control Nucleoids Behave Similarly with Respect to Brij 58-Mediated Compaction 79
3.4.4 Nucleoids Isolated Under Low- and High-Salt Conditions are Similar in Size 79
3.5 Discussion.....80
References 97

4 Conclusions and Future Directions 100
References 108

Appendix A Structural Studies of the *Escherichia Coli* Nucleoid with Electron Microscopy *In Situ* Hybridization 110
A.1 Abstract.....110
A.2 Introduction 110
A.3 Materials and Methods 112
A.3.1 Bacterial Strain and Growth Conditions.....112
A.3.2 Nucleoid Isolations for Electron Microscopy.....113

A.3.3 Electron Microscopy of Isolated Nucleoids 114
A.3.4 Digoxigenin-Labeled Oligonucleotide Probe Synthesis..... 114
A.3.5 Agarose Gel Electrophoresis and Northern Verification..... 115
A.3.6 Electron Microscopy *In Situ* Hybridization (EMISH)..... 115
A.3.7 Chromosomal Digestion and Pulsed Field Gel Electrophoresis (PFGE)..... 116
A.4 Results 117
A.4.1 *E. coli* Nucleoid Isolations..... 117
A.4.2 Nucleoid Visualization with Transmission Electron Microscopy 118
A.4.3 Verification of Digoxigenin-Labeled *lacZ* Oligonucleotide Probe Synthesis 121
A.4.4 Electron Microscopy *In Situ* Hybridization..... 123
A.4.5 Protein-free Nucleoids Exhibit Increased Accessibility to Restriction Enzymes Compared to Controls 123
A.5 Discussion..... 129
References 131

Appendix B Northern Verification of Microarray Experiments 133
B.1 Introduction..... 133
B.2 Materials and Methods..... 133
B.2.1 *E. coli* Cell Synchronization and RNA Isolation..... 133
B.2.2 Digoxigenin-labeled Oligonucleotide Probe Synthesis 134
B.2.3 Formaldehyde Agarose Gel Electrophoresis and Transfer to Nylon Membrane..... 134
B.3 Results..... 134

References 137

Appendix C Detailed Experimental Procedures 138

C.1 C-Medium Preparation 138

C.2 Bacterial Growth Rate Assay 138

C.3 Coulter Counter Operation 139

C.4 *E. coli* Population Synchronization by Membrane Elution 141

C.5 *E. coli* RNA Stabilization and Isolation 142

C.6 High-salt Nucleoid Isolation 143

C.7 Low-salt Nucleoid Isolation 144

C.8 Picogreen-DNA Assay 145

C.9 Transmission Electron Microscopy Grid Preparation 146

C.10 Attachment of DNA to TEM grids 147

C.11 Electron Microscopy *In Situ* Hybridization 148

LIST OF FIGURES

Figure 1.1 Diagram of Processes Involved in Efficient *E. coli* Cell Reproduction 17

Figure 2.1 *E. coli* B/r Cell Concentration Profile during a Typical Synchronous Experiment Performed in C-medium + 0.1% glucose.....36

Figure 2.2 *E. coli* Circular Genome Diagram Showing Location of Genes Included in Custom Microarrays 38

Figure 2.3 Comparison of *E. coli* Cell Cycle-Related Transcript Levels with Previous Measurements.....49

Figure 2.4 *E. coli* Transcript Levels during the Cell Division Cycle for Statistically Significant Genes Showing an Increase in Transcript Level Following Gene Replication 50

Figure 2.5 Differentially Expressed Transcript Levels during the *E. coli* Cell Division Cycle.....51

Figure 2.6 Compiled *E. coli* Transcript Levels for Nucleotide Biosynthesis Genes included in Microarray Analysis 55

Figure 3.1 Spermidine and Brij 58 Contributions to Maintaining Nucleoid Compaction after Release from *E. coli* Cells 73

Figure 3.2 Average Area of *E. coli* Nucleoids in Solution with Increasing Concentrations of Macromolecular Crowding Agent, Brij 58 76

Figure 3.3 Electron Micrographs of *E. coli* Nucleoids Isolated under Low Salt Conditions.....81

Figure 3.4 Electron Micrographs of *E. coli* Nucleoids Isolated under High Salt Conditions 86

Figure 3.5 Average Area of Condensed Region of Isolated Nucleoids in Electron Micrographs.....90

Figure 3.6 Proposed Model for Bacterial Nucleoid Compaction and the Physical Nature of the Biochemical Compaction Forces.....91

Figure A.1 Fluorescent and Differential Interference Contrast Images of DAPI-Stained *E. coli* Nucleoid Preparations 119

Figure A.2 DNA Concentration Measured for Sucrose Density Gradient Fractions Containing Nucleoid Isolations from High Salt and Low Salt Preparations 120

Figure A.3 Consequences of Attempts to Increase the Nucleoid Adsorption to Carbon/Butvar-Coated Nickel Grids 122

Figure A.4 Image of Chemiluminescent Reaction Showing *lacZ*-Digoxigenin

Oligonucleotide Probe bound to Total RNA Sample isolated from *E. coli* Cells 124

Figure A.5 Electron Micrograph with Digoxigenin-Labeled *lacZ* Oligonucleotide Probe Associated with 15 nm Gold Particles 125

Figure A.6 EcoRI- and NcoI-mediated *E. coli* Genome Fragmentation 127

Figure B.1 Images of 23S rRNA and Northern Hybridization of *nrdA*, *rpoA* and *rpoN* Transcripts during the *E. coli* Cell Division Cycle 135

LIST OF TABLES

Table 1.1 Essential Characteristics of a Biotechnological Platform Cell 8

Table 2.1 Oligonucleotide Probes Used for Custom Microarrays 39

Table 2.2 Compiled *E. coli* Transcript Level Measurements from Oligonucleotide Microarrays 41

Table 2.3 Genes Displaying Statistically Significant Changes in Transcript Level during the Cell Division Cycle.....47

Table 3.1 Average Area in Square Micrometers of Treated *E. coli* Nucleoids Compacted by Brij 58 78

CHAPTER 1

CONSIDERATIONS FOR THE DESIGN AND CONSTRUCTION OF A SYNTHETIC PLATFORM CELL FOR BIOTECHNOLOGICAL APPLICATIONS

1.1 Introduction

Engineers in the field of synthetic biology have a variety of aims, however they generally fall into two categories: (1) to develop a biological components and systems that can be combined to produce a pre-programmed outcome in a biological system, and (2) to build a complete, self-replicating biological system capable of performing some useful task. Towards the former goal, biological switches (Gardner *et al.*, 2000), oscillators (Elowitz and Leibler, 2000; Stricker *et al.*, 2008), and signal transduction mechanisms (Bashor *et al.*, 2008; Ullner *et al.*, 2008; Wang *et al.*, 2008) have been designed and synthesized in recent years. These systems have already uncovered details of natural system design that have enhanced our understanding of the natural world. In addition, these biological 'tools' could potentially be integrated into an existing biological system and thereby convey a novel property or activity to that system. Several recent review articles that examine these systems are available (McDaniel and Weiss 2005; Drubin *et al.*, 2007).

Other researchers focus on the design and construction of an artificial cell (Keasling, 2008; Forster and Church, 2006; Noireaux and Libchaber, 2004; Zimmer, 2003; Pohorille and Deamer, 2002). From an engineer's perspective, a functional organism capable of completing some pre-defined task, whether that be producing therapeutics or decontaminating waste streams, is desired. In addition, to facilitate future optimization of the organism for other tasks, a completely-defined system is

envisioned. In this thesis, we examine the unique factors that must be considered when designing a synthetic organism from an engineering perspective, and propose that *Escherichia coli* should serve as a model organism for the design and construction of a synthetic organism.

1.2 Defining a Hypothetical Minimal Cell

As a first step towards designing a useful synthetic organism, several studies have focused on the composition and development of a minimal cell (Gil *et al.*, 2004; Forster and Church, 2006; Zimmer, 2003; Pohorille and Deamer, 2002), defined as a cell with the minimum components that are required for life. To accomplish this, we first must define what constitutes a 'living' cell. To delineate the basis on which a man-made system can be considered to be living, synthetic biologists have identified three criteria. A 'living' cell must be capable of metabolic homeostasis, cellular reproduction, and Darwinian evolution (Rasmmussen *et al.*, 2004; Pohorille and Deamer, 2002). Attempts to construct a synthetic cell can be classified as either bottom-up or top-down. Bottom-up approaches do not assume the basic molecular machinery that is found in today's organisms, but alternatively utilize compounds that could plausibly self-assemble into biological entities (Segré *et al.*, 2001; Hanczyc and Szoskak, 2004; Luisi *et al.*, 2006). This technique typically investigates scenarios and chemical compositions that are anticipated to yield insights about the origin of life. Conversely, top-down approaches aim to utilize modern cellular machinery, including DNA genomes, transcription and translation machinery, and phospholipid bilayers, in the design of a synthetic cell (Forster and Church, 2006; Zimmer, 2003). A top-down approach is anticipated to reveal basic biological principles that we do not yet fully understand as well as serve as a template for translating biology into a platform that

can be truly engineered rather than merely investigated.

A reasonable initial effort to build a top-down synthetic bacterium is the design and construction of a 'minimal modern cell'. We define a 'minimal cell' as a hypothetical bacterial cell consisting of the minimum number of genes required for the cell to perform essential cellular functions including growth and reproduction in an optimum environment (Koonin, 2003; Browning and Shuler, 2001). The hypothetical cell is considered modern because it contains the basic molecular machinery of today's organisms. Our hypothetical minimal modern cell would exist in an optimum environment, described as a medium containing ample amounts of all necessary nutrients at a constant temperature and pH. In addition, the cell would exist in culture at a low enough cell density that metabolic waste products would be maintained at a low level. A key step in building a minimal modern cell is the design and construction of a functional synthetic genome.

Theoretically, a minimal gene set would include only genes that are essential to the viability of a cell. Since the advent of large-scale DNA analysis and modification techniques, several studies have examined the essentiality of bacterial genes, and identified genes that are essential and non-essential for viability in *Mycoplasma genitalium* (Glass *et al.*, 2006), *Mycoplasma plumonis* (French *et al.*, 2008), *Helicobacter pylori* (Salama *et al.*, 2004), *Staphylococcus aureus* (Forsyth *et al.*, 2002), *Bacillus subtilis* (Kobayashi *et al.*, 2003), and *E. coli* (Gerdes *et al.*, 2003; Baba *et al.*, 2006). However, it is anticipated that only a fraction of genes that are essential in each specific organism are globally essential. Mushegian and Koonin were the first to define a full set of genes as globally essential for life(Mushegian and Koonin, 1996). Shortly after the complete genomes of two bacteria were sequenced, they compared the gene sets for Gram-positive *M. genitalium* and Gram-negative *Haemophilus influenzae.* They defined the genes that were conserved between the two

phylogenetically diverse bacteria as essential based on the assumption that all non-essential genes would have been naturally eliminated from at least one of these reduced genomes. The authors' essential gene set included 256 genes. More recently, Gil *et al.* performed a similar analysis using genome sequences for five endosymbionts and *M. genitalium* to more closely approximate the minimal gene set (Gil *et al.*, 2003). Later the same group combined these findings with a functional analysis of gene products, and a minimal gene set of 206 genes was defined (Gil *et al.*, 2004). Genes included in their minimum gene set are involved in the following essential processes: information storage and processing; protein processing, folding and secretion; cell structure and cellular processes; and energetic and intermediate metabolism. The authors also include eight poorly characterized genes based on their presence in several small genomes. Gabaldón *et al.* constructed a minimal metabolic network based on the 206 minimal gene set identified by Gil *et al.* (Gabaldon *et al.*, 2007), and found that random mutations introduced into the minimal metabolism in general caused significant damage to the network. This behavior was expected for a minimal metabolism, and therefore reinforced the essentiality of genes included in Gil *et al.*'s selected minimal gene set.

Defining the gene set required for life is not sufficient for synthesizing life. In addition, several technical obstacles, such as the synthesis and assembly of large DNA molecules with high fidelity and the efficient encapsulation of synthetic genomes into a cell-like structure, must be overcome. Some groups have focused on these specific challenges and are developing new technologies that are anticipated to be necessary for synthetic cell construction. Notably, researchers are now able to synthesize genome-sized DNA molecules (Gibson *et al.*, 2008; Itaya *et al.*, 2008; Smith *et al.,* 2003). In addition, researchers at the Venter Institute developed a procedure for the transplantation of a complete *Mycoplasma mycoides* genome into a *Mycoplasma*

capricolum cell, and subsequently completely removed the native chromosome (Lartigue *et al.*, 2007). Currently it is still unclear if these techniques are applicable to genomes that are more phylogenetically distant, as would be the case for a synthetic genome.

1.3 Experimental Approaches to De-Constructing Existing Microbes

Ultimately, it may be that shortcomings in our understanding of bacterial systems rather than technical difficulties limit our ability to design and assemble a complete genome *de novo*. A research strategy that complements the determination of a minimal gene set for synthetic genome design is the serial reduction of the genomes of existing organisms. This approach will shed light on minimal genome estimates as the removal of one or more essential genes will be immediately apparent. In addition to complementing minimal gene set estimates, vital design criteria and components for a synthetic organism will be identified and evaluated. A number of researchers have already begun efforts to eliminate chromosomal regions containing non-essential genes in industrially relevant microbes. (Mizoguchi *et al.*, 2007; Ara *et al.*, 2007; Giga-Hama *et al.*, 2007; Pósfai *et al.*, 2006; Hashimoto *et al.*, 2005; Yu *et al.*, 2002; Trinh *et al.*, 2008). In addition to exposing the non-essentiality of removed genes, these studies yield useful insights about construction of a synthetic genome. For example, Kato and Hashimoto determined that *oriC* is the only essential cis-acting genetic element in *E. coli*, but *ter* significantly increases the growth rate of the cells (Kato and Hashimoto, 2007). Pósfai *et al.* observed the properties of an *E. coli* strain with a genome reduced in size by 15% and found that replichore imbalance did not affect growth rate, and genome reductions decreased mutation rates (which may be expected based on the removal of transposons) and increased electroporation

efficiency (Pósfai *et al.*, 2006).

As part of a 'Minimum Genome Factory' project undertaken in 2001, researchers in Japan have produced strains of *E. coli*, *B. subtilis* and *Schizosaccharomyces pombe* with reduced genomes optimized for biotechnological applications (Mizoguchi *et al.*, 2007; Ara *et al.*, 2007; Giga-Hama *et al.*, 2007). These species exhibit increased protein productivity, indicating that a synthetic organism with a reduced genome might ultimately improve bioprocess efficiencies. Other groups have also evaluated productivity in reduced genome *E. coli* strains. Chloramphenicol acetyltransferase variants were produced in *E. coli* strain MDS40 (developed by Pósfai *et al.*), and the reduced genome strain and parent strain showed similar growth and production characteristics (Sharma *et al.*, 2007). Using a different approach, Trinh *et al.* increased production efficiency of an *E. coli* strain by reducing available metabolic pathways as opposed to large-scale gene deletions. Due to the deletion of a small number of genes, available metabolic pathways were reduced from >15,000 to 6 functional pathways. As a result, metabolic processes were tied to production pathways, which made product formation beneficial to cell viability (Trinh *et al.*, 2008).

Further reduction of these genomes, especially by removal of unnecessary metabolic pathways, would certainly yield a useful host strain for biomolecule production, as well as provide more insights regarding construction of a synthetic genome. However it is unlikely we will attain an equal level of biological system comprehension by de-constructing existing organisms as would be achieved by constructing an organism *de novo*. These complimentary approaches will each prove to have specific advantages.

1.4 A Minimal Modern Cell versus a Biotechnology Platform Cell

Ultimately, synthetic organisms should be designed to perform a biotechnological task. A minimal cell is, by definition, a living biological system with the minimum number of genes necessary for life. Therefore, a minimal cell will lack processes that enable robust and predictable growth that are present in modern bacterial cells because any gene that is not absolutely essential to survival would not exist in a minimal genome. Forster and Church have outlined a roadmap to the design and development of a minimal synthetic cell (Forster and Church, 2006). The creation of a minimal synthetic cell would advance our understanding of biology and elucidate possible factors related to the origin of life. However the utility of a minimal cell in a biotechnological context would be limited. A more practical application of synthetic biology would be the design and construction of a minimally complex organism that retains the properties that are required for robust and predictable growth. This cell would serve as a 'microbial chassis' or 'factory cell' (Keasling, 2008; Prather and Martin, 2008; Forster and Church, 2007; Zimmer, 2003) for the construction of microbes optimized to perform specific chemical processes such as synthesis of a complex biomolecule or degradation of an organic wastewater contaminant.

A set of criteria necessary for a biotechnologically useful platform cell can be defined to guide efforts for its design and construction. Here, we identify and discuss five essential characteristics that a biotechnological platform cell must exhibit beyond the requirements of a minimal modern cell (Table 1.1).

1.4.1 Cellular Growth and Reproduction

The first two requirements for a biotechnological platform cell minimize the

Table 1.1 Essential Characteristics of a Biotechnological Platform Cell

• Physically robust structure (e.g. capable of withstanding bioreactor shear stresses)
• Efficient and faithful cellular reproduction system
• Simplified transcription, regulation and translation systems that are compatible with existing biological systems
• Decreased evolutionary ability (e.g. reduced mutation)
• Well-defined interactions and predictable kinetics of system

cell's energy use for unnecessary biomass generation. Because chemical energy is required for cell growth, both physically-induced cell lysis and aberrant cell divisions would decrease the efficiency of a system by decreasing the biomass yield coefficient (defined as the total biomass produced divided by the mass of substrate utilized). As a result, the product yield coefficient (mass of product / mass substrate consumed) would be lower in cells lacking a robust cell wall and efficient cellular reproduction because the fraction of viable biomass capable of product formation would be reduced.

A key advantage of microbial cell culture over alternative cell culture systems is the high productivity that can be achieved with these systems over relatively short time periods. The doubling time for industrially relevant microbes is on the order of one hour, which allows for complete production runs of less than one week. Because bioreactor operation accounts for a large fraction of the overall production cost, short production runs are ideal. To achieve high growth rates, natural bacteria use a cell cycle that allows concurrent DNA replication cycles. In these organisms, cell division and DNA replication cycles are coupled at the point of septum constriction to avoid Z-ring contraction prior to the completion of chromosome replication and segregation. Because cell doubling times dictate the length of a production run and its overall productivity, a synthetic cell will only be useful for biotechnology applications if it can exhibit high growth rates. Therefore, efficient chromosome replication and

segregation mechanisms should be incorporated into cell design. Furthermore, cell division mechanisms capable of controlled septum formation and constriction are necessary.

Controlled cell division is also necessary for osmotic and shear stress resistant cells because the constriction and separation of a physically-resilient cell wall must be carefully controlled to ensure an intact barrier at all times during cell division. Resistance to shear stress is an important advantage of microbial cell culture systems in comparison to mammalian, plant, and insect cell culture systems. *E. coli* cells remain viable at shear stress levels up to 1000 Pa (Lange *et al.*, 2001), as compared with shear stress limits of approximately 1 Pa for mammalian and insect cell systems (Ma *et al.*, 2002). Shear stress is an especially important consideration in bioreactor design as optimal growth and product formation require a well-mixed, aerated bioreactor environment. Due to mass transfer limitations, vigorous agitation and forced aeration are often required to provide sufficient nutrient levels, particularly in the case of fast-growing cells. Therefore a balance between adequate mixing and acceptable shear stress levels must be achieved. Since bacteria exhibit high shear stress resistance due to their cell wall, genes required for cell wall synthesis, maintenance and division pathways should be included in a synthetic platform cell to confer hydrodynamic resistance.

1.4.2 Enhanced Metabolic Control and Expanded Synthetic Capabilities

It is anticipated that synthetic biology will eventually yield a completely defined biological system that can perform biological processes currently carried out by modified natural organisms, or for which efficient and robust organisms have not yet been defined. Perhaps the main advantage of a synthetic system over a modified

natural system will be increased control over intracellular processes. Ideally, a synthetic organism will possess streamlined metabolic pathways designed specifically to utilize pre-defined substrates (e.g. components of a chemically-defined medium) for growth and product formation. This will allow a significant reduction in the number of metabolic enzymes that the cell will require. In addition, a synthetic cell could be designed to code for the 20 common amino acids using only 21 of the 64 available codons (including one codon for transcription termination), which would free a number of codons for future incorporation of non-natural amino acids into synthetic protein products (Drubin *et al.*, 2007). This translational simplification would also reduce the number of genes required for translational machinery, thereby decreasing the number of possible contaminants in eventual biological products. Recent advances in technologies for *in vitro* DNA synthesis (Tian *et al.*, 2004; Smith *et al.*, 2003) will permit sequences taken from natural systems to be converted into the reduced-codon sequence necessary for expression in the hypothetical platform cell. Besides reducing the number of translational genes required in the synthetic cell, the use of a reduced set of codons will circumvent limitations associated with heterologous protein products that use rare codons in bacterial systems (i.e. reduced protein expression and amino acid mis-incorporation) (Burgess-Brown *et al.*, 2008; Gustafsson *et al.*, 2004) because the most efficient codon for each amino acid would be included in the minimal set. However, rare codon usage has been shown to increase protein folding, transport and stability (Kahili *et al.*, 2008; Zalucki *et al.*, 2008; Zalucki and Jennings, 2007; Cortazzo *et al.*, 2002). These codons are thought to affect protein folding by slowing the rate of translation, and therefore the rate of translation in a synthetic organism should be optimized to ensure the stability of highly expressed proteins in synthetic genomes.

Recent studies have shown that active proteins can be produced with a reduced

set of amino acids (Walter *et al.*, 2005; Akanuma *et al.*, 2002), which would allow a further reduction in the number of genes necessary for translation. However, it is important to note that the transcription and translation machinery of a biotechnological platform cell must be compatible with existing biological systems as it is likely that the systems would be used to produce biomolecules identified in natural systems. In addition, significant effort would be required to identify a reduced amino acid sequence with comparable activity to the native polypeptide, and this would be required for every protein in the cell.

Finally, a major limitation in current microbial cell culture is our incomplete understanding of transcriptional controls in existing microbes. Ideally, simplified transcriptional regulation would be incorporated into a synthetic cell, and expression systems could be optimized with only essential interference from metabolic controls that have evolved in natural systems.

1.4.3 Reduced Genetic Drift in a Synthetic Organism

Natural microbial systems that are exploited for biotechnological purposes possess various DNA repair and recombination mechanisms to maintain functional and dynamic genomes. We anticipate synthetic genomes will require some mutability to remain functional, but consider two specific genetic variation mechanisms to be non-essential for synthetic genomes, namely transposons and stress response mechanisms. Insertion elements, or transposons, account for a significant amount of genetic variation in natural bacterial systems. These elements, which are capable of integrating themselves and adjacent fragments of DNA into new positions within a genome, can disrupt genes by inserting into its length, as well as alter gene regulation by rearranging gene positions. A synthetic genome lacking transposons is anticipated

to exhibit reduced mutability based on recent studies that show transposon removal reduced mutation rates in *E. coli* (Pósfai *et al.*, 2006).

Bacteria also possess mechanisms designed to increase genetic variation when a microbial population is exposed to environmental stresses. Specifically, when a cell population is exposed to environmental stresses, genetic diversity is increased by the induction of low fidelity DNA polymerases through the SOS response and the RpoS regulon. Increased genetic diversity is hypothesized to increase the fitness of microbial populations (Galhardo *et al.*, 2007) and therefore is advantageous to natural systems, especially under changing environmental conditions. However, considering that a synthetic cell system will be maintained in a constant bioreactor environment, the SOS response and RpoS regulon are unlikely to be necessary for synthetic species. Therefore to decrease genetic drift and ultimately minimize unintended mutations to biological products or enzymes involved in synthetic pathways, these pathways should be absent in a synthetic organism.

Homologous recombination mechanisms are essential to maintain long-term cell viability since single strand DNA breaks resulting in replication fork arrest are common in bacterial cultures (Capaldo-Kimball and Barbour, 1971). In addition, recombination events allow the exchange of large fragments of DNA, which is central to today's genetic engineering technologies. Because the utilization of a biotechnological platform cell would require both robust growth and a mechanism for the addition of application specific genes for the final biological or chemical objective, a relatively efficient and well-defined system for future genetic manipulations must exist. For these two reasons, we anticipate basic homologous recombination machinery would be necessary in a platform cell. Incorporation of cellular machinery for homologous recombination will also confer transduction and female conjugation capabilities on the synthetic organism as these pathways utilize the same cellular

mechanisms. Because recombination resulting from unintended transduction and conjugation may have deleterious effects on the synthetic organism, precautions to minimize genetic drift in stock cultures will still be necessary. Although it may in the future be possible to synthesize readily a new, modified genome from basic components for each application, eliminating the need for transformation capabilities, it is unlikely that the homologous recombination genes could be eliminated completely from a synthetic cell based on the substantially reduced viability observed in recombination-deficient cells.

Finally, bacteria exhibit increased mutability due to defects in the mismatch repair system (Sundin and Weigand, 2007). Although a mismatch repair mechanism is not strictly required for cell viability, we propose that it would be necessary in a biotechnologically useful cell to ensure genome stability. It is anticipated that mutations resulting from defects in the mismatch repair system will not be eliminated from a synthetic organism as they result from random mutations to one of the genes involved in mismatch repair. This reinforces the need to maintain stock cultures under conditions that minimize mutant selection.

1.4.4 Mathematical Model of a Synthetic Cell

Advances in systems biology promise to expand its applicability from understanding biological events and confirming concepts and hypotheses to predicting the effects of modifying complex biological systems. A mathematical cell model of a synthetic organism would greatly enhance the value of the biological system by providing an *in silico* platform in which proposed modifications to the system could be evaluated and potential bottlenecks in production could be identified. Several mathematical models of whole cell microbial systems, especially metabolic pathway

models of microbial systems, have already been developed with this application in mind (Nikolaev *et al.*, 2006; Ishii *et al.*, 2004; Browning and Shuler, 2001; Tomito *et al.*, 1999). However, the utility of these models is limited by gaps in our understanding of existing intracellular processes. Although we do not anticipate that it would be feasible to construct a fully-defined mathematical model concurrently with synthetic organism development, an eventual *in silico* counterpart to the synthetic cell should be considered when incorporating components into the cell. Therefore, incorporation of well characterized systems and components should be preferred to poorly described systems. We anticipate that a functional mathematical model will eventually include a detailed representation of all metabolic pathways including stoichiometric and kinetic relationships, as well as physical and geometric constraints associated with ultrastructures involved in critical cellular processes such as cell division and DNA replication. The development of an *in silico* counterpart to the synthetic cell will be one of the key advantages of designing a synthetic cell *de novo* as opposed to reducing existing genomes to achieve a minimally complex synthetic cell.

1.5 *E. coli* as a Model for Synthetic Cell Design

Three microbial species stand out as plausible model cells for the design and construction of a synthetic cell: *M. genitalium*, *B. subtilis* and *E. coli. M. genitalium* is seen as an attractive model system because the species has undergone substantial genome reductions naturally, and contains the smallest known genome for a free-living organism (Glass *et al.*, 2006; Zimmer, 2003). However, the characterization of enzyme kinetics and cellular processes in Mycoplasmas is incomplete when compared to either *E. coli* or *B. subtilis*. Indeed, when Tomito *et al.* developed an *in silico* minimal cell based on *M. genitalium*, several of the parameters were derived from

studies in *E. coli* (Tomito *et al.*, 1999). In addition to poor characterization, natural Mycoplasmas do not exhibit many of the properties that will be necessary for a viable and robust biotechnology platform cell, e.g., high shear stress resistance, and efficient cell division mechanisms.

There has been considerable interest in developing a platform microbial cell by reducing the genome of *B. subtilis* (Morimoto *et al.*, 2008; Ara *et al.*, 2007; Westers *et al.*, 2004; Westers *et al.*, 2003). *B. subtilis* has several characteristics that are advantageous for bioproduction strategies such as good synthesis and secretion capabilities (Zweers, 2008). In addition, *B. subtilis* is a Gram-positive bacterium and therefore lacks an endotoxin-containing outer membrane. However, there are some drawbacks to designing a synthetic cell based on *B. subtilis*. Notably, *B. subtilis* excretes proteases thought to be involved in cell division, which may ultimately interfere with target protein production (Schallmey *et al.*, 2004). Strains that lack several extracellular proteases have been developed (Wu *et al.*, 2002; Lee *et al.*, 2000), however heterologous protein product yields in *B. subtilis* remains relatively low compared to native protein product yields (~0.3 g/L versus 30 g/L; Schumann, 2007). Finally, although *B. subtilis* has been studied extensively compared to other Gram-positive species, our knowledge of this system and components is still limited when compared to *E. coli*. For these reasons, we suggest that *E. coli* and its components should be used to design and construct a first-generation synthetic cell. Specific advantages of *E. coli*-based cell division and chromosome design are discussed below.

1.5.1 Cell Division in *E. coli*

An efficient and robust cell division mechanism is essential for any

biotechnologically relevant microbe. Division control mechanisms facilitate a high level of daughter cell viability by ensuring that each daughter cell will receive a full genome complement, as well as ensuring that a cell initiates replication and division only after a critical cell mass is achieved. Figure 1.1 diagrams three essential processes for required for cell reproduction: growth, DNA replication and cell division. Mechanisms for these three processes would be required at some level in a synthetic minimal cell (Gil *et al.*, 2004). Genes that are involved in coupling growth, replication and division are responsible for bestowing predictable and robust cell reproduction, and therefore are also essential for a robust cell.

There are four basic characteristics of *E. coli* cell division that allow for faithful and efficient cell reproduction, making it a good template for synthetic cell design. These are: (1) well-controlled replication initiation and septal ring constriction processes that occur only once per cell cycle; (2) mechanisms that ensure complete chromosome segregation prior to cell constriction; (3) a robust division site selection system; and (4) mechanisms to synthesize and maintain strong, intact cell wall and membrane structures throughout cell division.

In *E. coli*, replication initiation is thought to be limited to once per cell cycle by Regulatory Inactivation of DnaA (RIDA), titration of DnaA-ATP by the newly replicated *datA* locus, and oriC sequestration (Kaguni, 2006; Kato, 2005). Briefly, replication initiation is triggered by DnaA-ATP binding to DnaA boxes located close to *oriC*, the origin of replication. Immediately following initiation, DnaA-ATP is both titrated by an increase in the number of DnaA boxes in the *datA* locus due to replication and inactivated by conversion to DnaA-ADP, which is catalyzed by the beta-subunit of DNA polymerase and Hda protein (Camara *et al.*, 2005). In addition to DnaA-mediated control, SeqA inhibits re-initiation by sequestering *oriC* for a significant fraction of the cell cycle (estimated to be 1/3 of the cycle), thereby

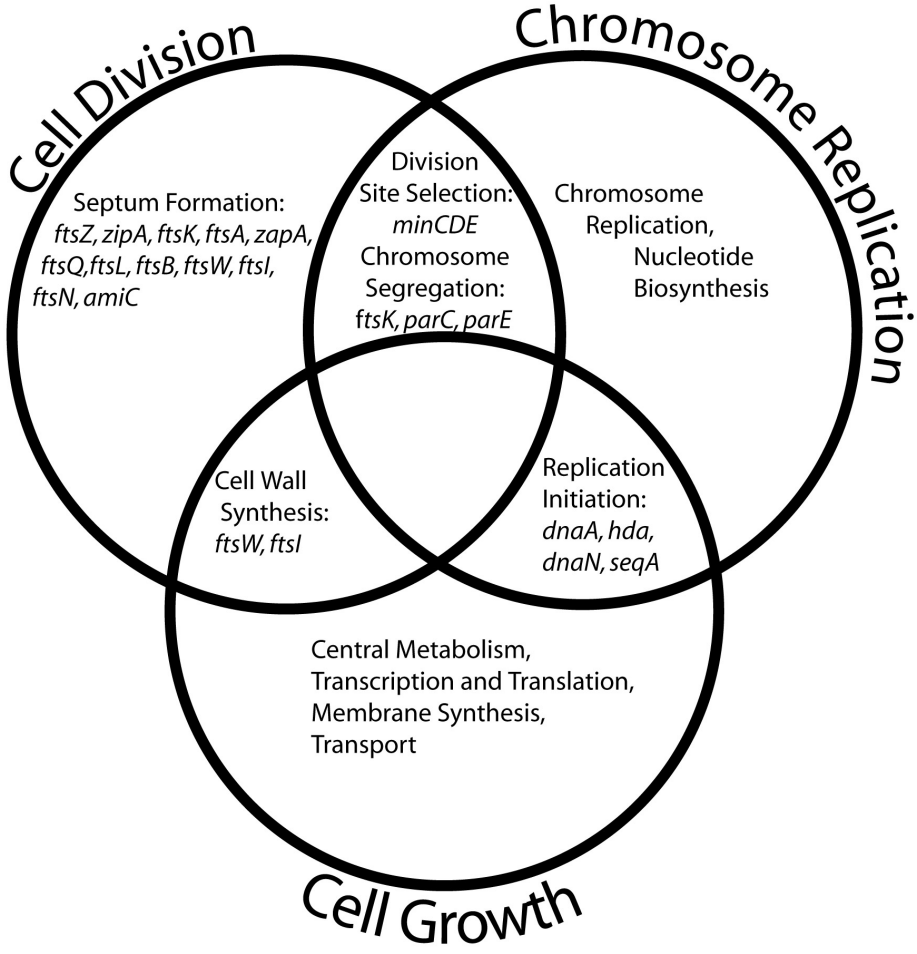

Figure 1.1 Diagram of processes involved in efficient *E. coli* cell reproduction. Intersections between two cellular processes represent nonessential genes that increase the efficiency and fidelity of cellular reproduction.

preventing methylation by DNA adenine methyltransferase (Dam). The small number of genes (*oriC, dnaA, hda, dnaN, seqA,* and *dam*) thought to be required for regulation of replication initiation makes the *E. coli* system ideal for incorporation into a synthetic organism.

Chromosomal segregation also appears to be a biochemically simple process in *E. coli*. Recently, it has been suggested that in *E. coli* the bulk of the chromosome segregates spontaneously upon replication due to its macromolecular properties (Woldringh and Nanninga, 2006; Jun and Mulder, 2006; Reyes-Lamothe *et al.*, 2008). This physical mechanism, possible requiring only *ftsK*, *parC* and *parE* for decatenation and final separation of chromosomes, would again be ideal for incorporation into a synthetic cell. However, future studies will reveal if in fact this is the case.

Finally, a surprisingly small number of genes appear to be involved in division site selection and septum formation in *E. coli* (recently reviewed by Margolin, 2005; Vincente *et al.*, 2006; Harry *et al.*, 2006). FtsZ is the first known protein to localize to the division site. Its positioning at mid-cell is controlled by the MinCDE system (Lutkenhaus, 2007), as well as SlmA, a protein that was recently implicated in the nucleoid occlusion system (Bernhardt and de Boer, 2005). FtsZ is thought to form filaments *in vivo* and trigger additional septal ring proteins to assemble at the division site. These proteins stabilize FtsZ filaments and form the septal ring which eventually constricts to split the cell into two daughter cells. In addition, septal ring components redirect peptidoglycan synthesis, and decatenate and clear chromosomal DNA from the septal plane prior to constriction. No proteins besides the septal ring components are known to be involved in septal ring formation or constriction, indicating that the system could operate independently of additional genes, which is an important characteristic for systems to be transplanted into synthetic organisms. We propose that

the basic septum machinery from *E. coli* (*ftsZ, zipA, ftsA, zapA, ftsQ, ftsL, ftsB, ftsW, ftsI, ftsN, ftsK* and *amiC*), as well as *minCDE* for proper division site placement in *E. coli*, should be incorporated into synthetic organisms designed for biotechnological purposes.

It is worth noting that many of the important factors required for physical structures and processes in bacterial cells remain only partially elucidated (Morris and Jensen, 2008). Therefore, prior to cell construction, studies designed to provide a more detailed understanding of these processes are required. Ultimately, the development of a synthetic cell that incorporates these basic, physical processes could significantly advance our knowledge of natural bacterial systems.

1.5.2 *E. coli* Genome Structure

Because transcription is affected by the structural constraints of the nucleoid (Ryter and Chang, 1975; Brewer, 1990; Claverie-Martin and Magasanik, 1991; Rabin *et al.*, 1992; Wang and Lynch, 1996), the physical structure of the bacterial nucleoid is an important factor to consider when designing synthetic organisms. Similarly to *E. coli* cell division coordination, the mechanisms used by *E. coli* to structure, organize and compact its genome appear to be relatively simple in comparison to other natural systems. The *E. coli* nucleoid consists of chromosomal DNA, nascent transcripts and polysomes, as well as DNA binding proteins including HU, Fis, H-NS, IHF, DNA topoisomerases and RNA polymerases. *In vivo*, the nucleoid is compacted over one thousand fold during the log-growth phase (Murphy and Zimmerman, 2000). Despite this compaction, during exponential phase the majority of the bacterial chromosome is in a transcriptionally accessible state throughout the cell cycle (Stonington and Pettijohn, 1971). Currently, the *E. coli* nucleoid is thought to be compacted by both

physical and biochemical forces (Zimmerman, 2006b; Cunha *et al.*, 2001). Physical forces including negative supercoiling and macromolecular crowding are expected to be inherent to any organism. Specific nucleoid-associated proteins (NAPs) may be involved in chromosome condensation (Johnson *et al.*, 2005). However, the *E. coli* cell can compensate for the loss of any particular NAP with other NAPs, which indicates that roles in condensation are not protein specific (Johnson *et al.*, 2005). In addition, evidence that NAPs may play a minimal role in nucleoid compaction has recently been presented (Zimmerman, 2006a). These results indicate that the compaction and accessibility of the *E. coli* nucleoid may be determined by physical properties of the molecules that are inherent to both natural and synthetic systems.

However, recent studies have shown the bacterial nucleoid is spatially and temporally organized (Niki *et al.*, 2000; Ryan and Shapiro, 2003; Viollier *et al.*, 2004), and suggest that nucleoid structure may not merely affect gene expression, but regulate transcription (Peter *et al.*, 2004; Kar *et al.*, 2005). These factors may be important for synthetic genomes. Notably, Hashimoto *et al.* found that the nucleoids of cells with reduced genomes tend to localize to several small nucleoids at the cell periphery as opposed to one, centrally located mass, as observed in wild type cells (Hashimoto *et al.*, 2005). Therefore, it will be important to elucidate the forces and processes that determine the structure and organization of the chromosome of a synthetic organism based on *E. coli*.

1.6 Preview of Subsequent Chapters

The development of a synthetic cell for biotechnological applications requires that we first determine the important design criteria and physical limitations. We propose that *E. coli* represents the best natural organism upon which to model

synthetic systems. We hypothesize that the physical structure and organization of the *E. coli* chromosome may yield insights regarding important design criteria for synthetic genomes. The work described in this dissertation is an initial step towards investigating the implications of the physical arrangement of the *E. coli* chromosome.

Chapter 2 examines the transcriptional effects of the *E. coli* cell division cycle, as this may be an important factor to consider when designing synthetic bacterial genomes. Transcript levels of 58 genes in *E. coli* B/r A were determined at five times during the cell division cycle. Approximately 17% of the transcript levels were found to be cell cycle dependent. These genes were divided into two classes: genes displaying increased transcript concentrations following their replication and genes displaying an increased transcript concentration prior to replication initiation. Transcripts levels for *hns*, *uspA*, and *zwf* were also affected by the cell division cycle, but did not fit well into either class. These results indicated that both physical gene position and the physiological function of a gene affect when it is transcribed. We concluded that gene position, with regard to the C period, and gene function are important factors to incorporate into design criteria for synthetic bacterial genomes.

Chapter 3 investigates *E. coli* chromosomal compaction mechanisms to determine whether the structure of the bacterial nucleoid affects the accessibility of genetic material to the transcriptional machinery in natural systems. We proposed that chromosomal DNA can be represented as a large polyelectrolyte in solution, and nascent transcripts can be viewed essentially as branches emanating from the DNA polyelectrolyte backbone. Experiments were designed to examine the nature and contribution of RNA- and protein-based forces to nucleoid compaction in *E. coli*. We found that RNA-free nucleoids adopted a compact structure similar in size to exponential-phase nucleoids when the concentration of a macromolecular crowding agent was increased, indicating the RNAse-sensitive constraint to nucleoid

decompaction resulted from changes in the macromolecular structure of the nucleoid. This chapter also contains evidence that control and protein-free nucleoids behaved similarly in solutions containing a macromolecular crowding agent, which indicated that the contribution to DNA compaction by nucleoid-associated proteins was small when compared to macromolecular crowding effects. Thus, nucleoid condensation in bacterial cells seems to be dominated by the physical characteristics of the structure of the DNA, indicating that proper condensation of chromosomes could be easily achieved in synthetic organisms.

Finally, in Chapter 4, we explore the implications of this research and proposed future studies that may contribute to the knowledge relating the physical and biochemical characteristics that will be important for the eventual design and construction of a synthetic organism.

REFERENCES

Akanuma, S., Kigawa, T. & Yokoyama, S. (2002). Combinatorial mutagenesis to restrict amino acid usage in an enzyme to a reduced set. *Proceedings of the National Academy of Sciences of the United States of America* **99**(21), 13549-13553.

Ara, K., Ozaki, K., Nakamura, K., Yamane, K., Sekiguchi, J. & Ogasawara, N. (2007). *Bacillus* minimum genome factory: effective utilization of microbial genome information. *Biotechnology and Applied Biochemistry* **46**, 169-178.

Baba, T., Ara, T., Hasegawa, M., Takai, Y., Okumura, Y., *et al.* (2006). Construction of *Escherichia coli* K-12 in-frame, single-gene knockout mutants: the Keio collection. *Molecular Systems Biology* **2**(1).

Bashor, C. J., Helman, N. C., Yan, S. D. & Lim, W. A. (2008). Using engineered scaffold interactions to reshape MAP kinase pathway signaling dynamics. *Science* **319**(5869), 1539-1543.

Bernhardt, T. G. & de Boer, P. A. J. (2005). SimA, a nucleoid-associated, FtsZ binding protein required for blocking septal ring assembly over chromosomes in *E coli*. *Molecular Cell* **18**(5), 555-564.

Brewer, B. J. (1990). Replication and the transcriptional organization of the *Escherichia coli* chromosome. In *The Bacterial Chromosome* (Drlica, K. & Riley, M., eds.), pp. 61-83. American Society for Microbiology Press, Washington D. C.

Browning, S. T. & Shuler, M. L. (2001). Towards the development of a minimal cell model by generalization of a model of *Escherichia coli*: Use of dimensionless rate parameters. *Biotechnology and Bioengineering* **76**(3), 187-192.

Burgess-Brown, N. A., Sharma, S., Sobott, F., Loenarz, C., Oppermann, U. & Gileadi, O. (2008). Codon optimization can improve expression of human genes in Escherichia coli: A multi-gene study. *Protein Expression and Purification* **59**(1), 94-102.

Camara, J. E., Breier, A. M., Brendler, T., Austin, S., Cozzarelli, N. R. & Crooke, E. (2005). Hda inactivation of DnaA is the predominant mechanism preventing hyperinitiation of *Escherichia coli* DNA replication. *EMBO Reports* **6**(8), 736-741.

Capaldo-Kimball, F. & Barbour, S. D. (1971). Involvement of recombination genes in growth and viability of *Escherichia coli* K-12. *Journal of Bacteriology* **106**, 204-212.

Claverie-Martin, F. & Magasanik, B. (1991). Role of Integration Host Factor in the regulation of the *glnHp2* promoter of *Escherichia coli*. *Proceedings of the National Academy of Sciences* **88**(5), 1631-1635.

Cortazzo, P., Cervenansky, C., Marin, M., Reiss, C., Ehrlich, R. & Deana, A. (2002). Silent mutations affect *in vivo* protein folding in *Escherichia coli*. *Biochemical and Biophysical Research Communications* **293**(1), 537-541.

Cunha, S., Odijk, T., Suleymanoglu, E. & Woldringh, C. L. (2001). Isolation of the *Escherichia coli* nucleoid. *Biochimie* **83**(2), 149-154.

Drubin, D. A., Way, J. C. & Silver, P. A. (2007). Designing biological systems. *Genes & Development* **21**(3), 242-254.

Elowitz, M. B. & Leibler, S. (2000). A synthetic oscillatory network of transcriptional regulators. *Nature* **403**(6767), 335-338.

Forster, A. C. & Church, G. M. (2006). Towards synthesis of a minimal cell. *Molecular Systems Biology*, Article 45.

Forster, A. C. & Church, G. M. (2007). Synthetic biology projects *in vitro*. *Genome Research* **17**(1), 1-6.

Forsyth, R. A., Haselbeck, R. J., Ohlsen, K. L., Yamamoto, R. T., Xu, H., *et al.* (2002). A genome-wide strategy for the identification of essential genes in *Staphylococcus aureus*. *Molecular Microbiology* **43**(6), 1387-1400.

French, C. T., Lao, P., Loraine, A. E., Matthews, B. T., Yu, H. L. & Dybvig, K. (2008). Large-scale transposon mutagenesis of *Mycoplasma pulmonis*. *Molecular Microbiology* **69**(1), 67-76.

Gabaldón, T., Pereto, J., Montero, F., Gil, R., Latorre, A. & Moya, A. (2007). Structural analyses of a hypothetical minimal metabolism. *Philosophical Transactions of the Royal Society B-Biological Sciences* **362**(1486), 1751-1762.

Galhardo, R. S., Hastings, P. J. & Rosenberg, S. M. (2007). Mutation as a stress response and the regulation of evolvability. *Critical Reviews in Biochemistry and Molecular Biology* **42**(5), 399-435.

Gardner, T. S., Cantor, C. R. & Collins, J. J. (2000). Construction of a genetic toggle switch in *Escherichia coli*. *Nature* **403**(6767), 339-342.

Gerdes, S. Y., Scholle, M. D., Campbell, J. W., Balazsi, G., Ravasz, E., *et al.* (2003). Experimental determination and system level analysis of essential genes in *Escherichia coli* MG1655. *Journal of Bacteriology* **185**(19), 5673-5684.

Gibson, D. G., Benders, G. A., Andrews-Pfannkoch, C., Denisova, E. A., Baden-Tillson, H., *et al.* (2008). Complete chemical synthesis, assembly, and cloning of a *Mycoplasma genitalium* genome. *Science* **319**(5867), 1215-1220.

Giga-Hama, Y., Tohda, H., Takegawa, K. & Kumagai, H. (2007). *Schizosoccharomyces pombe* minimum genome factory. *Biotechnology and Applied Biochemistry* **46**, 147-155.

Gil, R., Silva, F. J., Zientz, E., Delmotte, F., Gonzalez-Candelas, F., *et al.* (2003). The genome sequence of *Blochmannia floridanus*: Comparative analysis of reduced genomes. *Proceedings of the National Academy of Sciences of the United States of America* **100**(16), 9388-9393.

Gil, R., Silva, F. J., Pereto, J. & Moya, A. (2004). Determination of the core of a minimal bacterial gene set. *Microbiology and Molecular Biology Reviews* **68**(3), 518-537.

Glass, J. I., Assad-Garcia, N., Alperovich, N., Yooseph, S., Lewis, M. R., *et al.* (2006). Essential genes of a minimal bacterium. *Proceedings of the National Academy of Sciences* **103**(2), 425-430.

Gustafsson, C., Govindarajan, S. & Minshull, J. (2004). Codon bias and heterologous protein expression. *Trends in Biotechnology* **22**(7), 346-353.

Hanczyc, M. M. & Szostak, J. W. (2004). Replicating vesicles as models of primitive cell growth and division. *Current Opinion in Chemical Biology* **8**(6), 660-664.

Harry, E., Monahan, L. & Thompson, L. (2006). Bacterial cell division: The mechanism and its precison. *International Review of Cytology - a Survey of Cell Biology, Vol 253* **253**, 27-94.

Hashimoto, M., Ichimura, T., Mizoguchi, H., Tanaka, K., Fujimitsu, K., *et al.* (2005). Cell size and nucleoid organization of engineered *Escherichia coli* cells with a reduced genome. *Molecular Microbiology* **55**(1), 137-149.

Ishii, N., Robert, M., Nakayama, Y., Kanai, A. & Tomita, M. (2004). Toward large-scale modeling of the microbial cell for computer simulation. *Journal of Biotechnology* **113**(1-3), 281-294.

Itaya, M., Fujita, K., Kuroki, A. & Tsuge, K. (2008). Bottom-up genome assembly using the *Bacillus subtilis* genome vector. *Nature Methods* **5**(1), 41-43.

Johnson, R. C., Johnson, L. M., Schmidt, J. W. & Gardner, J. F. (2005). Major nucleoid proteins in the structure and function of the *Escherichia coli* chromosome. In *The bacterial chromosome* (Higgins, N. P., ed.), pp. 65-132. ASM Press, Washington, D. C.

Jun, S. & Mulder, B. (2006). Entropy-driven spatial organization of highly confined polymers: Lessons for the bacterial chromosome. *Proceedings of the National Academy of Sciences of the United States of America* **103**(33), 12388-12393.

Kaguni, J. M. (2006). DnaA: Controlling the initiation of bacterial DNA replication and more. *Annual Review of Microbiology* **60**, 351-371.

Kahali, B., Basak, S. & Ghosh, T. C. (2008). Delving deeper into the unexpected correlation between gene expressivity and codon usage bias of the *Escherichia coli* genome. *Journal of Biomolecular Structure and Dynamics* **25**(6), 655-661.

Kar, S., Edgar, R. & Adhya, S. (2005). Nucleoid remodeling by an altered HU protein: reorganization of the transcriptional program. *Proceedings of the National Academy of Sciences* **102**(45), 16397-16402.

Kato, J. (2005). Regulatory network of the initiation of chromosomal replication in *Escherichia coli*. *Critical Reviews in Biochemistry and Molecular Biology* **40**(6), 331-342.

Kato, J. I. & Hashimoto, M. (2007). Construction of consecutive deletions of the *Escherichia coli* chromosome. *Molecular Systems Biology* **3**.

Keasling, J. D. (2008). Synthetic biology for synthetic chemistry. *ACS Chemical Biology* **3**(1), 64-76.

Kobayashi, K., Ehrlich, S. D., Albertini, A., Amati, G., Andersen, K. K., *et al.* (2003). Essential *Bacillus subtilis* genes. *Proceedings of the National Academy of Sciences of the United States of America* **100**(8), 4678-4683.

Koonin, E. V. (2003). Comparative genomics, minimal gene-sets and the last universal common ancestor. *Nature Reviews Microbiology* **1**(2), 127-136.

Lange, H., Taillandier, P. & Riba, J. P. (2001). Effect of high sheer stress on microbial viability. *Journal of Chemical Technology and Biotechnology* **76**(5), 501-505.

Lartigue, C., Glass, J. I., Alperovich, N., Pieper, R., Parmar, P. P., *et al.* (2007). Genome transplantation in bacteria: Changing one species to another. *Science* **317**(5838), 632-638.

Lee, S. J., Kim, D. M., Bae, K. H., Byun, S. M. & Chung, J. H. (2000). Enhancement of secretion and extracellular stability of staphylokinase in *Bacillus subtilis* by *wprA* gene disruption. *Applied and Environmental Microbiology* **66**(2), 476-480.

Luisi, P. L., Ferri, F. & Stano, P. (2006). Approaches to semi-synthetic minimal cells: a review. *Naturwissenschaften* **93**(1), 1-13.

Lutkenhaus, J. (2007). Assembly dynamics of the bacterial MinCDE system and spatial regulation of the Z ring. *Annual Review of Biochemistry* **76**, 539-562.

Ma, N. N., Koelling, K. W. & Chalmers, J. J. (2002). Fabrication and use of a transient contractional flow device to quantify the sensitivity of mammalian and insect cells to hydrodynamic forces. *Biotechnology and Bioengineering* **80**(4), 428-437.

Margolin, W. (2005). FtsZ and the division of prokaryotic cells and organelles. *Nature Reviews Molecular Cell Biology* **6**(11), 862-871.

McDaniel, R. & Weiss, R. (2005). Advances in synthetic biology: on the path from prototypes to applications. *Current Opinion in Biotechnology* **16**(4), 476-483.

Mizoguchi, H., Mori, H. & Fujio, T. (2007). *Escherichia coli* minimum genome factory. *Biotechnology and Applied Biochemistry* **46**, 157-167.

Morimoto, T., Kadoya, R., Endo, K., Tohata, M., Sawada, K., *et al.* (2008). Enhanced recombinant protein productivity by genome reduction in *Bacillus subtilis*. *DNA Research* **15**(2), 73-81.

Morris, D. M. & Jensen, G. J. (2008). Toward a biomechanical understanding of whole bacterial cells. *Annual Review of Biochemistry* **77**, 583-613.

Murphy, L. D. & Zimmerman, S. B. (2000). Multiple restraints to the unfolding of spermidine nucleoids from *Escherichia coli*. *Journal of Structural Biology* **132**(1), 46-62.

Mushegian, A. R. & Koonin, E. V. (1996). A minimal gene set for cellular life derived by comparison of complete bacterial genomes. *Proceedings of the National Academy of Sciences of the United States of America* **93**(19), 10268-10273.

Niki, H., Yamaichi, Y. & Hiraga, S. (2000). Dynamic organization of chromosomal DNA in *Escherichia coli*. *Genes and Development* **14**, 212-223.

Nikolaev, E., Altas, J. C. & Shuler, M. L. (2006). Computer models of bacterial cells: from generalized coarse-grained to genome-specific modular models. *Journal of Physics: Conference Series* **4b**, 322-326.

Noireaux, V. & Libchaber, A. (2004). A vesicle bioreactor as a step toward an artificial cell assembly. *Proceedings of the National Academy of Sciences of the United States of America* **101**(51), 17669-17674.

Peter, B. J., Arsuaga, J., Breier, A. M., Khodursky, A. B., Brown, P. O. & Cozzarelli, N. R. (2004). Genomic trascriptional response to loss of chromosomal supercoiling in *Escherichia coli*. *Genome Biology* **5**, R87.

Pohorille, A. & Deamer, D. (2002). Artificial cells: prospects for biotechnology. *Trends in Biotechnology* **20**(3), 123-128.

Pósfai, G., Plunkett, G., Feher, T., Frisch, D., Keil, G. M., *et al.* (2006). Emergent properties of reduced-genome *Escherichia coli*. *Science* **312**(5776), 1044-1046.

Prather, K. L. J. & Martin, C. H. (2008). *De novo* biosynthetic pathways: rational design of microbial chemical factories. *Current Opinion in Biotechnology* **19**, 468-474.

Rabin, R. S., Collins, L. A. & Stewart, V. (1992). In vivo requirement of Integration Host Factor for *nar* (Nitrate reductase) operon expression in *Escherichia coli* K-12. *Proceedings of the National Academy of Sciences* **89**(18), 8701-8705.

Rasmussen, S., Chen, L. H., Deamer, D., Krakauer, D. C., Packard, N. H., *et al.* (2004). Transitions from nonliving to living matter. *Science* **303**(5660), 963-965.

Reyes-Larnothe, R., Wang, X. D. & Sherratt, D. (2008). *Escherichia coli* and its chromosome. *Trends in Microbiology* **16**(5), 238-245.

Ryan, K. R. & Shapiro, L. (2003). Temporal and spatial regulation in prokaryotic cell cycle progression and development. *Annual Review of Biochemistry* **72**, 367-394.

Ryter, A. & Chang, A. (1975). Localization of transcribing genes in the bacterial cell by means of high resolution autoradiography. *Journal of Molecular Biology* **98**, 797-810.

Salama, N. R., Shepherd, B. & Falkow, S. (2004). Global transposon mutagenesis and essential gene analysis of *Helicobacter pylori*. *Journal of Bacteriology* **186**(23), 7926-7935.

Schallmey, M., Singh, A. & Ward, O. P. (2004). Developments in the use of *Bacillus species* for industrial production. *Canadian Journal of Microbiology* **50**(1), 1-17.

Schumann, W. (2007). Production of recombinant proteins in *Bacillus subtilis*. *Advances in Applied Microbiology, Vol 62* **62**, 137-189.

Segré, D., Ben-Eli, D., Deamer, D. W. & Lancet, D. (2001). The lipid world. *Origins of Life and Evolution of the Biosphere* **31**(1-2), 119-145.

Sharma, S. S., Blattner, F. R. & Harcum, S. W. (2007). Recombinant protein production in an *Escherichia coli* reduced genome strain. *Metabolic Engineering* **9**(2), 133-141.

Smith, H. O., Hutchison, C. A., Pfannkoch, C. & Venter, J. C. (2003). Generating a synthetic genome by whole genome assembly: phi X174 bacteriophage from synthetic oligonucleotides. *Proceedings of the National Academy of Sciences of the United States of America* **100**(26), 15440-15445.

Stonington, O. & Pettijohn, D. (1971). Folded Genome of *Escherichia coli* Isolated in a Protein-DNA-Rna Complex. *Proceedings of the National Academy of Sciences of the United States of America* **68**(1), 6-&.

Stricker, J., Cookson, S., Bennett, M. R., Mather, W. H., Tsimring, L. S. & Hasty, J. (2008). A fast, robust and tunable synthetic gene oscillator. *Nature* **456**(7221), 516-U39.

Sundin, G. W. & Weigand, M. R. (2007). The microbiology of mutability. *FEMS Microbiology Letters* **277**(1), 11-20.

Szostak, J. W., Bartel, D. P. & Luisi, P. L. (2001). Synthesizing life. *Nature* **409**(6818), 387-390.

Tian, J. D., Gong, H., Sheng, N. J., Zhou, X. C., Gulari, E., *et al.* (2004). Accurate multiplex gene synthesis from programmable DNA microchips. *Nature* **432**(7020), 1050-1054.

Tomita, M., Hashimoto, K., Takahashi, K., Shimizu, T. S., Matsuzaki, Y., *et al.* (1999). E-CELL: software environment for whole-cell simulation. *Bioinformatics* **15**(1), 72-84.

Trinh, C. T., Unrean, P. & Srienc, F. (2008). Minimal *Escherichia coli* cell for the most efficient production of ethanol from hexoses and pentoses. *Applied and Environmental Microbiology* **74**(12), 3634-3643.

Ullner, E., Koseska, A., Kurths, J., Volkov, E., Kantz, H. & Garcia-Ojalvo, J. (2008). Multistability of synthetic genetic networks with repressive cell-to-cell communication. *Physical Review E* **78**(3).

Vicente, M., Rico, A. I., Martinez-Arteaga, R. & Mingorance, J. (2006). Septum enlightenment: Assembly of bacterial division proteins. *Journal of Bacteriology* **188**(1), 19-27.

Viollier, P. H., Thanbichler, M., McGrath, P. T., West, L., Meewan, M., *et al.* (2004). Rapid and sequential movement of individual chromosomal loci to specific subcellular locations during bacterial DNA replication. *Proceedings of the National Academy of Sciences* **101**(25), 9257-9262.

Walter, K. U., Vamvaca, K. & Hilvert, D. (2005). An active enzyme constructed from a 9-amino acid alphabet. *Journal of Biological Chemistry* **280**(45), 37742-37746.

Wang, J. C. & Lynch, A. S. (1996). Effects of DNA supercoiling on gene expression. In *Regulation of gene expression in Escherichia coli* (Lin, E. C. C. & Lynch, A. S., eds.), pp. 127-147. R. G. Landes Company, Austin, TX.

Wang, W. D., Chen, Z. T., Kang, B. G. & Li, R. (2008). Construction of an artificial intercellular communication network using the nitric oxide signaling elements in mammalian cells. *Experimental Cell Research* **314**(4), 699-706.

Westers, H., Dorenbos, R., van Dijl, J. M., Kabel, J., Flanagan, T., *et al.* (2003). Genome engineering reveals large dispensable regions in *Bacillus subtilis*. *Molecular Biology and Evolution* **20**(12), 2076-2090.

Westers, L., Westers, H. & Quax, W. J. (2004). Bacillus subtilis as cell factory for pharmaceutical proteins: a biotechnological approach to optimize the host organism. *Biochimica Et Biophysica Acta-Molecular Cell Research* **1694**(1-3), 299-310.

Woldringh, C. L. & Nanninga, N. (2006). Structural and physical aspects of bacterial chromosome segregation. *Journal of Structural Biology* **156**(2), 273-283.

Wu, S.-C., Yeung, J. C., Duan, Y., Ye, R., Szarka, S. J., Habibi, H. R. & Wong, S.-L. (2002). Functional Production and Characterization of a Fibrin-Specific Single-Chain Antibody Fragment from *Bacillus subtilis*: Effects of Molecular Chaperones and a Wall-bound Protease on Antibody Fragment Production. *Applied and Environmental Microbiology* **68**(7), 3261-3269.

Yu, B. J., Sung, B. H., Koob, M. D., Lee, C. H., Lee, J. H., *et al.* (2002). Minimization of the *Escherichia coli* genome using a Tn5-targeted Cre/loxP excision system. *Nature Biotechnology* **20**(10), 1018-1023.

Zalucki, Y. M. & Jennings, M. P. (2007). Experimental confirmation of a key role for non-optimal codons in protein export. *Biochemical and Biophysical Research Communications* **355**(1), 143-148.

Zalucki, Y. M., Gittins, K. L. & Jennings, M. P. (2008). Secretory signal sequence non-optimal codons are required for expression and export of beta-lactamase. *Biochemical and Biophysical Research Communications* **366**(1), 135-141.

Zimmer, C. (2003). Genomics - Tinker, tailor: Can Venter stitch together a genome from scratch? *Science* **299**(5609), 1006-1007.

Zimmerman, S. B. (2006a). Cooperative transitions of isolated *Escherichia coli* nucleoids: Implications for the nucleoid as a cellular phase. *Journal of Structural Biology* **153**, 160-175.

Zimmerman, S. B. (2006b). Shape and compaction of *Escherichia coli* nucleoids. *Journal of Structural Biology* **156**(2), 255-261.

Zweers, J. C., Barak, I., Becher, D., Driessen, A. J. M., Hecker, M., Kontinen, V. P., *et al.* (2008). Towards the development of *Bacillus subtilis* as a cell factory for membrane proteins and protein complexes. *Microbial Cell Factories* **7**.

CHAPTER 2

CELL CYCLE PROGRESSION IN *ESCHERICHIA COLI* B/R AFFECTS TRANSCRIPTION OF CERTAIN GENES: IMPLICATIONS FOR SYNTHETIC GENOME DESIGN[1]

2.1 Abstract

We propose that transcript levels for some genes are affected by the bacterial cell division cycle and this may be an important factor to consider when designing synthetic bacterial genomes. To test this hypothesis, transcript levels of 58 genes in *Escherichia coli* B/r A were determined at five times during the cell division cycle. A two-step ANOVA technique was used to analyze data from custom oligonucleotide microarrays containing genes involved in important cellular processes including central metabolism, macromolecular synthesis, and transport and secretion. Consistent with results previously found in *Caulobacter*, approximately 17% of the transcript levels were cell cycle dependent. Cell cycle regulation can be divided into two classes: genes displaying increased transcript concentrations following gene replication and genes displaying an increased transcript concentration prior to replication initiation. Transcripts levels for *hns*, *uspA*, and *zwf* were affected by the cell division cycle, but did not fit well into either class. These results indicate that transcription of a significant fraction of the genome is affected by replication cycle progression. The results also show that both physical gene position and the physiological function of a gene affect when it is transcribed. In addition to the simple association with

[1]Reproduced with permission from *Biotechnology and Bioengineering*, accepted for publication August 2008.

replication fork progression, other phenomena must be occurring to account for some of our observations. In conclusion, gene position, with regard to the C period, and gene function are important factors to incorporate into design criteria for synthetic bacterial genomes.

2.2 Introduction

Although synthetic biologists have made significant progress toward designing and synthesizing a minimal cell (Kobayashi *et al.*, 2004; Forster and Church, 2006; Filipovska *et al.*, 2008; Gibson *et al.*, 2008), the effects and implications of bacterial genome organization on transcription are still poorly understood. The dynamic nature of bacterial gene transcription is crucial to the survival of bacterial populations. With average mRNA half-lives in *Escherichia coli* ranging from 5.2 to 6.8 minutes (Bernstein *et al.*, 2002; Selinger *et al.*, 2003), transcription and RNA degradation play important roles in cellular dynamics and adaptability. Bernstein *et al.* showed that RNA degradation rates for individual transcripts are relatively constant, indicating that dynamic transcript levels reflect changes in transcription rates.

Several factors can affect transcription in bacteria including environmental and intracellular changes. In addition, crucial cellular processes may affect transcription. The cell cycle for all organisms involves mass doubling, chromosome replication and segregation, and cell division. Replication and division cause significant perturbations of cellular physiology and must be carefully coordinated to ensure viable daughter cells and prevent aberrant cell division. In bacteria, DNA replication forks change local DNA structure by increasing positive supercoiling in front of the replication fork and dislodging DNA-associated proteins, including the transcriptional machinery (French, 1992). We hypothesize that transcript levels for some genes are affected by

the bacterial cell cycle and for this reason the cell cycle is an important factor to consider when designing synthetic bacterial genomes. It may be that not only the genes selected for inclusion in a minimal gene set, but also their physical arrangement within the chromosome are important for the optimum physiological response.

Transcript levels throughout the cell cycle are dynamic in all three kingdoms. Cell cycle-related fluctuations were detected for 2, 5 and 3-13% of the transcripts in human primary fibroblasts (Cho *et al.*, 2001), HeLa cells (Whitfield *et al.*, 2002) and yeast cells (Rustici *et al.*, 2004; Peng *et al.*, 2005; Oliva *et al.* 2005; Spellman *et al.* 1998; Cho *et al.*, 1998), respectively. Despite the range of organisms studied, one characteristic common to these gene sets was that functionally related genes were co-transcribed. More recently, two groups reported that 3% and 10% of transcripts show cell cycle related changes in the archaea *Halobacterium salinarum* and *Sulfolobus acidocaldarius*, respectively (Baumann *et al.*, 2007; Lundgren and Bernander, 2007). Again, functional relationships could be identified for groups of genes that showed similar transcript level profiles.

Less is known about cell cycle related changes to bacterial transcription. Global transcriptional profiles during the cell cycle are reported for only one bacterial species, *Caulobacter crescentus*. Using populations synchronized by centrifugation, Laub *et al.* showed that at least 19% of *Caulobacter* genes have cell cycle-related expression profiles, and that at least 25% of those genes are regulated by CtrA, a DNA-binding response regulator (Laub *et al.*, 2000). However, the regulator for the remaining 75% of the cell cycle-regulated genes remains a mystery (Ryan and Shapiro, 2003). Stalk formation and compartmentalization accompany cell division in *Caulobacter*, making it difficult to determine whether cell cycle related transcriptional changes in *Caulobacter* are relevant for the greatly simplified genome of a hypothetical synthetic bacterium. The goals of this work were a) to determine whether

transcript levels for genes not related to replication or division processes are affected by the cell cycle for a simple model bacterium, *E. coli*, and b) to identify design criteria important for developing transcriptionally-efficient synthetic genomes.

Here we present evidence that both the location of a gene and its function can affect transcript levels during the cell cycle. Relative RNA abundances were measured for 58 genes in synchronous populations of *E. coli* B/r A at five points during the cell division cycle. The genes are located at different physical positions on the *E. coli* chromosome, and are involved in important processes within the bacterium. We detected changes in transcript levels related to the cell cycle for 10 genes (17%). Two patterns were seen for genes with dynamic transcript levels: increased transcript concentrations following gene replication and increased transcript concentration prior to replication initiation. These results show that both physical gene position and physiological function of a gene affect when a gene is transcribed, indicating that the cell cycle is an important factor to consider when designing synthetic bacterial chromosomes.

2.3 Materials and Methods

2.3.1 Bacterial strain, growth conditions and synchronization

E. coli B/r A (ATCC 12407) were grown in C medium (17.2 mM dibasic potassium phosphate, 11.0 mM monobasic potassium phosphate, 9.5 mM ammonium sulfate, 0.41 mM magenesium sulfate, 0.17 mM sodium chloride, 3.6 μM ferrous sulfate, 1.0 μM EDTA) containing 0.1% glucose (Roberts *et al.,* 1955). Populations were synchronized using the membrane elution technique developed by Helmstetter (Helmstetter, 1969; Helmstetter, 2003). Briefly, cells were attached to a 0.22 μm pore

diameter nitrocellulose membrane. C-medium containing 0.1% glucose was continuously pumped through the membrane at 4.5 mL/minute. As the cells divided, newborn daughter cells were collected for two minutes (<5% of the doubling time) and incubated at 37°C and 400 RPM. To analyze the synchrony of the *E. coli* populations, the cell concentration was measured using a Coulter Counter Model ZM (Beckman-Coulter, Inc., Fullerton, CA) with a 30 µm aperture diameter. The settings utilized were I = 500 µA, polarity = auto, T_L = 7.0, T_U = out, attenuation = 1, preset gain = 4 and manometer volume = 50 µL. Synchronous populations were approximately 9 mL with a concentration of approximately 6 X 10^6 cells/mL (Figure 2.1).

2.3.2 Microarray Sample Preparation and Hybridization

At 5, 12, 20, 27, 35 and 49 minutes after cell division and collection, synchronous *E. coli* populations were chilled in a swirling ice bath for 60 seconds, centrifuged and treated with RNAprotect bacterial reagent (Qiagen, Inc., Valencia, CA). Suspensions were incubated at room temperature for a minimum of ten minutes and the cells were pelleted by centrifugation. Total RNA was isolated using RNeasy mini-kits including DNAse I digestion according to the manufacturer's recommendations (Qiagen, Inc., Valencia, CA). Samples from asynchronous *E. coli* populations were collected analogously. RNA from several asynchronous populations was pooled to obtain a consistent control.

Aminoallyl cDNA was synthesized from one to three micrograms of isolated RNA and cDNA was synthesized and indirectly labeled with Cy3- or Cy5-monoreactive esters as previously described (Hedge *et al.*, 2000). Two-color

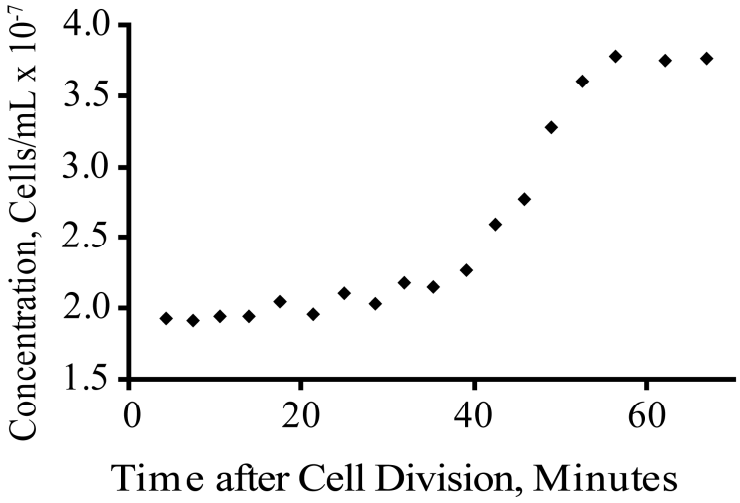

Figure 2.1 *E. coli* B/r cell concentration profile during a typical synchronous experiment performed in C-medium + 0.1% glucose. Average cell division occurs 44 minutes after collection (0 minutes).

hybridizations were performed as described earlier (Rhee *et al.*, 2004), with minor modifications. Briefly, slides were prehybridized for 45 minutes at 42˚C in prehybridization solution (50% formamide, 3x SSC, 0.31% SDS, 1 μg/mL salmon sperm DNA). Labeled cDNA samples (20 pmol dye each) were combined with hybridization solution to yield the following final concentrations: 50% formamide, 3x SSC, 0.31% SDS, 0.01 μg/mL salmon sperm DNA. Samples were boiled for two minutes, cooled by pulse centrifugation and hybridized to the microarrays for 20 hours at 42˚C. The microarrays were scanned using a GenePix 4000B scanner (Axon Instruments, Inc., Union City, CA) with GenePix Pro 4.0 software.

2.3.3 Oligonuceotide Microarray Design and Analysis

Microarrays contained 760 elements (8 replicates of 95 gene probes), that were covalently attached to aminosilane coated, 3 inch x 1 inch microscope slides. The genes included in the arrays were chosen to represent important cellular processes (central metabolism, macromolecular synthesis, nucleotide biosynthesis, transport/secretion and cell structure). In addition, several genes previously shown to have cell cycle-related transcription in either *E. coli* or *C. crescentus* were included in the array. Finally, genes were located throughout the genome (see Figure 2.2).

The oligonucleotide probes were 50 to 55 bases in length. Sequences were designed using Oligoarray 2.1 software (Rouillard *et al.*, 2003) and probes were synthesized by Illumina, Inc. (San Diego, CA). Complete probe sequences and microarray locations are included in Table 2.1.

Of the genes included in the microarray, cDNA hybridized to 58 probes with intensities at least three times greater than the background intensity. Gene probes that

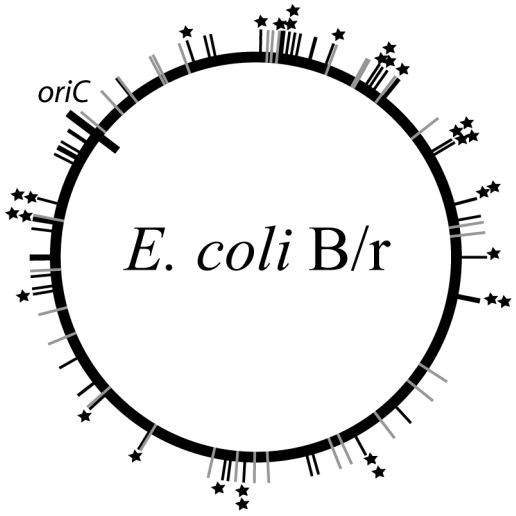

Figure 2.2 *E. coli* circular genome diagram showing location of genes included in custom microarrays. Black lines represent genes with successful transcript hybridizations; gray lines represent genes with unsuccessful transcript hybridizations. Transcripts for genes marked by stars showed statistically significant fluctuations during the division cycle. Double stars indicate the transcript level was verified at the 49 min time point.

Table 2.1 Oligonucleotide Probes Used for Custom Microarrays

Location	Gene	Synthetic Single-Stranded Oligonucleotide Probe (5' - 3')
D3	*aceE*	tgagaacctgcgtcaccacttcgaagttgatgcttcttatgtcgtggttg
C4	*ackA*	gatcatgaacgcaacctggctgcacgtttcggcaaatctggtttcatcaa
A7	*acpS*	atattaggtttaggcacggatattgtggagatcgctcgcatcgaagcggt
G11	*adk*	gaagagaccgtacgtaaacgtctggttgaataccatcagatgacagcacc
G8	*agp*	tgtgtatcagagtgcggaacagttacgtaatgccgatgcgttaaccctgc
E10	*alkB*	aggttatctctattcgcccattgatccgcaaacaaataaaccgtggcccg
F9	*amtB*	atcgtctggtccggtgttgtggcatttatcggctacaaattggcggatct
B3	*apt*	aaacttacgacctggaatacggcaccgatcagctggagatccacgttgat
F1	*araC*	cagtacatcagcgatcacctggcagacagcaattttgatatcgccagcgt
B6	*araG*	cactccgttcgcgacaatatcaacatcagtgccagacgtaaacatgtgctc
F2	*asd*	tattcgccaatgatcttgttgattgggtgtccgttgcaacctaccaggcc
C1	*atpA*	gcaagctgaaaggcatcctcgattccttcaaagcaacccaatcctggtaa
E6	*atpI*	tgctggtggttcagatactggcaccggctgtaattaacaacaaagggtaa
A2	*caiF*	tgtcagcgactggttaaagtggtcgatatcgatgagcaaatttacgcgcg
A1	*cel5A*	cggaacggaagatcgggtggaccaagtggaactactcggacgacttccgt
F3	*cmk*	ccgatgctttagtgttggattccaccaccttaagcattgagcaagtgatt
E7	*cycA*	caaacagcgtcctcatctacatgagaagtcgatctacaagatgccgctcg
C6	*cyoD*	catgaataccaaatcagatgaaggctggaacatgacggcgtttgtcttca
G12	*dapE*	gtttaacttccgcttcagcaccgaactgactgatgagatgatcaaagcgc
F10	*dicB*	tttcaatgctggctcgtttacgtctgatgccaaaaggatgtgcacaatga
G4	*dnaA*	attcagaagacggtggcggagtactacaagatcaaagtcgcggatctcct
H12	*dnaK*	aagttaccttcgatatcgatgctgacggtatcctgcacgtttccgcgaaa
B10	*dnaX*	ttcgccatcagcttgagcacatcctcaacgaagaacatatcgctcacgag
A3	*dut*	ccggtagtacaggctgaatttaatctggtggaagatttcgacgccaccga
F6	*eno*	tacactgcagttatctctcaccgttctggcgaaactgaagacgctaccat
D6	*era*	caaaaccatcgggattgaagcgcgtaaagacatgcaggaaatgttcgaag
H11	*fadL*	cctttgatgacagcccagttcctgcacagaatcgttctatctccattccg
C12	*feoA*	cactccagatactgcgtggaaaatcactggcttttcccgtgaaatcagcc
G6	*folA*	cagcgaattccacgatgctgatgcgcagaactctcacagctattgctttg
A8	*frr*	tcccgtacactgaaaatcaacgtgtttgatcgttcaatgtctccggccgt
H7	*fruK*	tgaaagatgtgattgaagctgcacatgcgctacgtgaacaaggcatcgcg
H10	*ftsI*	agtagatacttactcacgttttggactgggaaaagcgaccaatttggggt
D12	*ftsL*	actctgcctgttcatttgcattattttgacggcggtgactgtggtaacca
C9	*ftsN*	ccaccaaaaccagaagaacgctggcgctacattaaagagctggaaagtcg
H9	*ftsZ*	ttgatgaacgtggactttgcagacgtacgcaccgtaatgtctgagatggg
B2	*fumB*	aaaccgtcaagttagcaagcgctcactattacgatgaactgccgacggaa
B4	*gadB*	attatgtgtcgtcgcggcttcgaaatggactttgctgaactgttgctgga
F11	*glgA*	gtgggcgttcagattggctatcacgaagcattttcgcatcgcattatggg
D4	*glnG*	ctcaagcagattaaacagcgccatccaatgcttccggtcatcattatgac
B8	*glpA*	ctggttcacaagaacccgctgaagttaccttgcgtaaagtcatctccctg
H3	*gltA*	cgctgaacgacccgtactttatcgagaagaaactgtacccgaacgtcgat
B12	*gmk*	tgacttcgataccgcgttgaccgatttgaagaccattattcgcgccgaac
D1	*gnd*	cctgcagaaaatcaccgatgcttatgccgaaaatccacagatcgctaacctgttg
G1	*groS*	caatggccgtatccttgaaaatggcgaagtgaagccgctggatgtgaaagttg
E9	*gyrB*	gaactgaacgacaaagaacagcacggcagccagtggaagtttgatgttca
G2	*hflB*	tgaaatatgagactatcgacgcaccgcagattgatgacctgatggcacgt
H4	*hns*	ggtattgacccgaacgaactgctgaatagccttgctgccgttaaatctgg
E12	*hpt*	ttatcggtttctcgatcccggatgagtttgtggtgggttacggcattgat

Table 2.1 (Continued)

Location	Gene	Synthetic Single-Stranded Oligonucleotide Probe (5' - 3')
D7	*hyaA*	aaggttactgcctgtacaaaatgggctgcaaagggcctaccacctataac
G5	*lacI*	ggttttcaacaaaccatgcaaatgctgaatgagggcatcgttcccactgcg
E1	*lacZ*	tgtcgctccacaaggtaaacagttgattgaactgcctgaactaccgcagc
F4	*lgt*	taaaccacgcccaatgggagctgtctcaggtttgttcctgattggttacg
H6	*lpp*	ctcgtgctaaccagcgtctggacaacatggctactaaataccgcaagtaa
D8	*malF*	tttaactttaacaacttcgtgctgattcaactgttaaccaacggcggccc
B7	*mbrA*	tcgaaagggctggagtttccttatgtctacatggtcggtatggaagaagg
A6	*mdh*	ttgaacagaacgcgctggaaggtatgctggatacgctgaagaaagatatc
A5	*mrdB*	tcacagcttgaatttctccccgaacgccatactgactttatcttcgcggtactgg
E4	*mukB*	tatgtcgattctggtgatggtggtacaaagctgggaagatgaatctcgcc
E8	*nadE*	ctttataagaaagcgccaacggccgatctggaagatgatcgcccttctctg
F8	*nlpA*	caaagttgatgtagcgattatcagcaccacttacattcagcagaccgggctttct
C7	*nrdA*	tttatcgatcagtcgatctctgccaacaccaactacgatccgtcacgctt
D11	*nuoK*	caacttcaccgtcgtcgccagaacctgaacatcgattcagtaagtgagat
B5	*ompA*	aagtctgacgttctgttcaacttcaacaaagcaaccctgaaaccggaagg
A12	*oppA*	agcagaacaacagctggataaggattcggccattgttcctgtttattactacgtg
B1	*parC*	agctgtcgaagggcaaaggcaacaagattatcaacattccatcggcagaa
C10	*pgk*	tcgaattcgtggaaggtaaagtactgcctgcagtagcgatgctcgaagag
E2	*phoE*	atcgctgggttatgtcttatcgaaagggaaagatattgaaggtatcggtgatgaa
D9	*plsB*	gttgctggcggagttgattacatcagacgtgcgtttgacgattgagagtg
G10	*potF*	catatttccgaccatgtgttctatgccaacgccaataaagcagccacgcc
A4	*ppa*	tgttctatccatgcaactacggttacatcaaccacaccctgtctctggacggt
H5	*proA*	aagagtatgacgatgagtttctgtcattagatttgaacgtcaaaatcgtcagcga
D10	*proB*	cgttattggtgatgtgatggaaggcatttccgtcggtacgctgttccatg
H1	*rbsA*	aacgtgacggtttagtgttgggcatgtcagtaaaagagaacatgtcgctgac
C2	*rcsA*	cgaatcgagtatgttgcgaatgtggatggcaggtcagggaaccattcaaatctct
D2	*rfaD*	aaactgaaaggccgctatcaggcgttcactcaggcagatctgacaaatct
C11	*rplD*	tcgtaatgactgctgatgctgttaagcaagttgaggagatgctggcatga
A10	*rplR*	cacatttacgcacaggtaattgcaccgaacggttctgaagttctggtagc
C5	*rpoA*	gtgatctggtacagcgtaccgaggttgagctccttaaaacgcctaaccttt
H8	*rpoN*	caaatggttgatcaagagtctggaaagccgtaacgatacgctactgcgcgtg
C8	*rpsA*	aaacagctcgcagaagatccgttcaacaactgggttgctctgaacaagaa
G9	*rpsB*	ccggacgctctgtttgtaatcgatgctgaccacgaacacattgctatcaa
F7	*sdhA*	atctgctgaacaaacatggcgaacgttttatggagcgttatgcgccgaac
G3	*secD*	gacgtactgttcaacaggcaattgatgaaggttatcgtggcgcattcagt
D5	*secF*	ttccatcggtactgcatcttccatctatgtggcatctgcgttggctctga
A11	*tdcA*	aagaacgaacagtgggtgttgccacaaactaatatggggtactacagcgaactgc
H2	*thyA*	tcgaagactttgagattgaaggctacgatccgcatccgggcattaaagcg
E3	*tktA*	agagctgctgtttgaagagttcggcttcactgttgataacgttgttgcga
B9	*tmk*	actggcagcacaagataaaagcattcataccattgatgccacccagccgc
G7	*tpiA*	cgctaacatcgctgaacaagtgatcattcagtacggcggctctgtaaacg
E11	*trpR*	atctccatttaccgttgttaaacctgatgctgacgccagatgagcgcgaa
F12	*ugpB*	tcagaaaaccggttatctgccaatcaccaaagcagcgtatgacctgaccc
A9	*upp*	acttaacttctccattttcgttgataccccgctggatatctgcctgatgc
C3	*uspA*	tcttccgcacgtcagctgatcaacaccgttcacgttgatatgctgattgt
F5	*yhdJ*	caaaacgaagccggttaagcgaagttgaccccgatctcattacaaagtaa
B11	*zipA*	gatttcactactccgggtgtcactatctttatgcaggtaccgtcttacgg
E5	*zwf*	aataaagttcctggccttgaccacaaacataacctgcaaatcaccaagct

Table 2.2 Compiled Transcript Level Measurements from Microarrays

Gene	Gene product	p-value	5 min	12 min	20 min	27 min	35 min	49 min
Central metabolism [a]								
mdh	Malate dehydrogenase	0.1499	-0.02 ± 0.32	-0.18 ± 0.08	-0.60 ± 0.59	0.22 ± 0.13	0.36 ± 0.17	-
atpA	ATP synthase, F1 complex a-subunit	0.6043	-0.14 ± 0.19	-0.00 ± 0.15	-0.06 ± 0.22	0.17 ± 0.06	-0.10 ± 0.12	0.10 ± 0.23
cyoD	Cytochrome O ubiquinol oxidase subunit IV	0.0483	0.14 ± 0.14	-0.00 ± 0.07	0.22 ± 0.12	-0.09 ± 0.07	-0.24 ± 0.10	-0.00 ± 0.13
nuoK	NADH-dehydrogenase	0.0891	0.10 ± 0.15	0.14 ± 0.17	0.09 ± 0.14	-0.19 ± 0.07	-0.58 ± 0.35	0.64 ± 0.02
atpI	ATP synthase component, nonessential protein	0.0483	-0.16 ± 0.08	0.18 ± 0.15	-0.03 ± 0.07	0.16 ± 0.03	-0.04 ± 0.05	0.15 ± 0.05
sdhA	Succinate dehydrogenase	0.0025	0.68 ± 0.11	-0.08 ± 0.11	-0.35 ± 0.14	0.07 ± 0.07	-0.20 ± 0.35	0.65 ± 0.16
ackA	Acetate kinase A	0.0088	-0.12 ± 0.06	0.15 ± 0.06	-0.08 ± 0.02	-0.00 ± 0.05	-0.26 ± 0.12	0.32 ± 0.04
pgk	Phosphoglycerate kinase	0.0984	-0.00 ± 0.21	0.14 ± 0.08	-0.28 ± 0.19	0.15 ± 0.11	-0.35 ± 0.16	0.41 ± 0.29
ppa	Inorganic pyrophosphatase	0.9144	0.05 ± 0.04	0.06 ± 0.19	-0.07 ± 0.11	0.07 ± 0.12	0.09 ± 0.11	-0.23 ± 0.30
gnd	6-Phosphoglucanate dehydrogenase	0.1558	-0.04 ± 0.08	-0.01 ± 0.09	0.19 ± 0.10	-0.16 ± 0.05	0.11 ± 0.16	-0.07 ± 0.19
aceE	Component of pyruvate dehydrogenase complex	0.5806	0.06 ± 0.15	-0.12 ± 0.14	-0.02 ± 0.18	0.02 ± 0.10	-0.22 ± 0.08	0.28 ± 0.11
zwf	Glucose-6-phosphate-1-dehydrogenase	0.0017	-0.04 ± 0.25	-0.24 ± 0.10	0.45 ± 0.05	-0.33 ± 0.07	0.36 ± 0.13	-0.24 ± 0.23
proB	Glutamate kinase	0.0467	0.11 ± 0.06	-0.04 ± 0.15	-0.31 ± 0.13	0.07 ± 0.06	-0.17 ± 0.64	0.49 ± 0.11
asd	Aspartate semialdehyde dehydrogenase	0.013	-0.11 ± 0.23	0.05 ± 0.18	-0.50 ± 0.15	0.32 ± 0.05	0.21 ± 0.13	-0.05 ± 0.29
eno	Enolase	0.0161	0.34 ± 0.21	-0.10 ± 0.09	0.60 ± 0.25	-0.35 ± 0.12	0.22 ± 0.23	-0.63 ± 0.17
tpiA	Triose phosphate isomerase	0.5072	-0.06 ± 0.12	0.02 ± 0.03	0.09 ± 0.20	0.05 ± 0.10	0.31 ± 0.21	-0.43 ± 0.19
gltA	Citrate synthase	0.0011	0.35 ± 0.06	0.01 ± 0.09	-0.50 ± 0.12	0.06 ± 0.11	-0.18 ± 0.14	0.24 ± 0.31
proA	Glutamylphosphate reductase	0.0318	0.35 ± 0.12	-0.36 ± 0.17	0.20 ± 0.33	-0.22 ± 0.03	0.13 ± 0.17	-
glgA	Glycogen synthase	0.1675	0.10 ± 0.28	-0.33 ± 0.20	-0.38 ± 0.35	0.13 ± 0.12	0.45 ± 0.28	-
Macromolecular synthesis [b]								
frr	Ribosome recycling factor	0.2175	0.11 ± 0.06	0.07 ± 0.04	0.11 ± 0.10	-0.10 ± 0.07	0.19 ± 0.15	-0.34 ± 0.06

Table 2.2 (Continued)

Gene	Gene product	p-value	5 min	12 min	20 min	27 min	35 min	49 min
rplR	50S ribosomal subunit protein L18	0.5683	0.02 ± 0.16	-0.03 ± 0.18	0.124 ± 0.210	0.121 ± 0.078	-0.194 ± 0.117	-0.065 ± 0.185
rpoA	RNA polymerase, alpha subunit	0.1551	-0.08 ± 0.09	0.07 ± 0.07	0.103 ± 0.174	0.182 ± 0.058	-0.143 ± 0.068	-0.180 ± 0.045
rpsA	30S Ribosomal subunit protein S1	0.6671	-0.02 ± 0.18	0.13 ± 0.08	0.177 ± 0.266	0.065 ± 0.061	-0.151 ± 0.186	-0.215 ± 0.193
rplD	50S ribosomal subunit protein L4	0.3874	0.05 ± 0.20	-0.07 ± 0.16	0.10 ± 0.16	0.06 ± 0.05	-0.28 ± 0.13	0.13 ± 0.26
rpsB	30S ribosomal subunit protein S2	0.4519	-0.01 ± 0.09	0.15 ± 0.07	0.17 ± 0.18	0.11 ± 0.05	-0.07 ± 0.11	-0.38 ± 0.12
dnaX	DNA polymerase III	0.0224	0.50 ± 0.11	-0.02 ± 0.17	0.22 ± 0.11	-0.23 ± 0.07	-0.35 ± 0.31	-
groS	GrpE co-chaperone protein	0.0305	-1.22 ± 0.38	-0.23 ± 0.63	-0.01 ± 0.32	0.35 ± 0.17	0.61 ± 0.29	0.47 ± 0.19
rpoN	s54 transcriptional factor	0.2227	0.16 ± 0.14	0.048 ± 0.068	-0.21 ± 0.14	0.16 ± 0.13	-0.25 ± 0.25	-
dnaK	DnaK chaperone (hsp70 family)	0.0128	-1.60 ± 0.38	-0.14 ± 0.73	-0.10 ± 0.29	0.49 ± 0.16	0.42 ± 0.27	0.81 ± 0.21
rfaD	ADP-L-glycero-D-mannoheptose-6-epimerase	0.2129	-0.14 ± 0.09	0.12 ± 0.12	-0.17 ± 0.17	0.08 ± 0.04	-0.09 ± 0.04	0.36 ± 0.37
Nucleotide biosynthesis								
dut	Deoxyuridine triphosphatase	0.2292	-0.11 ± 0.06	0.09 ± 0.12	-0.13 ± 0.07	0.08 ± 0.08	0.00 ± 0.07	0.06 ± 0.24
upp	Uracil phosphoribosyltransferase	0.1069	0.08 ± 0.12	0.12 ± 0.04	0.19 ± 0.13	-0.08 ± 0.08	-0.22 ± 0.14	-
apt	Adenine phosphoribosyltransferase	0.1504	0.04 ± 0.09	0.13 ± 0.16	-0.24 ± 0.06	0.08 ± 0.16	-0.24 ± 0.09	0.29 ± 0.14
tmk	Thymidylate kinase	0.0208	-0.16 ± 0.14	0.25 ± 0.03	0.15 ± 0.15	0.02 ± 0.07	-0.30 ± 0.14	-
gmk	Guanylate kinase	0.1847	-0.16 ± 0.10	0.17 ± 0.05	-0.03 ± 0.11	0.09 ± 0.12	0.01 ± 0.02	-0.10 ± 0.08
nrdA	Ribonucleotide reductase	0.0017	-0.10 ± 0.15	0.48 ± 0.14	0.50 ± 0.23	-0.42 ± 0.08	-0.45 ± 0.25	0.18 ± 0.14
hpt	Guanine phosphoribosyltransferase	0.2144	-0.03 ± 0.19	0.11 ± 0.12	-0.23 ± 0.05	0.15 ± 0.14	-0.17 ± 0.04	0.15 ± 0.09
cmk	Cytidylate kinase	0.0312	0.13 ± 0.20	0.12 ± 0.05	0.02 ± 0.08	-0.16 ± 0.05	-0.31 ± 0.05	0.23 ± 0.16
adk	Adenylate kinase	0.1318	0.21 ± 0.16	-0.20 ± 0.06	0.14 ± 0.11	-0.05 ± 0.06	-0.10 ± 0.13	0.03
thyA	Thymidylate synthase	0.0488	0.44 ± 0.22	0.03 ± 0.12	-0.15 ± 0.13	-0.18 ± 0.14	-0.28 ± 0.17	0.16 ± 0.18

Table 2.2 (Continued)

Gene	Gene product	p-value	5 min	12 min	20 min	27 min	35 min	49 min
Transport and secretion [c]								
oppA	Oligonucleotide ABC transporter	0.9142	0.03 ± 0.12	-0.05 ± 0.15	0.04 ± 0.09	-0.10 ± 0.10	-0.02 ± 0.14	0.23 ± 0.06
feoA	Iron II transport sytem protein	0.1551	-1.12 ± 0.75	0.83 ± 0.09	-0.70 ± 0.78	0.70 ± 0.21	0.49 ± 0.74	-
secF	SecF (component of Sec Secretion Complex)	0.0151	0.47 ± 0.26	-0.08 ± 0.07	0.25 ± 0.09	-0.27 ± 0.14	-0.11 ± 0.08	-
cycA	d-Serine, d-alanine, glycine transporter	0.7641	0.10 ± 0.35	-0.28 ± 0.12	0.19 ± 0.28	-0.07 ± 0.23	0.13 ± 0.33	-0.18 ± 0.24
secD	SecD (component of Sec Secretion Complex)	0.0006	0.31 ± 0.09	0.03 ± 0.04	0.02 ± 0.06	-0.21 ± 0.08	-0.20 ± 0.07	0.10 ± 0.12
ompA	Outer membrane protein 3a	0.4131	-0.12 ± 0.18	-0.02 ± 0.09	0.22 ± 0.24	-0.20 ± 0.15	0.33 ± 0.38	-0.16 ± 0.14
Cell structure [d]								
nlpA	Lipoprotein-28	0.1315	0.26 ± 0.22	0.48 ± 0.16	-1.12 ± 0.98	0.01 ± 0.17	0.37 ± 0.09	-0.02
lpp	Murein lipoprotein	0.0699	0.07 ± 0.49	-0.62 ± 0.58	1.25 ± 0.31	-0.30 ± 0.54	0.84 ± 0.30	-1.16 ± 0.49
ftsL	FtsL (essential cell division protein)	0.0023	-0.19 ± 0.11	0.07 ± 0.11	-0.45 ± 0.11	-0.09 ± 0.08	-0.08 ± 0.04	0.26 ± 0.04
gyrB	DNA gyrase subunit B	0.6414	0.09 ± 0.21	-0.21 ± 0.15	-0.20 ± 0.74	-0.05 ± 0.04	0.33 ± 0.19	-
ftsZ	FtsZ (essential cell division protein)	0.0063	0.08 ± 0.06	0.20 ± 0.05	-0.19 ± 0.06	-0.09 ± 0.03	-0.08 ± 0.09	0.26 ± 0.06
ftsI	FtsI (involved in septum formation)	0.8469	-0.04 ± 0.30	-0.07 ± 0.16	-0.19 ± 0.15	0.08 ± 0.06	-0.28 ± 0.43	0.58 ± 0.24
lgt	Phosphatidylglycerol-prolipoprotein diacylglyceryl transferase	0.0828	0.23 ± 0.10	0.13 ± 0.03	-0.08 ± 0.19	-0.01 ± 0.16	-0.37 ± 0.18	0.37
hns	H-NS, DNA binding protein	0.0148	-0.19 ± 0.29	0.10 ± 0.10	0.73 ± 0.08	-0.27 ± 0.18	0.60 ± 0.33	-0.90 ± 0.52

Table 2.2 (Continued)

Gene	Gene product	p-value	5 min	12 min	20 min	27 min	35 min	49 min
Other								
dnaA	DnaA transcriptional dual regulator	0.1538	-0.02 ± 0.13	-0.27 ± 0.13	-0.12 ± 0.11	0.28 ± 0.09	0.04 ± 0.25	-
hflB	FtsH, Integral membrane peptidase	0.009	0.15 ± 0.13	-0.23 ± 0.05	0.21 ± 0.12	-0.11 ± 0.14	0.39 ± 0.07	-0.37 ± 0.35
uspA	Universal Stress Protein	0.0109	-0.31 ± 0.15	-0.18 ± 0.03	-0.06 ± 0.25	-0.04 ± 0.08	0.73 ± 0.30	-0.49 ± 0.16
era	Essential GTP-binding protein	0.0354	0.50 ± 0.30	-0.10 ± 0.16	0.64 ± 0.31	-0.33 ± 0.08	-0.49 ± 0.39	-

Genes not successful hybridized:
[a] *acpS, agp, araC, araG, dapE, folA, fruK, fumB, gadB, glpA, hyaA, lacI, lacZ, nadE, plsB, tktA, trpR*
[b] *alkB, caiF, mbrA, parC, rcsA, tdcA, yhdJ*
[c] *amtB, fadL, glnG, malF, phoE, potF, rbsA, ugpB*
[d] *dicB, ftsN, mrdB, mukB, zipA*

did not hybridize to the cDNA were located throughout the genome (Table 2.2, Figure 2.2). Genes were distributed among classes, excluding nucleotide biosynthesis, but transport/secretion classified genes were over-represented in this subset, indicating these genes displayed lower average transcript levels.

To analyze the microarray data, a two-step ANOVA procedure was used (Lee, 2004). The 532 nm and 635 nm intensities of each gene spot were transformed as follows:

$$y = \sum_{i=8} \log_2 \left(\frac{Intensity_{\lambda_S} - Intensity_{\lambda,background_S}}{Intensity_{\lambda_A} - Intensity_{\lambda,background_A}} \right) \quad (2.1)$$

where $Intensity_{\lambda S}$ refers to the Intensity of the wavelength measuring the synchronous sample and $Intensity_{\lambda A}$ refers to the intensity of the wavelength measuring the asynchronous sample. Each biological replicate was averaged over the 8 technical replicates. The following model was used to normalize the data.

$$y_{gene,array,time,dye,replicate} = \mu + \alpha_{array} + \delta_{dye} + \tau_{time} + u_{gene,array,time,dye,replicate} \quad (2.2)$$

where μ represents the overall average transformed ratio of the hybridization intensity of the synchronous population to the hybridization intensity of the asynchronous population, α represents effects introduced by each array, δ represents effects introduced by the Cy3 or Cy5 dye, τ represents overall time effects and u represents the residuals. The residuals are the normalized microarray data, and were analyzed for cell cycle related changes specific to each gene as follows:

$$u_{gene,array,dye,time,replicate} = \gamma_{gene} + (\gamma\tau)_{gene \cdot time} + \varepsilon_{gene,array,dye,time,replicate} \quad (2.3)$$

Statistical analysis of the $(\gamma\tau)_{gene \cdot time}$ term identified differentially expressed genes during the cell cycle. A false discovery rate of 0.1 was utilized (Benjamini and Hochberg, 1995).

2.4 Results

2.4.1 *E. coli* Synchronous Cultures and Transcript Level Changes

E. coli B/r A cultures grown in a minimal glucose medium were synchronized according to the membrane-elution technique developed by Helmstetter (Helmstetter, 2003). We adopted this technique to isolate cell cycle-related changes in transcript levels and to avoid changes in the gene expression profiles caused by temperature shifts or nutrient starvation techniques. This procedure relies on separation and collection of newly-divided cells from a population of *E. coli* immobilized on a nitrocellulose membrane. Figure 2.1 shows a representative population profile of a synchronous *E. coli* culture. During exponential phase, the growth rate was 0.95 hr^{-1}, which corresponded to a doubling time of 44 minutes.

Transcript levels for 58 model genes were measured using two-color custom oligonucleotide microarrays. The genes included in these microarrays represent the following cellular processes: i. central metabolism, ii. macromolecular synthesis, iii. nucleotide biosynthesis, iv. transport and secretion, and v. cell structure (Table 2.2). In addition, the genes were located throughout the genome. Total RNA was isolated from populations of synchronous *E. coli* cells incubated at 37°C and 400 RPM for 5, 12, 20, 27, 35 and 49 minutes after cell division. To identify changes in transcript level, we used a two-step analysis of variance (ANOVA) technique (Lee, 2004) to analyze data collected from microarray hybridization experiments. Data was normalized to remove slide-specific and dye-specific effects, and subsequently each gene was analyzed for changes in transcript level during one cell cycle.

We detected statistically significant fluctuations in transcript level during the cell cycle for 21 of the 58 genes analyzed (36%) at a false discovery rate of 0.1

Table 2.3 Genes displaying statistically significant changes in transcript level during the cell division cycle

Gene	Protein Function	Map Position (centisomes)[a]	p-value
Cell cycle related			
secD	Sec secretion pathway component	9.2	0.0006
gltA	citrate synthase (central metabolism)	16.2	0.0011
nrdA	ribonucleotide reductase	50.5	0.0017
zwf	glucose-6-phosphate-1-dehydrogenase	41.7	0.0017
sdhA	succinate dehydrogenase	16.3	0.0025
ftsZ	Essential cell division protein FtsZ	2.3	0.0063
uspA	universal stress protein	78.4	0.0108
asd	aspartate semialdehyde dehydrogenase	77	0.0132
hns	H-NS, DNA binding protein	27.8	0.0147
cmk	cytidylate kinase	20.7	0.0313
Dynamic			
ftsL	FtsL (essential cell division protein)	2	0.0023
ackA	Acetate kinase A	52	0.0088
hflB	Integral membrane peptidase (degrades σ^{32})	71.6	0.0089
dnaK	DnaK chaperone (hsp70 family)	0.3	0.0128
secF	SecF (component of Sec Secretion Complex)	9.2	0.0151
eno	Enolase	62.6	0.0161
groS	GrpE co-chaperone protein	94.2	0.0305
Not verified at 49 min			
tmk	Thymidylate kinase	24.9	0.0208
dnaX	DNA polymerase III	10.6	0.0224
proA	Glutamylphosphate reductase	5.6	0.0318
era	Essential GTP-binding protein	58.2	0.0354

[a] values calculated by Ecocyc database (Keseler et al., 2005).

(Benjamini and Hochberg, 1995). To further distinguish cell cycle-induced changes, we compared transcript levels for populations incubated for 5 minutes and 49 minutes (τ_D + 5 minutes) after collection. Ten of the 21 genes (17% of the total) displayed similar expression levels, indicating the transcript dynamics were related to the cell cycle. Seven genes did not show the same expression levels at 5 and 49 minutes, and four genes were not verified at 49 minutes due to low hybridization intensity and high background in the 49 minute measurements. The genes displaying changes in transcript level are listed in Table 2.3. Transcript level profiles for the ten genes showing cell cycle related changes are shown in Figures 2.3, 2.4 and 2.5.

2.4.2 Changes in Transcript Levels are Related to the C-Period

To verify that our methodology is sufficiently robust to detect cell cycle related changes, we included three genes in our analyses that were shown previously to be cell cycle related. In addition, we included *rpoA*, a gene that has been shown to not fluctuate during the cell cycle (Theisen, 1993). As expected, in our studies *rpoA* transcript levels did not fluctuate during the cell cycle (data not shown). Transcript levels for both *ftsZ* and *nrdA* were detected as cell cycle related (Figure 2.3). Transcript levels for *dnaA* showed a profile similar to previous studies, but the fluctuations were not statistically significant (p-value = 0.154). The lack of statistical significance may be due to the relatively low level of hybridization, which increases errors between measurements, compared to the other genes in this study.

To visualize the relationship of cell cycle related changes in *E. coli* transcription with the cell replication and division cycles, we aligned our data for *ftsZ*, *dnaA* and *nrdA* with data collected from previous studies (Figure 2.3; Zhou *et al.*, 1994; Theisen *et al.*, 1993; Zhou *et al.*, 1997). Although all studies used *E. coli* B/r

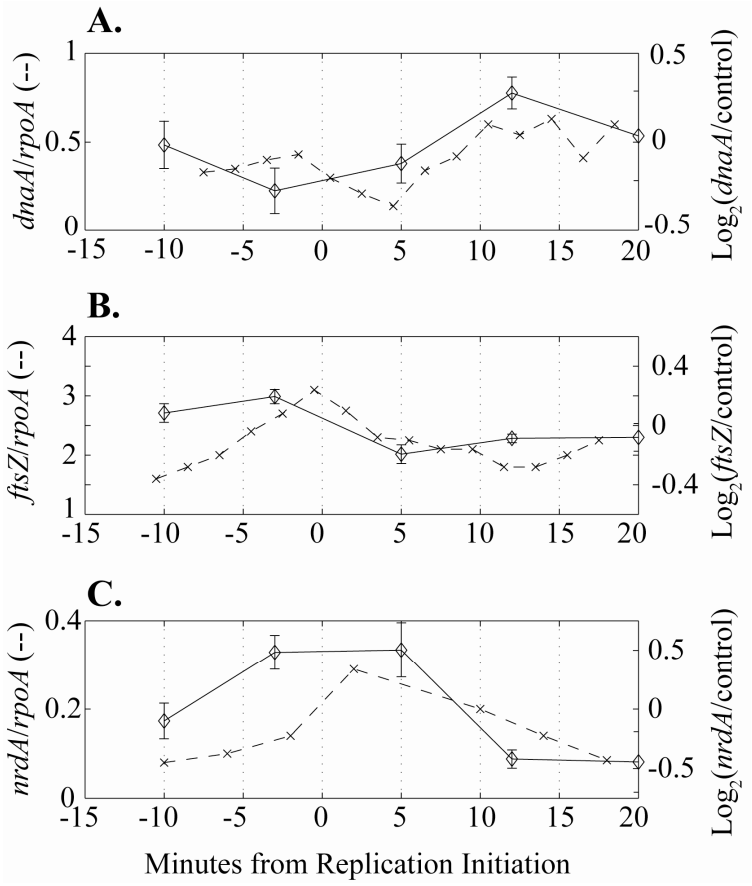

Figure 2.3 Comparison of *E. coli* cell cycle-related transcript levels with previous measurements. Solid lines represent data measured in these studies. Broken lines represent data from Theisen *et al*. (1993); Zhou *et al*. (1994) and Zhou *et al*. (1997) for *dnaA, ftsZ* and *nrdA* respectively. Data correlates well when plotted by C-period and aligned for replication initiation.

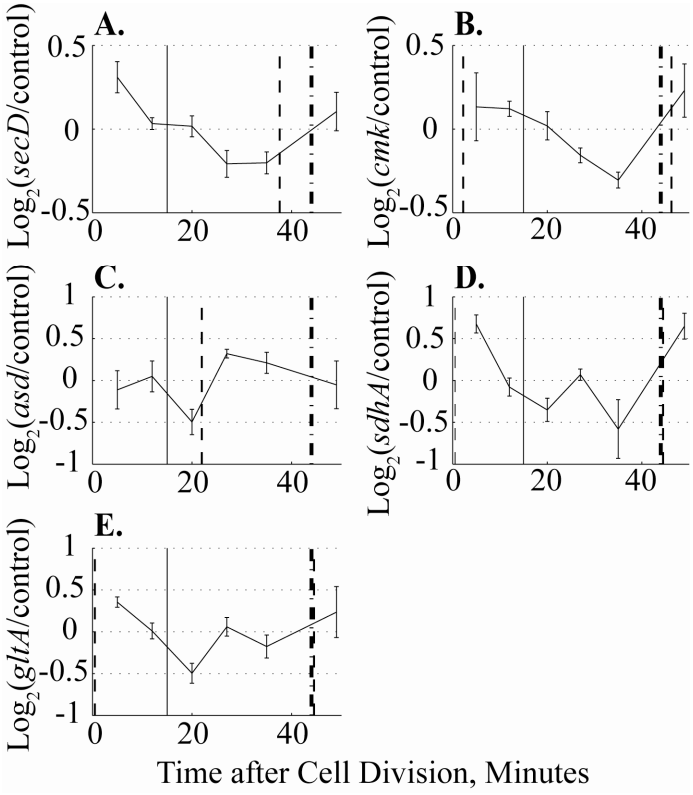

Figure 2.4 *E. coli* transcript levels during the cell division cycle for statistically significant genes showing an increase in transcript level following gene replication. The vertical solid line represents replication initiation; the vertical broken line represents gene replication and the vertical double broken line represents average time of cell division. Plot shows relative transcript levels for: A, *secD*; B, *cmk*; C, *asd*; D, *sdhA*; E, *gltA*.

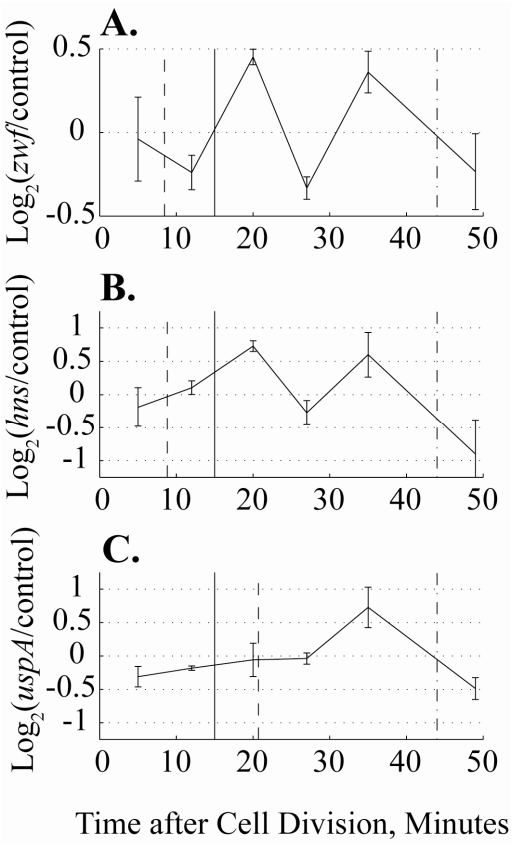

Figure 2.5 Differentially expressed transcript levels during the *E. coli* cell division cycle. The vertical solid line represents replication initiation; the vertical broken line represents gene replication and the vertical double broken line represents average time of cell division. Plot shows relative transcript levels for: A, *zwf*; B, *hns*; C, *uspA*.

populations synchronized by the membrane elution technique, the average doubling time and C period for the cells in previous studies were 22 minutes and 45 minutes, respectively. For our studies the average doubling time was 44 minutes while the C-period was 45 minutes, reflecting differences in the culture media used. As shown in Figure 2.3, the transcript level changes align well when considered with respect to the C period. This approach contrasts with attempts to correlate the data based on the fraction of the division cycle, where the correlation was much poorer. These results show that fluctuations in transcript levels are correlated with DNA replication and not cell division. The data corroborate previous results showing that changes in transcript levels are correlated with the C period (Zhou *et al.*, 1997). Our results are also consistent with the finding that transcription of *ftsZ,* a gene involved in cell division, is correlated with the replication cycle, and in particular replication initiation (Garrido *et al.*, 1993; Zhou *et al.*, 1994).

2.4.3 Transcript Level Increases Following Gene Replication for Some Genes

The C and D periods for *E. coli* B/r A grown in minimal glucose medium are 45 and 25 minutes respectively (Bremer and Chuang, 1981). Using these values and assuming a constant rate of DNA synthesis, we plotted the transcript level throughout the cell cycle with the average times of replication initiation, gene replication and cell division marked (Figures 2.4 and 2.5). Of the ten transcripts that showed cell cycle related changes, five displayed an increase in transcript level at the first time point following replication of the gene (*secD*, *cmk*, *asd*, *sdhA* and *gltA*; Figure 2.3). *SdhA* and *gltA* are adjacent genes and show very similar transcript level fluctuations during the cell cycle. These genes, and *asd*, encode products involved in central metabolism and therefore demand for their gene products is not expected to change during the cell

cycle. *Cmk*, a gene involved in nucleotide biosynthesis, may be expected to fluctuate based on DNA synthesis and will be discussed further below. The remaining gene, *secD*, is involved in transport and therefore we also would not expect it to be correlated with the cell cycle. The increase in transcript level detected shortly after replication of each of these genes indicates that replication fork progression may affect gene transcription.

2.4.4 Additional Transcriptional Mechanisms Exist for *zwf, hns* and *uspA*

Three genes that displayed differential expression during the cell cycle did not show fluctuations correlated to gene replication: *zwf*, *hns* and *uspA* (Figure 2.5). Our results show the transcript level peaks twice during the division cycle for both *zwf* and *hns*, indicating a transcriptional control mechanism beyond replication fork progression is somehow coupled to the division cycle for these genes. Although these genes are not functionally related to replication or division (the *zwf* gene product is involved in central metabolism and the *hns* gene product is a DNA-binding protein and environmental transcription regulator), they both show clear fluctuations in transcript level during the division cycle.

We also detected an increased *uspA* transcript level prior to cell division. Nachin *et al.* recently showed UspA is involved in oxidative stress resistance in *E. coli* (Nachin *et al.*, 2005), and therefore our results may indicate division induces expression of genes designed to protect cells from DNA-damaging agents.

2.4.5 Transcript Level for Nucleotide Biosynthesis Genes Increase Near Replication Initiation

Three of ten genes measured that were involved in nucleotide biosynthesis displayed statistically significant changes in transcript levels during the cell cycle (*nrdA*, *cmk*, *tmk*). In addition to analyzing each gene separately for transcript level fluctuations, we performed an ANOVA test on each class of genes. As a group, nucleotide biosynthesis genes (*dut*, *upp*, *apt*, *tmk*, *gmk*, *nrdA*, *hpt*, *cmk*, *adk*, *thyA*) displayed changes in transcript levels during the cell cycle (p-value <0.0001). The maximum average transcript level was detected 3 minutes prior to replication initiation, while the minimum transcript level occurred 20 minutes after replication initiation, or approximately mid-C period (Figure 2.6). To ensure the gene group was not dominated by the three genes showing cell cycle related transcript fluctuations (*nrdA, cmk, tmk*), the ANOVA test was also performed for only nucleotide biosynthesis genes not showing statistically significant transcript fluctuations on an individual level (*dut, upp, apt, gmk, hpt, adk, thyA*). This analysis yielded equivalent results (p-value = 0.0096). Although our results were not sensitive enough to detect cell cycle related changes for all genes involved in nucleotide biosynthesis individually, the gene class shows strong correlation with the C period, indicating that transcription of this set of genes is regulated during the cell cycle.

2.5 Discussion

In recent years, there has been a growing effort to construct a synthetic bacterium. A major step in this process is defining and assembling a minimal genome *de novo*. To this end, researchers have attempted to identify a minimal bacterial gene set necessary for life (reviewed by Koonin, 2003; Smalley *et al.*, 2003). However, our understanding of transcriptional organization in even the simplest organisms remains incomplete. Because DNA replication and division are major processes that must be

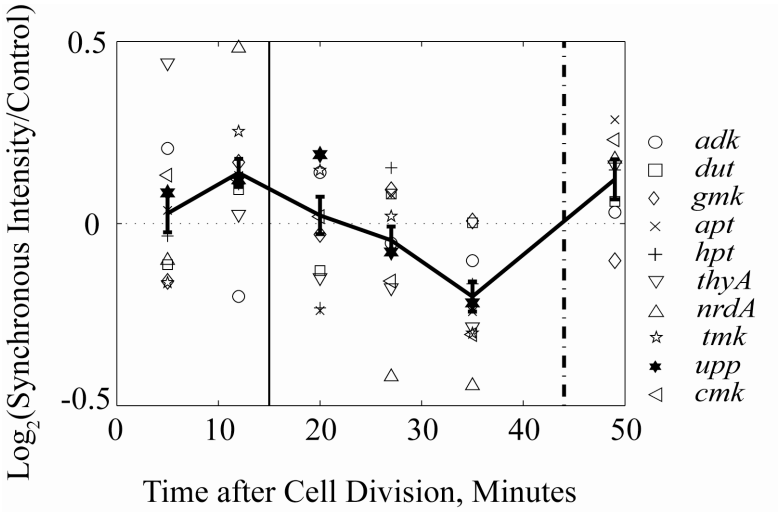

Figure 2.6 Compiled *E. coli* transcript levels for nucleotide biosynthesis genes included in microarray analysis. The vertical solid line represents replication initiation and the vertical double broken line represents average time of cell division. Symbols represent genes show in legend on right.

undertaken by any synthetic organism, it is important to understand their effects on transcript profiles. In this study, we identify two transcriptional phenomena related to cell cycle progression: transcription of some genes increases transiently after the gene is replicated; and transcription of genes involved in nucleotide biosynthesis are activated prior to replication initiation.

We employed an ANOVA procedure to analyze transcript measurements and did not limit our analysis to detecting only transcripts with cyclic profiles. To eliminate changes due to factors outside of cell cycle progression, we required that data collected for populations of cells at 49 minutes was statistically indistinguishable from the 5 minute time point. Ten of the 21 genes displaying dynamic transcript levels fit this criterion. Of the seven genes that did not fit this criterion, our results may show real cell cycle effects for some while others may be dynamic due to other cellular processes. For example, fluctuations for *ftsL* and *hflB* may be related to the cell cycle based on the division cycle related function of the gene products (e.g. FtsL and FtsH, respectively). In addition, we would expect to see changes in *secF* transcript levels similar to the *secD* transcript levels because these genes are expressed in the same operon. Indeed the *secD* and *secF* profiles are similar (Table 2.2). Both *dnaK* and *groS* also display dynamic transcript levels but do not recover to the 5 minute level at the 49 minute point. These genes are both stress-induced and could be up-regulated based on the minor changes in the cellular environment (i.e. shaking during incubation).

Several of the cell cycle related transcripts displayed a peak shortly after the replication fork progressed through the coding gene. Previously *E. coli* transcript levels for several genes (most not studied here) have been shown to fluctuate with the cell replication cycle (Theisen *et al.*, 1993; Garrido *et al.*, 1993; Zhou *et al.*, 1994; Zhou *et al.*, 1997). *E. coli* cultures that were synchronous with respect to either cell division or replication initiation showed that transcript levels for *mnmG (gidA)*, *mioC*,

dnaA, *dam*, *ftsZ*, *seqA*, *nrdA* and *mukB* all decreased transiently near gene replication. Due to the longer sampling intervals we employed, we would not expect to see this inhibition in our studies. However, several of the transcripts in previous studies also displayed a peak in transcript level following the decrease, which is consistent with our findings. In addition, previous studies found transcription of *rpoA*, *minE* and *tus* were unaffected by cell cycle progression, and transcription of *argP (iciA)* increased near the time of its replication. These results indicate that not all genes are affected by the cell cycle, which is corroborated by the data presented here. In previous studies, genes were analyzed based on their functional or structural relationship with the cell division or replication cycles. Our studies provide evidence that transcript levels for a significant fraction of genes in *E. coli* are affected by the cell cycle, whether or not the function or position of the gene product is related to cell cycle progression.

In addition to showing induction following replication of some genes, we show that fluctuations in transcript level depend on the length of the C period as opposed to the division cycle. The replication cycle in *E. coli* can be divided into I, C and D periods. The I period is simply defined as the time required between replication initiation events. The C period is defined as the time it takes to complete one round of replication and the D period is the time between replication termination and cell division. At high growth rates, *E. coli* replication cycles overlap as cell division is not a prerequisite for initiating the next round of replication, therefore the doubling time (τ_D) is often shorter than the sum of the C and D periods. Our results show that cell cycle related transcription is correlated to the C period, not the division cycle. Based on this relationship, we would expect changes in transcript level to be somewhat lower in *E. coli* populations synchronized by the division cycle rather than the replication cycle. Indeed, the fluctuations in transcript level that we measured, although statistically significant, were in general less than two-fold. Based on the observed

correlation with the C period, transcript level changes may be more pronounced in populations synchronized with respect to the replication cycle.

Finally, although we were able to detect two distinct phenomena affecting transcription, these do not fully account for all of our results. Specifically, the *zwf*, *hns* and *uspA* transcript profiles during the cell cycle are not predicted by either gene location or gene function. In addition, *hns* and *zwf* transcripts do not display a purely cyclic profile, but peak multiple times during the cell cycle. Therefore, other mechanisms must occur during the cell cycle to control transcript levels for important genes. Further study of these genes may reveal important information about transcriptional regulation.

The overall goal of this work was to identify important design criteria for construction of a bacterial genome *de novo*. Our results show the time at which a gene is replicated is an important factor to consider when organizing a synthetic genome. Because the transcriptional variations introduced by the cell cycle are related to replication, key design criteria that must be considered when designing synthetic genomes include replication initiation timing, the rate of DNA polymerization and the distance of the gene from the origin of replication. Our results show that transcription of 15-20% of the genome fluctuates with the cell cycle, and about half of the fluctuating transcripts reach a maximum following gene replication. Therefore genes should be arranged within the genome to allow for transcription at their optimum time within the cell cycle. The rate of DNA polymerization must also be considered, and this may be especially important when designing a minimal genome. Because DNA replication may serve as a key process to make regions of the genome accessible for transcription, it is possible that replication must persist for a specified amount of time to optimize the ratio between the fraction of the genome in a transcriptionally accessible state and the concentration of the transcriptional machinery, and to enable

efficient transcription of accessible genes. Consistent with this hypothesis, the chief DNA polymerase in *Mycoplasma capricolum*, a bacterium with a greatly reduced genome size, is approximately ten times slower than *E. coli* DNA polymerase III (Seto and Miyata, 1998).

Another interesting observation from this study is that nucleotide biosynthesis genes are up-regulated concurrently with DNA replication initiation. Although each of these genes is replication related, they are located throughout the genome and are replicated in different segments of the cell cycle. Therefore a hierarchy of gene regulation mechanisms may exist in bacterial systems. Further understanding of all transcription regulation mechanisms will aid in designing efficient and robust synthetic genomes.

REFERENCES

Baumann, A., Lange, C. & Soppa, J. (2007). Transcriptome changes and cAMP oscillations in an archaeal cell cycle. *BMC Cell Biology* **8**, 21.

Benjamini, Y. & Hochberg, Y. (1995). Controlling the false discovery rate: a practical and powerful approach to multiple testing. *Journal of the Royal Statistical Society. Series B (Methodological)* **57**(1), 289-300.

Bernstein, J. A., Khodursky, A. B., Lin, P.-H., Lin-Chao, S. & Cohen, S. N. (2002). Global analysis of mRNA decay and abundance in *Escherichia coli* at single-gene resolution using two-color fluorescent DNA microarrays. *Proceedings of the National Academy of Sciences of the United States of America* **99**(15), 9697-9702.

Bremer, H. & Chuang, L. (1981). The cell cycle in *Escherichia coli* B/r. *Journal of Theoretical Biology* **88**, 47-80.

Cho, R. J., Campbell, M. J., Winzeler, E. A., Steinmetz, L., Wolfsberg, T. G., *et al.* (1998). A genome-wide transcriptional analysis of the mitotic cell cycle. *Molecular Cell* **2**(1), 65-73.

Cho, R. J., Huang, M., Campbell, M. J., Dong, H., Steinmetz, L., *et al.* (2001). Transcriptional regulation and function during the human cell cycle. *Nature Genetics* **27**(1), 48-54.

Filipovska, A. & Rackham, O. (2008). Building a parallel metabolism within the cell. *ACS Chemical Biology* **3**(1), 51-63.

Forster, A. C. & Church, G. M. (2006). Towards synthesis of a minimal cell. *Molecular Systems Biology*, Article 45.

French, S. (1992). Consequences of replication fork movement through transcription units *in vivo*. *Science* **258**, 1362-1365.

Garrido, T., Sanchez, M., Palacios, P., Aldea, M. & Vicente, M. (1993). Transcription of *ftsZ* oscillates during the cell cycle of *Escherichia coli*. *EMBO Journal* **12**(10), 3957-3965.

Gibson, D. G., Benders, G. A., Andrews-Pfannkoch, C., Denisova, E. A., Baden-Tillson, H., *et al.* (2008). Complete chemical synthesis, assembly, and cloning of a *Mycoplasma genitalium* genome. *Science* **319**, 1215-1220.

Hegde, P., Qi, R., Abernathy, K., Gay, C., Dharap, S., *et al.* (2000). A concise guide to cDNA microarray analysis--II. *BioTechniques* **29**(3), 548-562.

Helmstetter, C. E. (1969). Methods for studying the microbial division cycle. In

Methods in Microbiology (Norris, J. R. & Ribbons, D. W., eds.), Vol. 1, pp. 327-363. 34 vols. Academic Press, London, New York.

Helmstetter, C. E., Thornton, M., Romero, A. & Eward, K. L. (2003). Synchrony in human, mouse and bacterial cell cycles. *Cell Cycle* **2**, 42-45.

Keseler, I. M., Collado-Vides, J., Gama-Castro, S., Ingraham, J., Paley, S., *et al.* (2005). EcoCyc: a comprehensive database resource for *Escherichia coli*. *Nucleic Acids Research* **33**, D334-D337.

Kobayashi, H., Kaern, M., Araki, M., Chung, K., Gardner, T. S., *et al.* (2004). Programmable cells: interfacing natural and engineered gene networks. *Proceedings of the National Academy of Sciences of the United States of America* **101**(22), 8414-8419.

Koonin, E. V. (2003). Comparative genomics, minimal gene sets and the last universal common ancestor. *Nature Reviews Microbiology* **1**(2), 127-136.

Laub, M. T., McAdams, H. H., Feldblyum, T., Fraser, C. M. & Shapiro, L. (2000). Global analysis of the genetic network controlling a bacterial cell cycle. *Science* **290**, 2144-2148.

Lee, M.-L. T. (2004). *Analysis of microarray gene expression data*, Kluwer Academic Publishers, Boston.

Lundgren, M. & Bernander, R. (2007). Genome-wide transcription map of an archaeal cell cycle. *Proceedings of the National Academy of Sciences of the United States of America* **104**(8), 2939-2944.

Nachin, L., Nannmark, U. & Nyström, T. (2005). Differential roles of the universal stress proteins of *Escherichia coli* in oxidative stress resistance, adhesion, and motility. *Journal of Bacteriology* **187**(18), 6265-6272.

Oliva, A., Rosebrock, A., Ferrezuelo, F., Pyne, S., Chen, H., *et al.* (2005). The cell cycle-regulated genes of *Schizosaccharomyces pombe*. *PLoS Biology* **3**(7), e225.

Peng, X., Karuturi, R. K. M., Miller, L. D., Lin, K., Jia, Y. H., *et al.* (2005). Identification of cell cycle-regulated genes in fission yeast. *Molecular Biology of the Cell* **16**(3), 1026-1042.

Rhee, S.-K., Liu, X., Wu, L., Chong, S. C., Wan, X. & Zhou, J. (2004). Detection of genes involved in biodegradation and biotransformation in microbial communities by using 50-mer oligonucleotide microarrays. *Applied and Environmental Microbiology* **70**(7), 4303-4317.

Roberts, R. B., Abelson, P. H., Cowie, D. B., Boulton, E. T. & Britten, R. J. (1955). *Studies of Biosynthesis in Escherichia coli*, Carnegie Institute of Washington,

Washington, D. C.

Rouillard, J.-M., Zuker, M. & Gulari, E. (2003). OligoArray 2.0: design of oligonucleotide probes for DNA microarrays using a thermodynamic approach. *Nucleic Acids Research* **31**(12), 3057-3062.

Rustici, G., Mata, J., Kivinen, K., Lio, P., Penkett, C. J., *et al.* (2004). Periodic gene expression program of the fission yeast cell cycle. *Nature Genetics* **36**(8), 809-817.

Ryan, K. R. & Shapiro, L. (2003). Temporal and spatial regulation in prokaryotic cell cycle progression and development. *Annual Review of Biochemistry* **72**, 367-394.

Selinger, D. W., Saxena, R. M., Cheung, K. J., Church, G. M. & Rosenow, C. (2003). Global RNA half-life analysis in *Escherichia coli* reveals positional patterns of transcript degradation. *Genome Research* **13**, 216-223.

Seto, S. & Miyata, M. (1998). Cell reproduction and morphological changes in *Mycoplasma capricolum*. *Journal of Bacteriology* **180**(2), 256-264.

Smalley, D. J., Whiteley, M. & Conway, T. (2003). In search of the minimal *Escherichia coli* genome. *Trends in Microbiology* **11**, 6-8.

Spellman, P. T., Sherlock, G., Zhang, M. Q., Iyer, V. R., Anders, K., *et al.* (1998). Comprehensive identification of cell cycle-related genes of the yeast *Saccharomyces cervisiae* by microarray hybridization. *Molecular Biology of the Cell* **9**(12), 3273-3297.

Theisen, P. W., Grimwade, J. E., Leonard, A. C., Bogan, J. A. & Helmstetter, C. E. (1993). Correlation of gene transcription with the time of initiation of chromosome replication in *Escherichia coli*. *Molecular Microbiology* **10**(3), 575-584.

Whitfield, M. L., Sherlock, G., Saldanha, A. J., Murray, J. I., Ball, C. A., *et al.* (2002). Identification of genes periodically expressed in the human cell cycle and their expression in tumors. *Molecular Biology of the Cell* **13**(6), 1977-2000.

Zhou, P. & Helmstetter, C. E. (1994). Relationship between *ftsZ* gene expression and chromosome replication in *Escherichia coli*. *Journal of Bacteriology* **176**(19), 6100-6106.

Zhou, P., Bogan, J. A., Welch, K., Pickett, S. P., Wang, H.-J., *et al.* (1997). Gene transcription and chromosome replication in *Escherichia coli*. *Journal of Bacteriology* **179**(1), 163-169.

CHAPTER 3

MACROMOLECULAR CROWDING CAN ACCOUNT FOR RNASE-SENSITIVE CONSTRAINT OF BACTERIAL NUCLEOID STRUCTURE

3.1 Abstract

The shape and compaction of the bacterial nucleoid may affect the accessibility of genetic material to transcriptional machinery in natural and synthetic systems. To investigate this phenomenon, the nature and contribution of RNA- and protein-based forces to nucleoid compaction in *Escherichia coli* were investigated. We propose that the removal of RNA from the bacterial nucleoid affects nucleoid compaction by altering the branching density of the nucleoid macromolecular structure. We show that RNA-free nucleoids adopt a compact structure similar in size to exponential-phase nucleoids when the concentration of the macromolecular crowding agent is increased, indicating that the RNase-sensitive nucleoid compaction force results from changes to the branch density of the chromosome. We also present evidence that control and protein-free nucleoids behave similarly in solutions containing a macromolecular crowding agent. These results show that the contribution to DNA compaction by nucleoid-associated proteins is small when compared to macromolecular crowding effects.

3.2 Introduction

The bacterial nucleoid consists of chromosomal DNA, nascent transcripts and polysomes, and DNA binding proteins including HU, Fis, H-NS, IHF, DNA

topoisomerases and RNA polymerases. *In vivo*, the nucleoid is compacted over one thousand fold during the log-growth phase (Murphy and Zimmerman, 2000). Despite this compaction, during exponential phase the majority of the bacterial chromosome exists in a transcriptionally accessible state throughout the cell cycle (Stonington and Pettijohn, 1971). This characteristic indicates that unique mechanisms exist in bacteria that allow transcriptional machinery to access the compacted DNA. Given the recent advances toward building synthetic genomes *de novo*, it is important to understand whether these mechanisms are physical properties of the biomolecules involved, or if specific molecular mechanisms enable this accessibility.

Several physical forces have been suggested to aid in bacterial nucleoid compaction. Chromosomal DNA is kept in a state of high negative supercoiling through the action of several topisomerases, and physiological levels of negative supercoiling ($\sigma \sim -0.025$) have been shown to compact DNA by 2.5 fold in solution (Boles *et al.*, 1990). However, this modest compaction is unlikely to serve as the main DNA compacting force *in vivo*. Cells also produce polyamines such as spermidine and spermine which have been suggested to aid in compaction by neutralizing the charge of the DNA backbone (Pelta *et al.*, 1996). Multiple studies show that physiological concentrations of cellular polyamines are capable of inducing a first order random coil to globule transition of naked DNA chains, resulting in a several-fold increase in compaction (Yoshikawa *et al.*, 1996; Baeza *et al.*, 1987; Tsumoto *et al.*, 2003; Oana *et al.*, 2002).

Macromolecular crowding is also thought to play a role in chromosomal compaction. The concentration of macromolecules (proteins and RNA) in bacterial cytoplasm is approximately 340 mg/mL, producing significant DNA compaction forces due to excluded volume effects (Cunha *et al.*, 2001; Murphy and Zimmerman, 1997; Murphy and Zimmerman, 2000, Woldringh *et al.*, 1995). The compaction of

DNA by macromolecular crowding has been observed *in vitro* as a model for *in vivo* processes (Zimmerman, 2006; Tsumoto *et al.*, 2003; Zimmerman and Murphy, 2001).

Notably, these physical DNA compaction forces are non-specific and therefore affect genomic DNA regardless of the primary structure or organization. In addition to physical forces, the nucleoid is thought to be compacted by biochemical forces, namely proteins and RNA that are known to be associated with chromosomal DNA. Several nucleoid-associated proteins (NAPs) exist in bacteria. Due to their histone-like characteristics (small, basic proteins with DNA-binding affinity) and abundance, NAPs are thought to participate in chromosomal compaction, albeit via different mechanisms than eukaryotic histones. HU, IHF and H-NS have higher affinities for curved DNA and these proteins bind to DNA independent of the DNA sequence *in vivo* (Johnson *et al.*, 2005). HU and IHF induce kinks in the DNA, and H-NS is thought to bind non-specifically to patches of DNA and form bridges between H-NS bound segments. Both activities affect local DNA structure, and are thought to enhance global compaction (Johnson *et al.*, 2005; Pettijohn 1996; Dame, 2005). Nucleoid-associated proteins IHF and Fis are known to bind to consensus sequences and are thought to provide sequence specific structure to chromosomal DNA in addition to non-specific binding effects. Evidence for the NAPs' role in chromosome compaction includes studies that show NAPs compact DNA *in vitro* (Murphy and Zimmerman, 1994). However, this function has recently been called into question. NAP-mediated DNA compaction *in vitro* requires levels of NAPs that are several times higher than intracellular levels. In addition, Brunetti *et al.* showed that genomic deletion of specific NAPs did not alter global DNA structure (Brunetti *et al.*, 2001). Zimmerman argued that NAPs may not compact DNA *in vivo,* since removing NAPs by washing has little effect on the size of isolated nucleoids (Zimmerman, 2006).

Evidence for an RNA-based DNA compaction force has also been observed in

both low-salt (Murphy and Zimmerman, 2000; Murphy and Zimmerman, 2002; Zimmerman, 2006) and high-salt (Dworsky, 1975; Dworsky and Schaechter, 1973) nucleoid preparations. It is known that the removal of RNA from isolated nucleoids causes instability and decompaction. The method of RNA removal does not affect the sensitivity of RNA-free nucleoids as both rifampicin-treated nucleoids (causing removal of RNA *in vivo*) and RNase-treated nucleoids (causing removal of RNA following cell lysis) are easily denatured. Yet the existence of an RNA constraint remains controversial because an RNA molecule responsible for nucleoid stabilization has not been identified. It has been suggested the sensitivity of RNA-free nucleoids results from removal of transertional linkages with the cytoplasmic membrane, as removal of RNA would free polysomes associated with nascent transcripts for membrane-associated proteins (Murphy and Zimmerman, 2002). However, RNA-free nucleoids isolated under high-salt conditions, which removes most proteins and membrane fragments from the compacted DNA, also decompact upon cell lysis, suggesting additional effects of RNA removal.

We hypothesize that nucleoid compaction is mediated mainly by physical forces, specifically macromolecular crowding effects. In solution, long polymer chains such as DNA do not exist in a linear conformation, but rather assume a random coil configuration (for detailed examination of polymer theory, see Flory, 1953; Grosberg and Khokhlov, 1994). The size of the polymer in solution can be described by its radius of gyration, which approximates the hydrodynamic radius of the polymer. A polymer's radius of gyration depends on the polymer length and structure, and the quality of its solvent. In a 'good solvent', interactions between the polymer and the solvent are more thermodynamically favorable than polymer interactions with itself therefore the polymer exists in an expanded conformation. In a 'poor solvent', the opposite situation exists and interactions of the polymer with itself are more

thermodynamically favorable, leading to a more compact configuration. In a Theta (Θ) solvent, attractive and repulsive forces between the polymer and solvent are balanced and the polymer assumes an ideal random coil conformation with a radius of gyration R_{gO}. The quality of the solvent can be determined from the swelling parameter of a polymer chain, α, where:

$$\alpha \approx \frac{R_g}{R_{gO}} \tag{3.1}$$

In a good solvent $\alpha > 1.0$, whereas in a poor solvent, $\alpha < 1.0$.

A polymer's radius of gyration also depends on its length and structure. The radius of gyration for an ideal, linear polymer chain is:

$$R_{gO}^{Linear} \sim aN^{1/2} \tag{3.2}$$

Where a is the length of a segment of the polymer and N is the number of segments in the polymer chain. Theoretically, branched polymers assume a more compact structure when compared to their linear counterparts as the radius of gyration for an ideal randomly branched polymer chain is:

$$R_{gO}^{Branched} \sim an^{1/4}N^{1/4} \tag{3.3}$$

Where n is the average length between branch points. For polymers with $N >> n$, the polymer chain assumes a compact configuration (Grosberg and Khokhlov, 1994).

We propose that previously observed RNA-based DNA compaction forces are actually the result of changes to the effective branching density of the nucleoid. We present a model of the bacterial nucleoid where chromosomal DNA is represented as a polyelectrolyte in a random coil configuration, and nascent transcripts are represented as branches emanating from the DNA backbone. The removal of RNA from the nucleoid alters the nucleoid's radius of gyration from $R_g \sim N^{1/4}$ to $R_g \sim N^{1/2}$, which results in nucleoid decompaction. To test this hypothesis, we investigated the nature

and the contribution of RNA- and protein-based factors to nucleoid condensation. We present evidence that Brij 58, a detergent used extensively in *E. coli* nucleoid preparations, also serves an unrecognized role as a macromolecular crowding agent in these preparations. The removal of RNA from the nucleoid either *in vivo* or following cell lysis resulted in reduced Brij 58-dependent nucleoid compaction. We propose that nucleoid-associated RNA increases the branching density of the chromosomal DNA, and the removal of RNA changes the nucleoid macromolecular structure and its interactions with the Brij 58 molecules, which results in nucleoid decompaction. In addition, we show native and protein-free nucleoids behaved similarly with respect to changes in macromolecular crowding indicating that the contribution of nucleoid-associated proteins to nucleoid compaction is small when compared to macromolecular crowding effects.

3.3 Materials and Methods

3.3.1 Bacterial Strain and Growth Conditions

E. coli B/r A (ATCC 12407) were grown in C-medium (17.2 mM dibasic potassium phosphate, 11.0 mM monobasic potassium phosphate, 9.5 mM ammonium sulfate, 0.41 mM magnesium sulfate, 0.17 mM sodium chloride, 3.6 μM ferrous sulfate, 1.0 μM EDTA) containing 0.1% glucose (Roberts *et al.*, 1955) at 37°C, shaking at 350 RPM to OD600 ~0.4. The doubling time for these cultures was 44 min. Where indicated, chloramphenicol or rifampicin was added to a final concentration of 30 μg/mL or 40 μg/mL, respectively, and cultures were incubated at 37°C, 350 RPM for 30 min. Cells were harvested by centrifugation at 14,000*g*, 4°C for 10 minutes.

3.3.2 Nucleoid Preparations for Fluorescence Microscopy

Nucleoids for fluorescent microscopy were isolated using a modified low-salt procedure developed by Kornberg *et al.* (Kornberg *et al.*, 1974). Briefly, harvested cell pellets were resuspended in 250 µL Solution A (20% sucrose, 10 mM Tris-HCl pH 8.1, 0.1 M sodium chloride) containing a 1/200 dilution of Picogreen (Invitrogen Co., Carlsbad, CA) and vortexed briefly. After a two minute incubation, 50 µL of Solution B (4 mg lysozyme per milliliter of 120 mM Tris-HCl pH 8.1, 50 mM EDTA) was added and suspensions were incubated at room temperature for 1 minute. Ten microliters of the suspension were diluted tenfold into Solution D (7.1% sucrose, 14 mM Tris-HCl pH 8.1, 36 mM sodium chloride, 10 mM EDTA, 5 mM spermidine, 5 mg Brij 58/mL, 0.22% sodium deoxycholate). The concentrations of Brij 58 and spermidine were varied as indicated. Cells were incubated at room temperature for >20 minutes to allow nucleoid release. The final nucleoid solution contained the same concentration of all components except Picogreen as the previously described low-salt procedure. Five microliters of the nucleoid suspensions were placed on a microscope slide and viewed with an Olympus BX-51 fluorescent microscope and imaged using a Cooke SensiCam CCD camera. The images were analyzed with ImageJ version 1.38x software (NIH, Bethesda MD). The contrast of the images was adjusted to the same level and the area of each nucleoid was measured three times using the freehand selection tool. The average area was taken to be the nucleoid area.

3.3.3 Fragmented *E. coli* Chromosomal DNA Preparations

Ten milliliters of *E. coli* B/r cell suspensions (OD 600 ~ 0.4) were centrifuged for 10 minutes at 14,000*g*, 4ºC. DNA was isolated from cell pellets using the

FastDNA® Kit and the FastPrep® Instrument (Qbiogene, Inc., CA). The size of the fragmented DNA ranged from 5000 – 6500 basepairs as measured by agarose gel electrophoresis. Fragmented DNA was diluted to 2.5 μg/mL in solutions containing a 1/200 dilution of Picogreen with Brij 58 and sodium chloride or spermidine. DNA compaction was observed by fluorescent microscopy as previously described.

3.3.4 Nucleoid Isolations for Electron Microscopy

Two procedures were used to isolate nucleoids from harvested *E. coli* B/r cells. The 'high-salt procedure' developed by Stonington and Pettijohn was employed with some modifications (Stonington and Pettijohn, 1971). Harvested cell pellets were resuspended in 250 μL Solution A and vortexed briefly. After two minutes, 50 μL of Solution B was added and the samples were inverted to mix. After one minute, 250 μL of Solution C (1% Brij 58, 0.4% sodium deoxycholate, 10 mM EDTA pH 8.0, 2 M sodium chloride) was added and the samples were incubated at room temperature for 10 - 20 minutes, until the suspensions began to clear. Nucleoid suspensions were loaded onto 10 - 30% sucrose continuous gradients in 10 mM Tris-HCl pH 8.1, 1 M NaCl, 1 mM EDTA, 1 mM β-mercaptoethanol. Gradients were centrifuged at 28,000*g*, 4°C for 45 minutes in a Beckman SW41 rotor. Acceleration and deceleration were set to 1. Nucleoids were also isolated using a 'low-salt procedure' based on Kornberg *et al.*'s modification of the Stonington and Pettijohn procedure, where the 2 M NaCl in Solution C was replaced with 10 mM spermidine (Kornberg *et al.*, 1974). In addition, cell suspensions were incubated at 37°C for 5 minutes to allow cell lysis. Nucleoid suspensions from low-salt preparations were loaded onto 15 - 30% sucrose continuous gradients in 20 mM sodium diethylmalonate pH 7.1, 5 mM magnesium chloride, 1 mM β-mercaptoethanol. Gradients were centrifuged at 3000*g*, 4°C for 35 minutes in a

Beckman SW41 rotor. Acceleration and deceleration were set to 1.

Gradients from both high- and low-salt preparations were fractionated into 0.3 mL aliquots. One hundred microliters of each fraction were combined with 100 µL of a 1/200 dilution of Picogreen in TE. The fluorescence was measured and the DNA concentration of each fraction was calculated. Calf thymus DNA (Sigma Chemical Co., St. Louis, MO) was used as a standard.

3.3.5 Electron Microscopy of Isolated Nucleoids

Nucleoids were attached to butvar-coated nickel grids that were freshly coated with carbon by glow-discharge as described by Postow *et al.* (Postow *et al.*, 2004). Eight microliter aliquots from the fraction containing the peak DNA concentration were adsorbed to the grid for 2 minutes. Grids were rinsed for consecutive 1 minute intervals in 0.1 M ammonium acetate, 0.01 M ammonium acetate and 2% uranyl acetate. Grids were viewed using a Tecnai T12 transmission electron (FEI Co., Hillsboro, Oregon), and imaged with an SIS Megaview III CCD camera. Images were analyzed with ImageJ software. The condensed area of each nucleoid was measured three times using the freehand selection tool, and averaged. Membrane fragments and single loops extending from the central body of the nucleoid were excluded. Individual images are included in Appendix A.

3.4 Results

3.4.1 Brij 58 Serves as Macromolecular Crowding Agent in Nucleoid Preparations

E. coli nucleoids were prepared using a low-salt procedure originally described

by Kornberg *et al.* (Kornberg *et al.*, 1974), and modified by Murphy and Zimmerman (Murphy and Zimmerman, 1997). In this procedure, cells are exposed sequentially to a sucrose/sodium chloride solution to disrupt the outer membrane (Solution A), lysozyme to degrade the peptidoglycan layer (Solution B), and finally Brij 58, deoxycholate and spermidine to solubilize the inner membrane and stabilize the nucleoid (Solution C). It has been noted previously that a long delay between the addition of Solutions B and C resulted in premature cell lysis and nucleoid decompaction (Murphy and Zimmerman, 1997). To investigate the mechanism by which Solution C stabilizes compacted nucleoids, we removed each solution component and observed the effect on nucleoid preparations via fluorescent microscopy. Removal of either EDTA or sodium deoxycholate resulted in incomplete cell lysis (data not shown). Interestingly, the removal of spermidine resulted in only partial decompaction of the nucleoids (Figure 3.1a), indicating that spermidine is partially but not fully responsible for nucleoid compaction after cell lysis. Removal of Brij 58 from the reaction resulted in nearly complete decompaction of the nucleoid DNA. Very few intact cells were observed in the nucleoid preparations lacking either spermidine or Brij 58 showing that cell lysis is not prevented by removal of either component from Solution C. These results indicate that both spermidine and Brij 58 play a role in nucleoid compaction and/or stabilization.

To further investigate the roles of spermidine and Brij 58 in DNA compaction, we observed the compaction of purified, fragmented *E. coli* chromosomal DNA in the presence of spermidine and Brij 58 (Figure 3.1b). This DNA preparation lacks the associated proteins and RNA found in nucleoid DNA. As expected, 5 mM spermidine caused DNA compaction. This is in agreement with previous studies showing that naked DNA assumed a compact form in solutions containing at least 0.14 - 1.15 mM spermidine (Yoshikawa *et al.*, 1996; Baeza *et al.*, 1987). Solutions with Brij 58 only

Figure 3.1 Spermidine and Brij 58 contributions to maintaining nucleoid compaction after release from *E. coli* cells. (a) Fluorescent micrographs of nucleoids released from exponential phase *E. coli* cells in the presence and absence of spermidine and Brij 58; (b) spermidine and Brij 58 mediated compaction of naked *E. coli* chromosomal DNA, and a table showing adequate levels of Brij 58 for DNA compaction in the presence of NaCl, where + indicates compact nucleoids were present, - indicates dispersed nucleoids were present and +/- indicates a mixture; (c) molecular structure of Brij 58.

a.

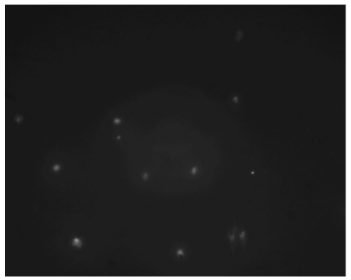

5 mg/mL Brij 58,
5 mM spermidine

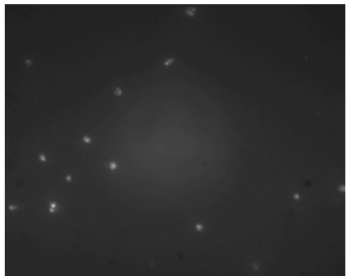

5 mg/mL Brij 58,
0 mM spermidine

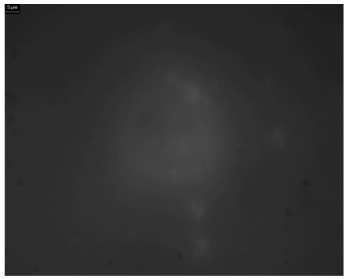

0 mg/mL Brij 58,
5 mM spermidine

b.

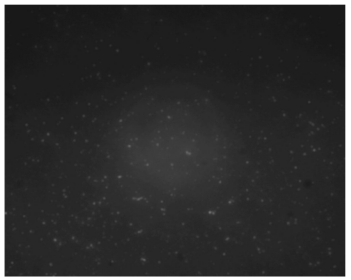

5 mM spermidine

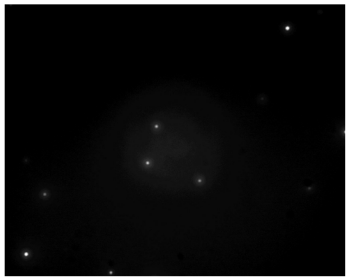

150 mg/mL Brij 58,
3 M NaCl

NaCl (M)	Brij 58 (mg/mL) 100	150	200
1	-	-	+/-
2	-	+/-	+
3	-	+	+
4	-	+	+
5	+	+	+

c.

Brij 58

PEG segment

required much higher levels than those found in nucleoid preparations to compact naked DNA independently of spermidine (>100 mg/mL Brij 58 versus 5 mg/mL Brij 58). The ionic strength of the solution affected Brij 58-mediated compaction of naked DNA; high levels of sodium chloride decreased the critical Brij 58 concentration required for DNA collapse (Figure 3.1b). These observations agree well with previous studies that characterized the conditions required for compaction of DNA molecules in the presence of macromolecular poly(ethylene glycol) (i.e. PEG) and poly(ethylene oxide) (i.e. PEO) (de Vries, 2001; Vasilevskaya *et al.*, 1995; Frisch and Fesciyan, 1979). Together with the structural similarities between Brij 58 and PEG (Figure 3.1c), our results show that Brij 58 participates in nucleoid compaction through a mechanism similar to PEG, presumably through macromolecular crowding effects.

3.4.2 Compaction of RNA-free Nucleoids Requires High Levels of Brij 58

Based on our observations that Brij 58 serves as a macromolecular crowding factor in nucleoid preparations, we hypothesized that the nucleoid decompaction observed in RNA-free nucleoids may result from changes in the effective branching density of the nucleoid that affect the nucleoid's response to Brij 58-induced crowding. We investigated Brij 58-mediated nucleoid compaction in native nucleoids (nucleoids isolated from cells in exponential phase, with no antibiotic, RNase or proteinase K treatment), and compared compaction levels with RNA-free nucleoid compaction levels (Figure 3.2, Table 3.1). Our results show that native nucleoids are compacted with concentrations of Brij 58 greater than or equal to 5 mg/mL, but become expanded at Brij 58 concentrations of 2.5 mg/mL and below. RNA-free nucleoids, produced both *in vivo* by treatment with rifampicin and after cell lysis by RNase A treatment, were not compacted at Brij 58 concentrations below 50 mg/mL.

Figure 3.2 Average area of *E. coli* nucleoids in solution with increasing concentrations of macromolecular crowding agent, Brij 58. The Brij 58 concentration is noted at the base of the each bar (1 - 50 mg/mL). (a) Native nucleoids from exponential phase cells; (b) RNA-free nucleoids from exponential phase cells treated for 30 min with rifampicin; (c) RNA-free nucleoids from exponential phase cells treated with RNase A for 1 hour after nucleoid release; (d) Nascent polypeptide-free nucleoids from exponential phase cells treated for 30 min with chloramphenicol; (e) Protein-free nucleoids from exponential phase cells treated with proteinase K for 1 hr after nucleoid release. Error bars represent standard error.

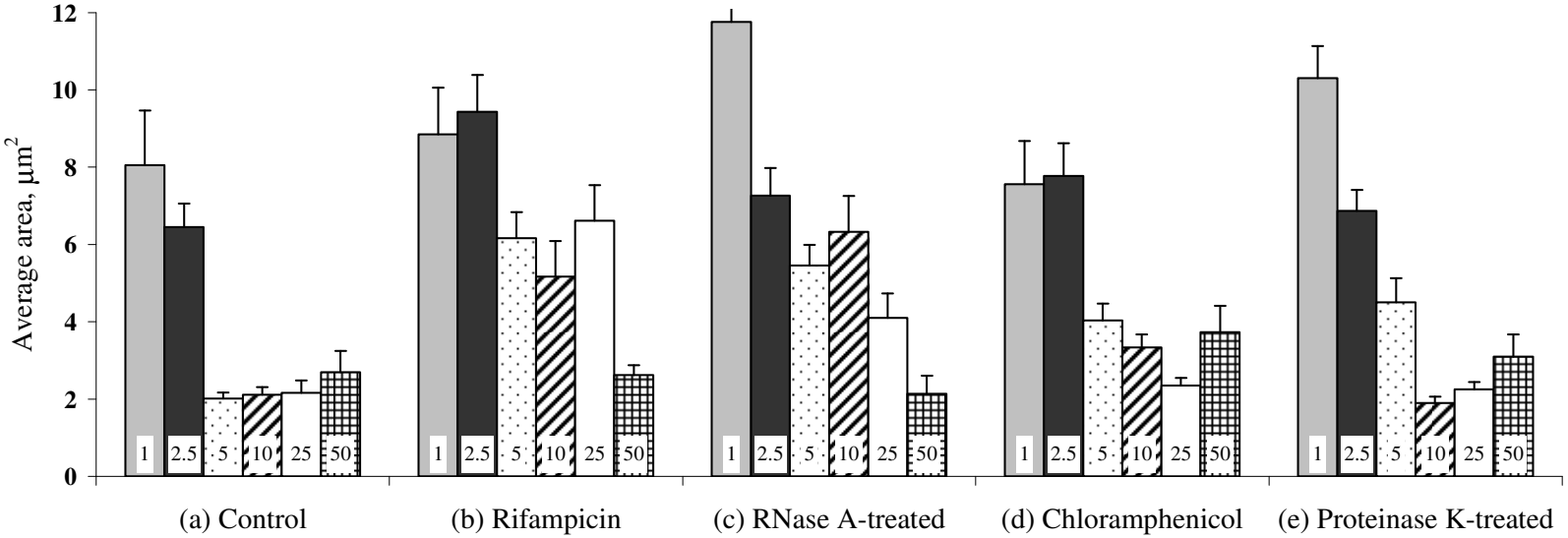
Average area, μm2
12
10
8
6
4
2
0
1
2.5
5
10
25
50
(a) Control
(b) Rifampicin
(c) RNase A-treated
(d) Chloramphenicol
(e) Proteinase K-treated

Table 3.2 Average area in square micrometers of treated nucleoids compacted by Brij 58

Brij 58, mg/mL	Control	Chloramphenicol	Proteinase K-treated	Rifampicin	RNase A-treated
1	8.05 ± 5.29 (*n* =14)	7.56 ± 4.16 (*n* =14)	10.31 ± 4.03 (*n* =24)	8.85 ± 4.38 (*n* =13)	11.76 ± 6.02 (*n* =18)
2.5	6.45 ± 2.35 (*n* =15)	7.77 ± 2.96 (*n* =12)	6.87 ± 1.80 (*n* =11)	9.43 ± 3.82 (*n* =16)	7.27 ± 3.32 (*n* =22)
5	2.01 ± 0.68 (*n* =18)	4.03 ± 1.77 (*n* =16)	4.50 ± 2.58 (*n* =17)	6.16 ± 3.24 (*n* =23)	5.45 ± 2.96 (*n* =30)
10	2.11 ± 0.95 (*n* =23)	3.33 ± 1.33 (*n* =15)	1.89 ± 0.77 (*n* =20)	5.17 ± 4.95 (*n* =29)	6.33 ± 2.93 (*n* =10)
25	2.16 ± 1.09 (*n* =12)	2.35 ± 0.90 (*n* =21)	2.25 ± 0.65 (*n* =12)	6.61 ± 4.02 (*n* =19)	4.10 ± 2.52 (*n* =16)
50	2.70 ± 2.33 (*n* =18)	2.35 ± 2.27 (*n* =11)	3.10 ± 2.34 (*n* =17)	2.62 ± 1.28 (*n* =26)	2.13 ± 1.84 (*n* =15)

However, a Brij 58 concentration of 50 mg/mL induced compaction of RNA-free nucleoids to sizes that were comparable to native nucleoids. These results show that Brij 58 participates in nucleoid compaction and stabilization after cell lysis, and that the removal of RNA from the nucleoid changes the compacting forces exhibited by Brij 58.

3.4.3 Protein-free Nucleoids and Control Nucleoids Behave Similarly with Respect to Brij 58-Mediated Compaction

Brij 58-mediated compaction of nascent polypeptide-free and protein-free nucleoids was examined to investigate the role of NAPs in nucleoid compaction. We hypothesized that the removal of NAPs, and therefore NAP-mediated compaction forces, would require higher levels of Brij 58 for nucleoid compaction. Our results show that control nucleoids, chloramphenicol-treated nucleoids and proteinase K-treated nucleoids all exhibited similar compaction characteristics in the presence of Brij 58 (Figure 3.2, Table 3.1). These results indicated that NAPs do not play a role in nucleoid compaction.

3.4.4 Nucleoids Isolated Under Low- and High-Salt Conditions are Similar in Size

To further investigate whether NAPs serve to compact chromosomal DNA, we prepared isolated nucleoids using both high- and low-salt procedures and observed the size of the compacted region using transmission electron microscopy. Nucleoids prepared using the high-salt isolation procedure lack nearly all nucleoid associated proteins excluding RNA polymerase (Pettijohn *et al.*, 1970), while nucleoids prepared with the low-salt procedure retain these proteins (Murphy and Zimmerman, 1997). We

observed no statistically significant difference in the area of the compacted region of nucleoids with and without NAPs (Figures 3.3, 3.4, 3.5). These results corroborate our previous findings that indicate removal of NAPs from the chromosome does not affect the level of compaction.

3.5 Discussion

The effects of macromolecular crowding on naked DNA molecules in solution have been characterized previously (Vasilevskaya *et al.*, 1995; de Vries, 2001; Pastré *et al.*, 2007). Large DNA molecules are known to collapse in the presence of macromolecular concentrations similar to the concentration of Brij 58 required in these studies to compact fragmented chromosomal DNA, provided the polymer solution also contained an adequate ionic strength to shield the charges between DNA chains. Here we show that Brij 58 is participating in nucleoid preparations not only as a detergent but also as a molecular crowding agent. Because Brij 58 is extensively used in nucleoid preparations we predict that macromolecular crowding plays a more extensive role in nucleoid condensation than previously thought.

In Figure 3.6, we present a model detailing how macromolecular crowding could dominate nucleoid compaction, both *in vivo* and *in vitro* in nucleoid preparations. We propose that chromosomal DNA can be represented as a large polyelectrolyte in solution with macromolecules. Nascent transcripts can be viewed essentially as branches emanating from the DNA polyelectrolyte backbone. These RNA branches increase both the branch density and molecular weight of the polymer. The nucleoids in these studies exist in solution with Brij 58, which acts as a macromolecular crowding agent. Presumably, the Brij 58 molecules decrease the

Figure 3.3 Electron micrographs of *E. coli* nucleoids isolated under low salt conditions. Outline indicates area included in condensed area measurement for analysis.

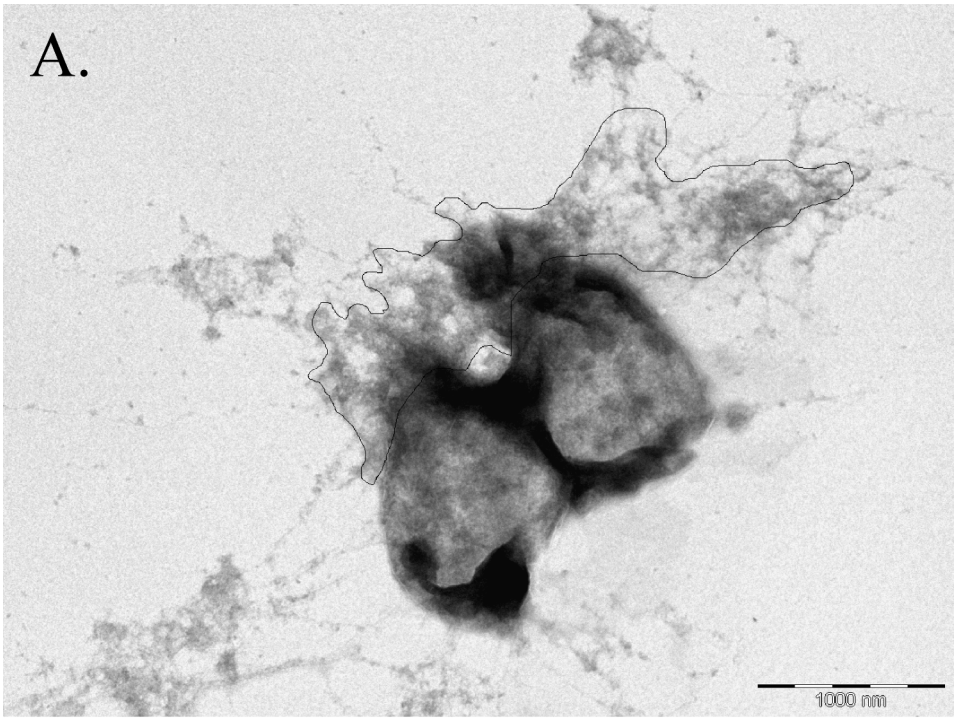
A.
1000 nm

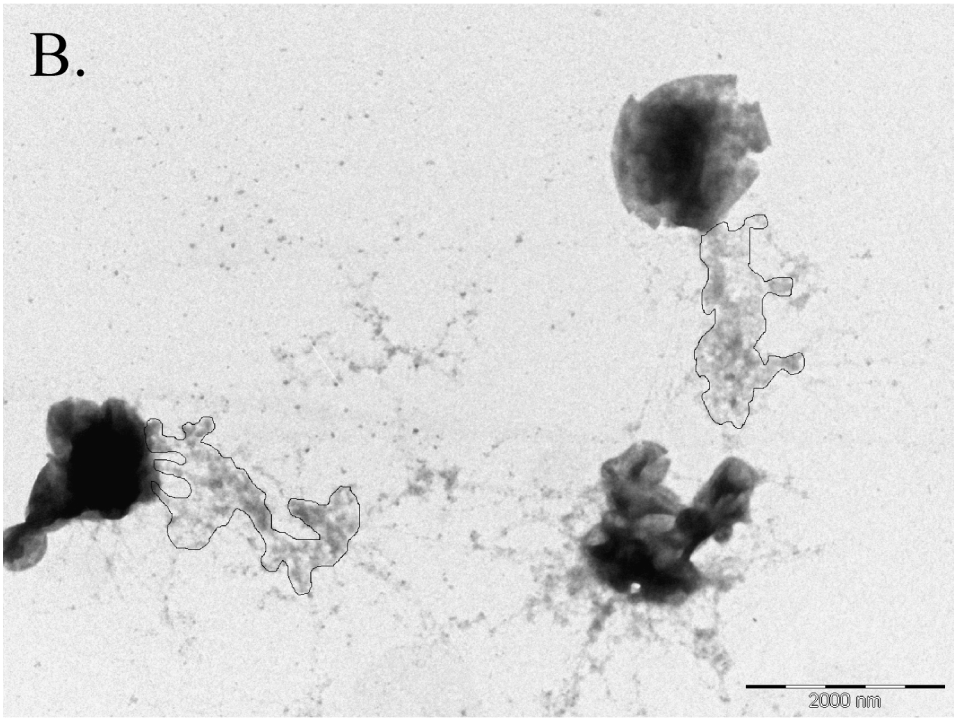
B.
2000 nm

Figure 3.3 Continued

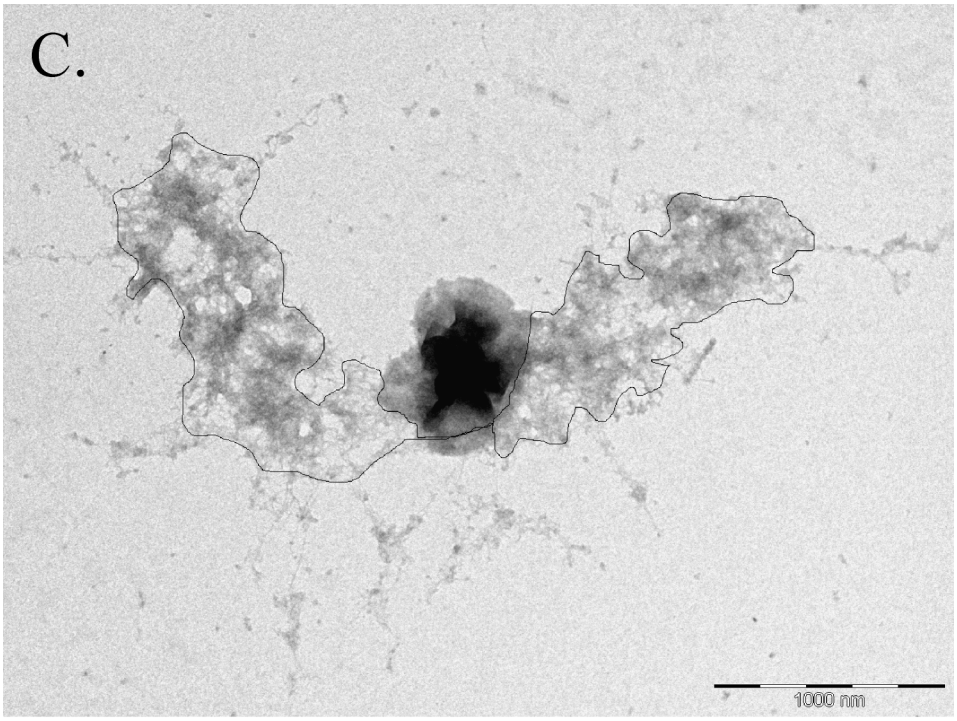

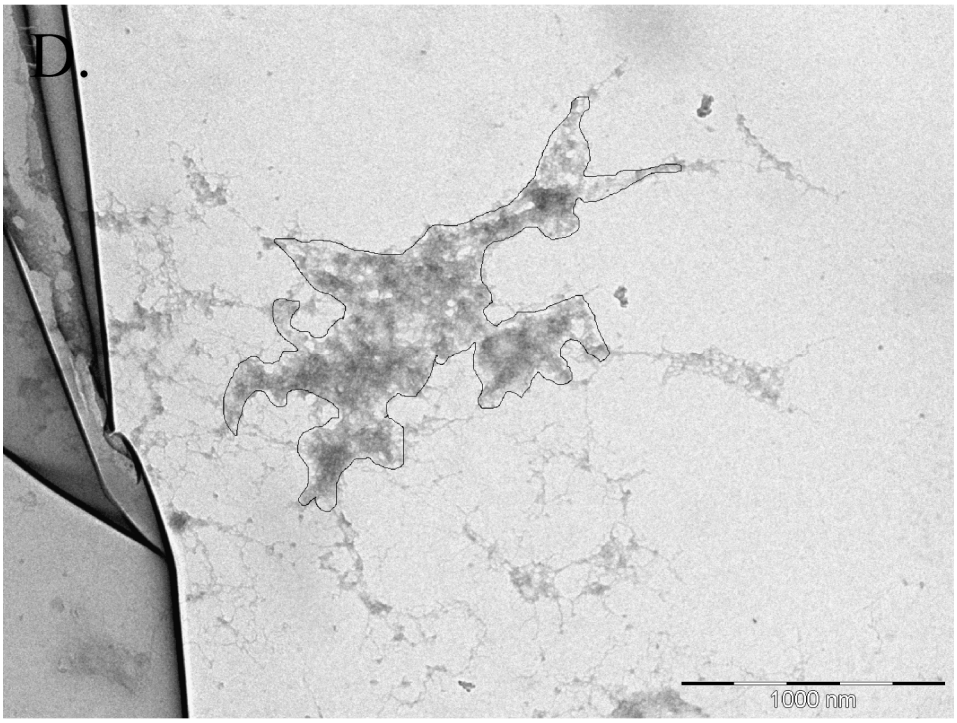

Figure 3.3 Continued

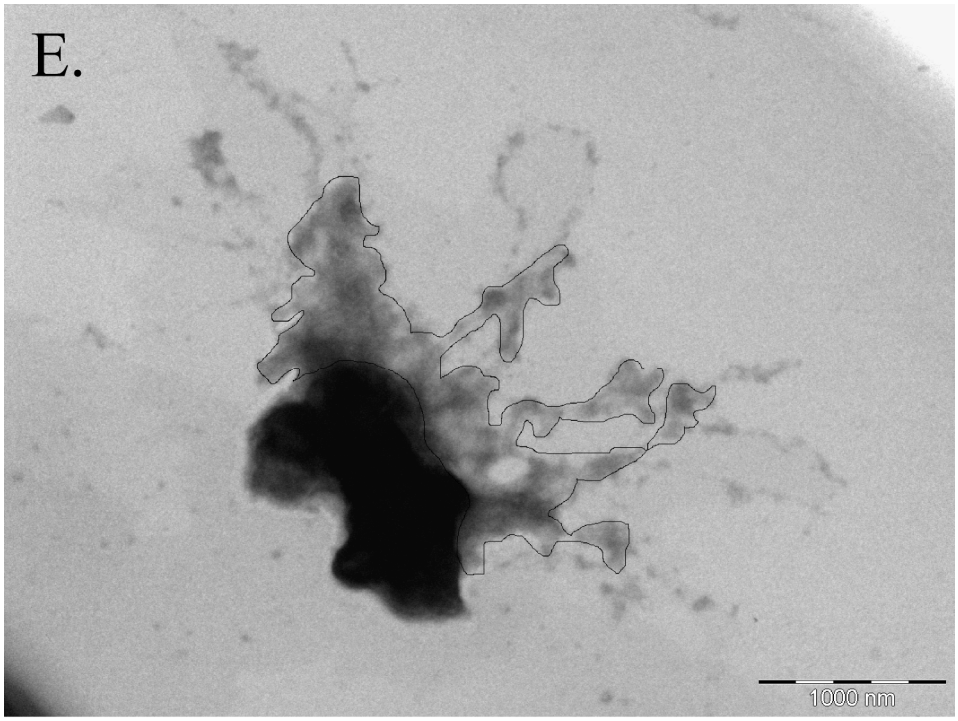

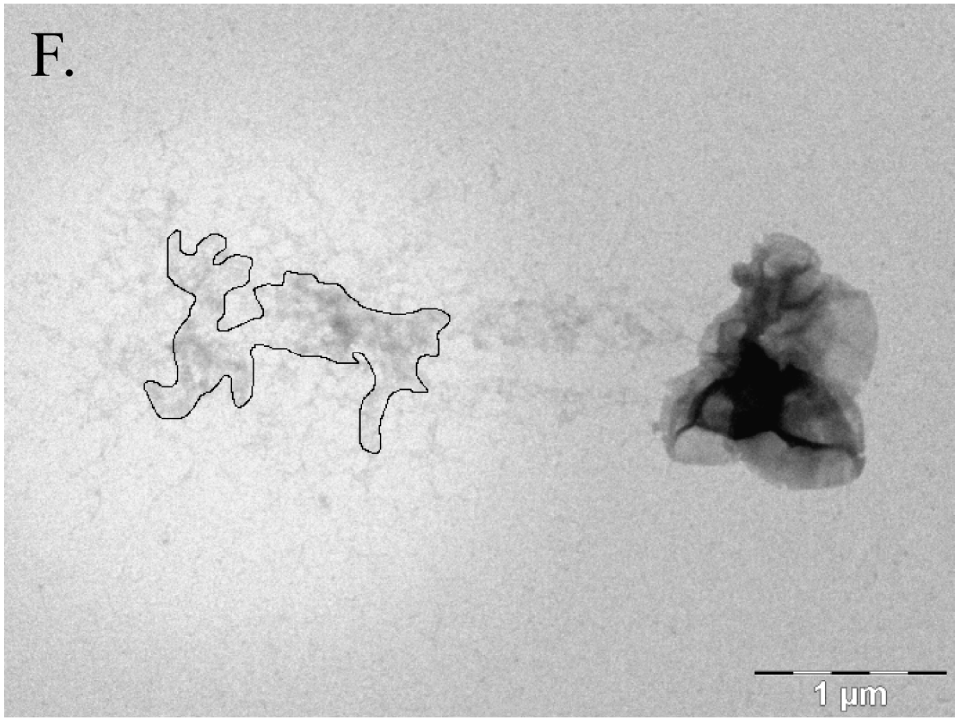

Figure 3.3 Continued

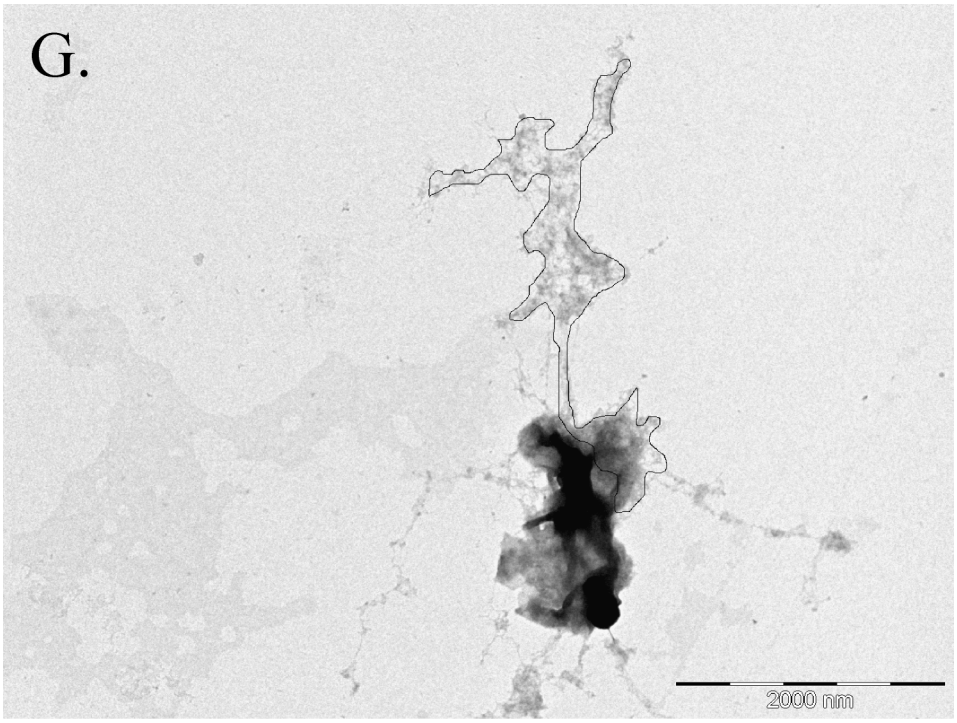

Figure 3.4 Electron micrographs of *E. coli* nucleoids isolated under high salt conditions. Outline indicates area included in condensed area measurement for analysis.

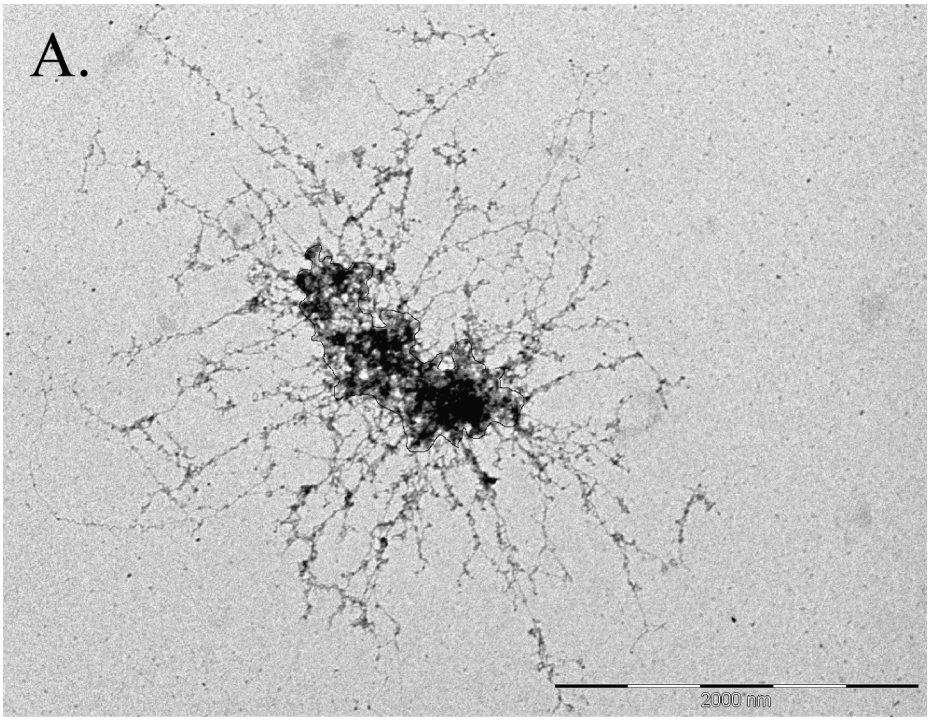
A.
2000 nm

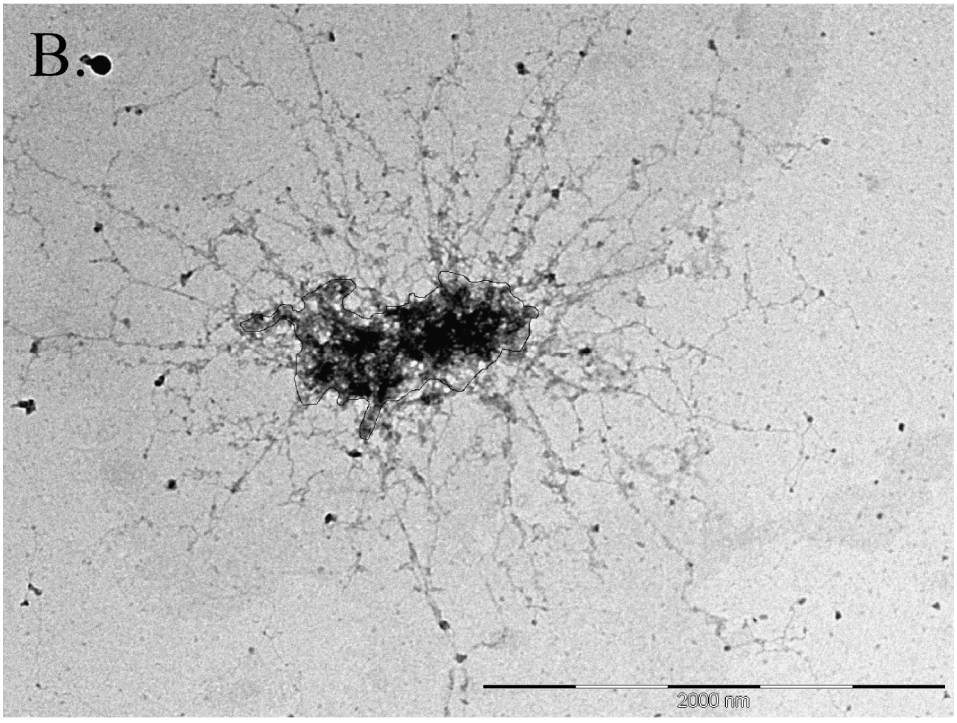
B.
2000 nm

Figure 3.4 Continued

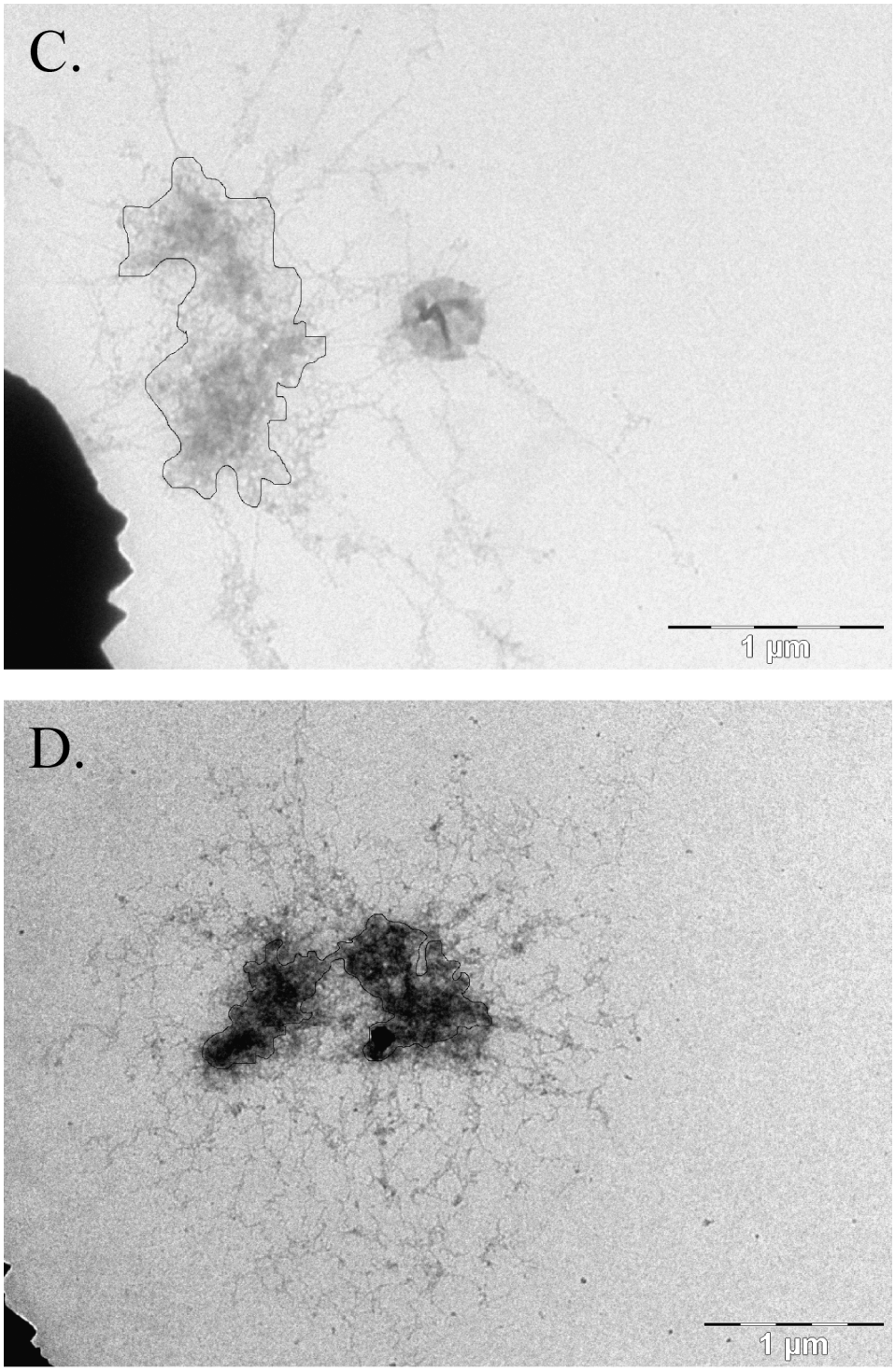

Figure 3.4 Continued

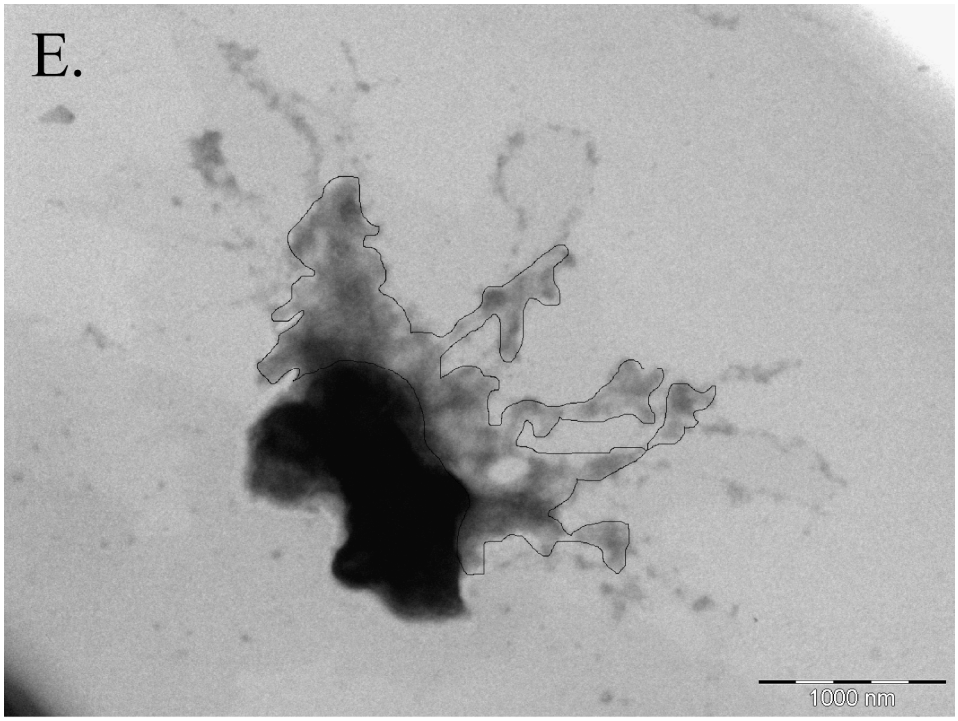

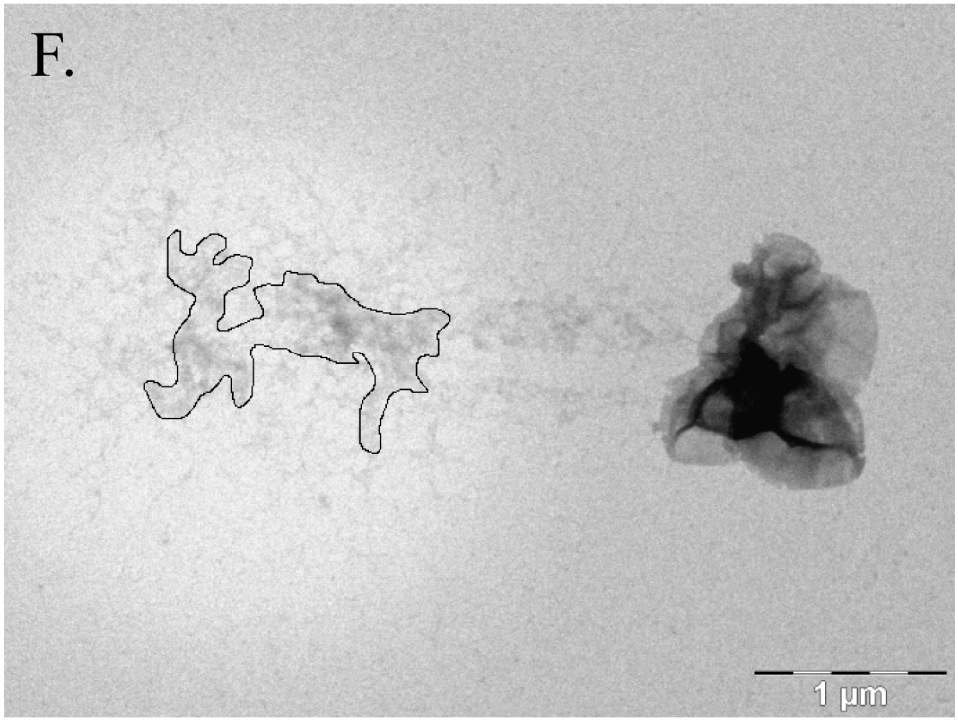

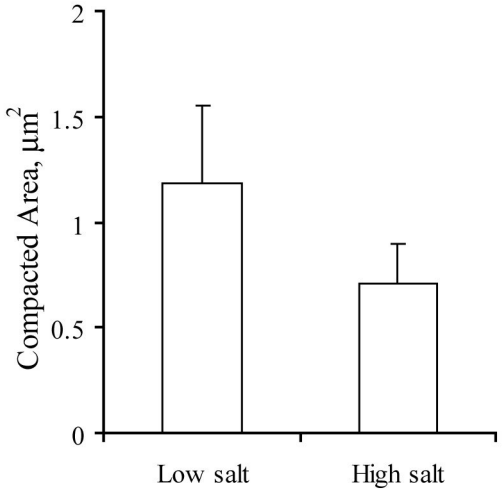

Figure 3.5 Average area of condensed region of isolated nucleoids in electron micrographs. Error bars represent the standard deviation for $n = 8$ and $n = 6$ replicates of low salt and high salt nucleoids, respectively.

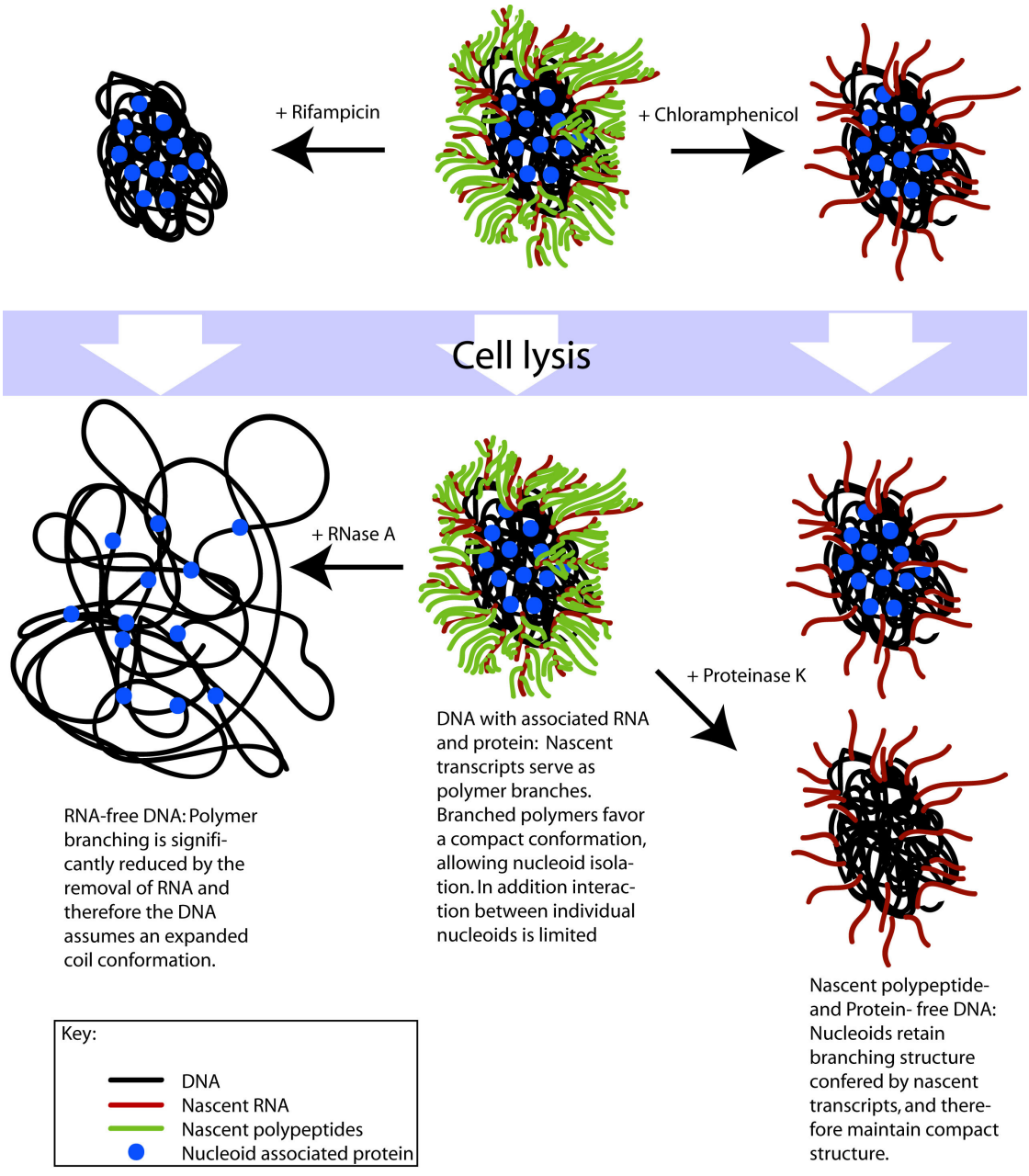

Figure 3.6 Proposed model for bacterial nucleoid compaction and the physical nature of the biochemical compaction forces

solvent quality ($\alpha < 1.0$), therefore the repulsive forces between DNA segments are outweighed by the repulsive forces between the DNA and the solvent. Under these conditions, the DNA assumes a compressed random coil conformation. We would expect native nucleoids and RNA-free nucleoids to interact similarly with the solvent, therefore:

$$\alpha^{Native} \cong \alpha^{RNA-free} \tag{3.4}$$

And:

$$\frac{R_g^{Native}}{R_g^{RNA-free}} \cong \frac{R_{gO}^{Native}}{R_{gO}^{RNA-free}} \tag{3.5}$$

Therefore, we can roughly approximate the theoretical expansion of a polymer due to branch removal. According to our model, the theoretical radius of gyration for our branched polymer (which represents native nucleoids), not accounting for volume interactions, depends on the length and branch density as follows:

$$R_{gO}^{Native} \sim a(N_{DNA+RNA})^{1/4} n^{1/4} \tag{3.6}$$

Where a is the size of a polymer link, $N_{DNA+RNA}$ is the total number of polymer links, and n is the average number of links between branch points. The theoretical radius of gyration for an unperturbed, linear polymer (which represents RNA-free nucleoids) depends on the polymer length as follows:

$$R_{gO}^{RNA-free} \sim a(N_{DNA})^{1/2} \tag{3.7}$$

Combining Equations 3.6 and 3.7, we find:

$$\frac{R_g^{Native}}{R_g^{RNA-free}} \sim \frac{a(N_{DNA+RNA})^{1/4} n^{1/4}}{a(N_{DNA})^{1/2}} = \frac{(N_{DNA+RNA})^{1/4} n^{1/4}}{(N_{DNA})^{1/2}} \tag{3.8}$$

Previously, the persistence length, or length of DNA that behaves as a stiff rod, has been estimated at 50 nm, or approximately 150 basepairs (Grosberg and Khokhlov, 1994). Therefore we represent the *E. coli* nucleoid as a polymer chain with $N_{DNA} \cong$

27,000 links that are a ≅ 50 nm long (4,000,000 base pairs in the *E. coli* genome / 150 base pairs per link). Dworsky and Schaechter estimated that 2.5% of the total RNA remained associated with isolated nucleoids in their preparations; and 90% of the DNA was recovered in the in the nucleoid fraction (Dworsky and Schaechter, 1973). The average mass of DNA and RNA in an exponential *E. coli* cell are 8.8 $x10^{-15}$ g and 58 $x10^{-15}$ g, respectively (Neidhardt and Umbarger, 1996). Based on these data, we estimate the number of links in our branched polymer model:

$$\frac{N_{DNA+RNA}}{N_{DNA}} \approx \frac{m_{DNA+RNA}}{m_{DNA}} \approx \frac{(90\% \cdot 8.8x10^{-15}\, g) + (2.5\% \cdot 58x10^{-15}\, g)}{(90\% \cdot 8.8x10^{-15}\, g)} = 1.2 \qquad (3.9)$$

Where $m_{DNA+RNA}$ is the mass of total DNA and RNA in an average cell and m_{DNA} is the mass of total DNA in an average cell. We estimate the average length of nascent transcripts as 1500 bp or 8.5$x10^{-19}$ g, because rRNA accounts for >50% of transcription in exponential phase cells (Pettijohn *et al.*, 1970) and 16S and 23S rRNAs are 1541 basepairs and 2904 basepairs, respectively. Therefore we estimate the number of branch points in an average *E. coli* nucleoid is 1,700 (mass of RNA / mass of transcript). We estimate the distance between branch points as follows:

$$n = \frac{N_{DNA} \cdot G.E.}{branches} = \frac{27{,}000 \cdot 2.1}{1700} = 33.3 \qquad (3.10)$$

Where N_{DNA} is the number of links in a single *E. coli* chromosome, and *G.E.* is the number of genome equivalents in the average cell (Neidhardt and Umbarger, 1996). Therefore, the ratio between the dependence of the radiuses of gyration for a linear versus branched polymer on polymer length and branch density is:

$$\frac{R_g^{Native}}{R_g^{RNA-free}} \sim \frac{(N_{DNA+RNA})^{1/4} n^{1/4}}{(N_{DNA})^{1/2}} \sim \frac{(1.2 \cdot 27{,}000)^{1/4} \cdot (33.3)^{1/4}}{(27{,}000)^{1/2}} \approx \frac{1}{5} \qquad (3.11)$$

Although this model is greatly simplified, it suggests that the removal of RNA could indeed affect nucleoid compaction. We find the ratio $R_{gO}^{Native} / R_{gO}^{RNA\text{-}free}$ is not sensitive to the value of n, indicating that our rough estimates of transcript size and number can qualitatively predict the polymer behavior. For example, if n is reduced to 5, reflecting approximately a seven fold increase in the number of transcripts, the ratio $R_{gO}^{Native} / R_{gO}^{RNA\text{-}free}$ is 1/8. If the branch density is decreased and the resulting n = 300, $R_{gO}^{Native} / R_{gO}^{RNA\text{-}free}$ increases to 1/3. Consistent with this analysis, the measured ratio of R_g^{Native} to $R_g^{RNA\text{-}free}$ is ~1/2 in these studies (where R_g was calculated from the average area of nucleoid measured in the fluorescent micrographs and the formula Area = πR_g^2).

A strong tendency for highly branched macromolecules to assume a compact state is not unexpected. It has been shown previously that hyperbranched polymers assume a more compact configuration than a homologous linear polymer in solution (Lue, 2000). Indeed, theoretical analysis of polymer behavior in dilute solutions predicts a branched polymer with a high molecular weight (i.e. a large number of links) will assume a compact configuration (Grosberg and Khokhlov, 1994). Furthermore, recently it has been shown using hyperbranched polyethers that the relative polymer compactness increased with increasing branch density (Behera and Ramakrishnan, 2004).

This model accounts for the RNase-sensitive constraint observed in both high- and low-salt nucleoid preparations, since it is known that nascent transcripts remain associated with the DNA under both conditions (Dworsky and Schaechter, 1973; Murphy and Zimmerman, 1997). In addition, our model explains why studies by both Cunha *et al.* and Murphy and Zimmerman found that nucleoids assumed a compact configuration at much lower concentrations of PEG than previously determined for naked DNA molecules (PEG concentrations of ~25 mg/mL versus ~120 mg/mL)

(Cunha *et al.*, 2001; Murphy and Zimmerman, 1997; Vasilevskaya *et al.*, 1995). Our model can also explain seemingly contradictory observations regarding the behavior of chloramphenicol-treated and rifampicin-treated nucleoids. Both treatments remove transertional linkages between the nucleoid and the cell membrane as translation is inhibited by both chemicals. However in chloramphenicol-treated cells the result is strong nucleoid compaction in nucleoid preparations, whereas in rifampicin-treated cells nucleoid decompaction occurs upon lysis. According to our model, a high level of compaction would occur for chloramphenicol-treated nucleoids as the RNA branches remain associated with the DNA while the transertional linkages are removed. On the other hand, RNA branches are removed from rifampicin-treated nucleoids which would allow a more dispersed configuration of the DNA in dilute polymer solutions, consistent with our model. Finally, we note that Zimmerman and Murphy were able to recover compact nucleoids from rifampicin-treated cells using a modified nucleoid preparation procedure that included 1 mg polylysine/mL in the preparation solution (Zimmerman and Murphy, 2001). Because polylysine would increase the macromolecular crowding forces in solution as well as partially neutralize repulsive forces between DNA chains, our model would predict that the addition of polylysine would decrease the critical concentration of Brij 58 needed to induce RNA-free nucleoid compaction.

Our model argues against a role for NAPs in nucleoid compaction as we hypothesize that the branching structure of actively transcribing chromosomes would provide a strong compaction force. This is supported by our results that chloramphenicol-treated and proteinase K-treated nucleoids behave similarly to native nucleoids in regard to macromolecular crowding-mediated compaction. In addition, if the NAPs were providing some compaction force, one would expect a partial decompaction upon removal of these proteins in a high-salt nucleoid preparation. Our

results show no statistically significant difference in the sizes of nucleoids prepared using high- versus low-salt isolation procedures. These data corroborate previous evidence indicating NAPs do not induce DNA compaction (Zimmerman, 2006). The high levels of NAPs associated with chromosomal DNA *in vivo* and the fact that their concentrations are altered during different phases of cell growth suggest the proteins may be performing some physiological function. Several studies have shown that upon compaction naked DNA assumes a conformation inaccessible to restriction endonucleases (Oana *et al.*, 2002; Pingoud *et al.*, 1984). It is conceivable that NAPs prevent these inaccessible conformations *in vivo* ensuring chromosome accessibility throughout the cell cycle.

In conclusion, we propose that alterations to the branch density of the chromosome by RNA removal can adequately explain the previously observed RNase-sensitive constraint. The fact that nucleoid condensation in bacterial cells appears to be dominated by the physical characteristics of the structure of the DNA indicates that proper condensation of chromosomes should be easily achieved in organisms using synthetic chromosomes.

REFERENCES

Baeza, I., Gariglio, P., Rangel, L. M., Chavez, P., Cervantes, L., Arguello, C., Wong, C. & Montanez, C. (1987). Electron-Microscopy and Biochemical-Properties of Polyamine-Compacted DNA. *Biochemistry* **26**(20), 6387-6392.

Behera, G. C. & Ramakrishnan, S. (2004). Controlled variation of Spacer segment in hyperbranched polymers: From densely branched to lightly branched systems. *Macromolecules* **37**(26), 9814-9820.

Boles, T. C., White, J. H. & Cozzarelli, N. R. (1990). Structure of Plectonemically Supercoiled DNA. *Journal of Molecular Biology* **213**(4), 931-951.

Brunetti, R., Prosseda, G., Beghetto, E., Colonna, B. & Micheli, G. (2001). The looped domain organization of the nucleoid in histone-like protein defective *Escherichia coli* strains. *Biochimie* **83**(9), 873-882.

Cunha, S., Woldringh, C. L. & Odijk, T. (2001). Polymer-mediated compaction and internal dynamics of isolated *Escherichia coli* nucleoids. *Journal of Structural Biology* **136**(1), 53-66.

Dame, R. T. (2005). The role of nucleoid-associated proteins in the organization and compaction of bacterial chromatin. *Molecular Microbiology* **56**(4), 858-870.

de Vries, R. (2001). Flexible polymer-induced condensation and bundle formation of DNA and F-actin filaments. *Biophysical Journal* **80**(3), 1186-1194.

Dworsky, P. & Schaechter, M. (1973). Effect of Rifampin on the Structure and Membrane Attachment of the Nucleoid of *Escherichia coli*. *Journal of Bacteriology* **116**, 1364-1374.

Dworsky, P. (1975). Unfolding of Chromosome of *Escherichia-Coli* after Treatment with Rifampicin. *Zeitschrift Fur Allgemeine Mikrobiologie* **15**(4), 243-247.

Flory, P. (1953). *Principles of Polymer Chemistry*, Cornell University Press, Ithaca, New York.

Frisch, H. L. & Fesciyan, S. (1979). DNA Phase Transitions - Psi Transition of Single Coils. *Journal of Polymer Science Part C-Polymer Letters* **17**(5), 309-315.

Grosberg, A. Y. & Khokhlov, A. R. (1994). *Statistical physics of macromolecules*. Trans. Atanov, Y. A. AIP Series in Polymers and Complex Materials (Larson, R. & Pincus, P. A., Eds.), AIP Press, Woodbury, NY.

Johnson, R. C., Johnson, L. M., Schmidt, J. W. & Gardner, J. F. (2005). Major nucleoid proteins in the structure and function of the *Escherichia coli* chromosome. In

The bacterial chromosome (Higgins, N. P., ed.), pp. 65-132. ASM Press, Washington, D. C.

Kornberg, T., Lockwood, A. & Worcel, A. (1974). Replication of the *Escherichia coli* chromosome with a soluble enzyme system. *Proceedings of the National Academy of Sciences* **71**(8), 3189-3193.

Lue, L. (2000). Volumetric behavior of athermal dendritic polymers: Monte Carlo simulation. *Macromolecules* **33**(6), 2266-2272.

Murphy, L. D. & Zimmerman, S. B. (1994). Macromolecular Crowding Effects on the Interaction of DNA with *Escherichia-Coli* DNA-Binding Proteins - a Model for Bacterial Nucleoid Stabilization. *Biochimica Et Biophysica Acta-Gene Structure and Expression* **1219**(2), 277-284.

Murphy, L. D. & Zimmerman, S. B. (1997). Isolation and characterization of spermidine nucleoids from *Escherichia coli*. *Journal of Structural Biology* **119**(3), 321-335.

Murphy, L. D. & Zimmerman, S. B. (2000). Multiple restraints to the unfolding of spermidine nucleoids from *Escherichia coli*. *Journal of Structural Biology* **132**(1), 46-62.

Murphy, L. D. & Zimmerman, S. B. (2002). Hypothesis: the RNase-sensitive restraint to unfolding of spermidine nucleoids from *Escherichia coli* is composed of cotranslational insertion linkages. *Biophysical Chemistry* **101**, 321-331.

Neidhardt, F. C. & Umbarger, H. E. (1996). Chemical Composition of *Escherichia coli*. In *Escherichia coli and Salmonella: Cellular and Molecular Biology* (Neidhardt, F. C., ed.), Vol. I, pp. 13-16. II vols. ASM Press, Washington, D. C.

Oana, H., Tsumoto, K., Yoshikawa, Y. & Yoshikawa, K. (2002). Folding transition of large DNA completely inhibits the action of a restriction endonuclease as revealed by single-chain observation. *Febs Letters* **530**(1-3), 143-146.

Pastré, D., Hamon, L., Mechulam, A., Sorel, I., Baconnais, S., Curmi, P. A., Le Cam, E. & Pietrement, O. (2007). Atomic force microscopy imaging of DNA under macromolecular crowding conditions. *Biomacromolecules* **8**(12), 3712-3717.

Pelta, J., Livolant, F. & Sikorav, J. L. (1996). DNA aggregation induced by polyamines and cobalthexamine. *Journal of Biological Chemistry* **271**(10), 5656-5662.

Pettijohn, D. E., Stonington, O. G. & Kossman, C. R. (1970). Chain termination of ribosomal RNA synthesis *in vitro*. *Nature* **228**, 235-239.

Pettijohn, D. E., Clarkson, K., Kossman, C. R. & Stonington, O. G. (1970). Synthesis of ribosomal RNA on a protein-DNA complex isolated from bacteria: a comparison of

ribosomal RNA synthesis *in vitro* and *in vivo*. *Journal of Molecular Biology* **52**, 281-300.

Pettijohn, D. E. (1996). The Nucleoid. In *Escherichia coli and Salmonella:cellular and molecular biology* (Neidhardt, F. C., ed.), Vol. 1, pp. 158-166. 2 vols. ASM Press, Washington D. C.

Pingoud, A., Urbanke, C., Alves, J., Ehbrecht, H.-J., Zabeau, M. & Gualerzig, C. (1984). Effect of polyamines and basic proteins on cleavage of DNA by restriction endonucleases. *Biochemistry* **23**, 5697-5703.

Postow, L., Hardy, C. D., Arsuaga, J. & Cozzarelli, N. R. (2004). Topological domain structure of the *Escherichia coli* chromosome. *Genes and Development* **18**, 1766-1779.

Roberts, R. B., Abelson, P. H., Cowie, D. B., Boulton, E. T. & Britten, R. J. (1955). *Studies of Biosynthesis in Escherichia coli*, Carnegie Institute of Washington, Washington, D. C.

Stonington, O. & Pettijohn, D. (1971). Folded Genome of *Escherichia-Coli* Isolated in a Protein-DNA-Rna Complex. *Proceedings of the National Academy of Sciences of the United States of America* **68**(1), 6-&.

Tsumoto, K., Luckel, F. & Yoshikawa, K. (2003). Giant DNA molecules exhibit on/off switching of transcriptional activity through conformational transition. *Biophysical Chemistry* **106**(1), 23-29.

Vasilevskaya, V. V., Khokhlov, A. R., Matsuzawa, Y. & Yoshikawa, K. (1995). Collapse of Single DNA Molecule in Poly(Ethylene Glycol) Solutions. *Journal of Chemical Physics* **102**(16), 6595-6602.

Woldringh, C. L., Jensen, P. R. & Westerhoff, H. V. (1995). Structure and partitioning of bacterial DNA: determined by a balance of compaction and expansion forces? *FEMS Microbiology Letters* **131**(3), 235-242.

Yoshikawa, K., Takahashi, M., Vasilevskaya, V. V. & Khokhlov, A. R. (1996). Large discrete transition in a single DNA molecule appears continuous in the ensemble. *Physical Review Letters* **76**(16), 3029-3031.

Zimmerman, S. B. & Murphy, L. D. (2001). Release of compact nucleoids with characteristic shapes from *Escherichia coli*. *Journal of Bacteriology* **183**(17), 5041-5049.

Zimmerman, S. B. (2006). Cooperative transitions of isolated *Escherichia coli* nucleoids: Implications for the nucleoid as a cellular phase. *Journal of Structural Biology* **153**, 160-175.

CHAPTER 4

CONCLUSIONS AND FUTURE DIRECTIONS

The design and construction of a synthetic genome is a major step in the eventual development of a biotechnologically relevant, synthetic organism. Efforts are currently underway to define the minimal gene set necessary for life; however the physical structure and organization of the genome may also play a significant role in genome function. Using *Escherichia coli* as a model, this dissertation investigates whether the organization of genes with respect to the cell division cycle and the physical conformation of the compacted chromosome are important factors to consider for synthetic genome design.

In Chapter 2, we presented evidence that both the chromosomal location of a gene and its function can affect transcript levels during the *E. coli* cell cycle. The cell cycle for all organisms involves mass doubling, chromosome replication and segregation, and cell division. In bacteria, DNA replication forks change local DNA structure by increasing positive supercoiling in front of the replication fork and dislodging DNA-associated proteins, including the transcriptional machinery. We hypothesized that transcript levels for some genes are affected by the bacterial cell cycle and for this reason the cell cycle is an important factor to consider when designing synthetic bacterial genomes. To test this hypothesis, transcripts were measured for 58 model genes that were located at different physical positions on the *E. coli* chromosome at several points during the cell cycle. We found dynamic transcript levels correlated with the cell cycle for 10 genes (17% of those measured). Two patterns were seen for genes with dynamic transcript levels: increased transcript concentrations following gene replication, and increased transcript concentration prior

to replication initiation. These results showed that both the physical gene position and the physiological function of a gene affect when a gene is transcribed. In conclusion, gene position, with regard to the C period, and gene function are important factors to incorporate into design criteria for synthetic bacterial genomes.

In these studies, transcription of only a subset of the total number of genes measured was affected by replication fork progression. We were unable to identify genetic markers that distinguish these genes from those that are unaffected by the replication cycle, however this could be due to the relatively small number of genes analyzed in these studies (58 of ~4000 *E. coli* genes). Future studies to analyze transcript levels throughout the cell division cycle using full genome microarrays would provide a more extensive list of genes with cell cycle-related fluctuations in transcript levels. In addition, to more clearly elucidate cell cycle-related fluctuations, the cells could be grown with an extended cell cycle (i.e. with doubling times ~150 minutes as opposed to 44 minutes). However, an inherent limitation of the membrane elution synchronization method employed in these studies is that only a small population of synchronous cells can be collected (~10^8 cells). This constraint would be exacerbated by increasing the cell doubling time because fewer cells would divide during a specific time interval. To overcome this limitation, Bates *et al*. recently developed a new synchronization method based on the membrane-elution technique: the baby cell column (Bates *et al*., 2005). Using this technique, the authors were able to achieve cell concentrations in eluant cultures that were 10-fold higher than the original membrane-elution technique. A similar approach may facilitate a more detailed study of cell cycle-related transcription in *E. coli*.

The results from Chapter 2 indicate that the replication cycle affects transcription of some genes. In particular, the transcription of some genes increases due to their replication. We hypothesize that this is due to the movement of the

replication fork through the chromosomal region. To test this, the chromosomal position of a gene exhibiting cell cycle related changes in transcript levels (detected in these studies) could be swapped with a gene showing no cell cycle dependence such as *rpoA*. The transcript levels for the two genes could then be evaluated throughout the cell cycle. This experiment would clearly show whether replication fork progression is affecting gene transcription. We would expect that the maximum transcript level for the gene showing cell cycle related transcription would shift to immediately following replication of its new chromosomal region. It would also be interesting to determine whether transcript fluctuations result from changes in chromosomal accessibility due to structural changes induced by replication fork progression. It is known that the DNA replication fork temporarily removes all DNA-associated proteins while the replication machinery passes (Humphery-Smith, 1999, French, 1992), and this could serve to 'reset' the genome. We hypothesize that replication fork movement through the genome facilitates a quicker change to gene expression level in response to environmental stimuli. To evaluate whether changes in DNA accessibility occur due to replication, the induction of a model gene (e.g. *lacZ*) could be evaluated in wild type *E. coli* and a replication initiation deficient temperature sensitive mutant strain. One would anticipate a change in genome accessibility due to replication processes would be manifested as a lower level of induction for the replication deficient strain, as the subset of cells with inaccessible *lacZ* genes (therefore not induced) would not be reset by the replication fork. These experiments would require the optimization of inducer concentration and the length of incubation as both replicating and non-replicating cells would be expected to reach an equilibrium induction level at long times. In addition, the replication-deficient strain and wild-type strain should originate from the same parent strain to ensure that differences in inducer transport into the cell that may exist between strains do not affect expression levels.

The physical conformation of the chromosome may also affect the accessibility of chromosomal DNA to transcriptional machinery. In Chapter 3, we investigated the nature and contribution of RNA- and protein-based forces to nucleoid compaction in *Escherichia coli*. We presented evidence that Brij 58, a detergent used extensively in *E. coli* nucleoid preparations, also serves a previously unrecognized role as a macromolecular crowding agent in these preparations. The removal of RNA from the nucleoid either *in vivo* or following cell lysis resulted in reduced Brij 58-dependent nucleoid compaction. We proposed that nucleoid-associated RNA increases the branching density of the chromosomal DNA, and that the removal of RNA changed the nucleoid macromolecular structure and its interactions with the Brij 58 molecules. These changes resulted in DNA decompaction in nucleoid preparations. In addition, we showed that native and protein-free nucleoids behaved similarly with respect to changes in macromolecular crowding, indicating that the contribution of nucleoid-associated proteins (NAPs) to nucleoid compaction is small when compared to macromolecular crowding effects. We concluded that nucleoid condensation in bacterial cells appears to be dominated by the physical characteristics of the structure of the DNA. These results indicate that proper condensation of chromosomes should be readily achieved in organisms using synthetic chromosomes.

Our results indicated that NAPs are not involved in chromosomal compaction. However, NAPs are bound in a sequence independent manner to ~20% of the chromosomal DNA *in vivo* (Johnson *et al.*, 2005), indicating that the proteins are providing some physiologically relevant structure to the genome. Notably, several studies show that naked DNA is rendered inaccessible to restriction endonucleases and transcriptional machinery by macromolecular- or polyamine-mediated compaction (Yamada *et al.*, 2005; Tsumoto *et al.*, 2003; Oana *et al.*, 2002; Pingoud *et al.*, 1984). These studies showed that in the presence of a low concentration of spermidine,

spermine, putrescine or a polyethylene glycol, naked DNA assumed an expanded conformation and was susceptible to restriction endonuclease cleavage. When the concentration of these agents was increased past a critical value, the DNA assumed a compact globule conformation, and became resistant to cleavage by restriction endonucleases. Peter *et al.* and Postow *et al.* showed that compacted chromosomal DNA is susceptible to restriction endonucleases *in vivo* (Peter *et al.*, 2004; Postow *et al.*, 2004), indicating that DNA compaction within the bacterial cell is physically distinct from compacted, naked DNA *in vitro*. It is plausible that NAPs associated with bacterial chromosomes serve to prevent complete compaction of the DNA via physical forces, thereby ensuring the chromosome remains in a transcriptionally accessible state. To investigate this phenomenon, studies that evaluate the accessibility of restriction sites within native and protein-free nucleoids to rare-cutting restriction endonucleases should be performed. If the NAPs do in fact serve to prevent inaccessible conformations, the protein-free nucleoids would be poorly digested compared to native nucleoids. Critically, temperature is known to affect branched polymer compaction in solutions of macromolecules (Gauthier *et al.* 1998), therefore the temperature at which these studies are performed should be carefully considered. Ideally, experiments would be performed over the range of temperatures at which *E. coli* growth is supported. We reason that if the NAPs act to increase chromosomal accessibility, then this activity should be observed over a wide range of temperatures.

Preliminary experiments to observe the accessibility of cut sites for rare-cutting restriction endonucleases were performed and are described in Appendix A. Unexpectedly, results indicated that the NAPs may protect certain regions of the chromosome from digestion by restriction endonucleases because chloramphenicol and proteinase K-treated nucleoids exhibited higher susceptibility to restriction endonucleases. If this is the case, chromosome accessibility studies performed with

mutant *E. coli* strains for each NAP may yield insights regarding the role of each protein in maintaining the structure or stability of the *E. coli* chromosome. It is also possible that nucleoid preparations do not accurately model the physical state of the chromosome *in vivo.* Digestion of chromosomal DNA *in vivo* using a restriction endonuclease expressed *in vivo* from a plasmid, similar to Peter *et al.*'s approach, would elucidate whether nucleoid preparations are an adequate model of nucleoid behavior *in vivo.*

Finally, we note that Cunha *et al.* failed to observe a coil to globule transition upon compaction for osmotically-released nucleoids (Cunha *et al.*, 2001). A coil to globule transition is observed for naked DNA compacted by macromolecular crowding (Kojima *et al.*, 2006; Yoshikawa *et al.*, 1996; Vasilevskaya *et al.*, 1995), indicating the nucleoid contains some component that prevents this behavior. As noted earlier, compacted *E. coli* nucleoid DNA differs from compacted naked DNA in its accessibility to restriction endonucleases and transcriptional machinery, and the coil-globule transition may reflect this difference. To more clearly understand the factors affecting the nucleoid's compaction behavior, and possibly elucidate how bacterial cells maintain transcriptionally-active chromosomes, the contributions of RNA, NAPs, and polyamines to the coil to globule transition behavior of both naked DNA and nucleoid preparations could be evaluated using fluorescent microscopy as described in Chapter 3. It may be that the physical characteristics of the bacterial chromosome maintain the DNA in an inherently accessible state, thereby eliminating the need for mechanisms that are common in eukaryotic systems. It is worth noting that the maximum resolution of a fluorescent microscope is ~0.5 μm. Because compact bacterial nucleoids approach this limit, a large number of replicates may be required to determine whether a coil to globule transition is observed as the precision of individual measurements will be limited, and therefore may blur the boundary

between the coil and globule state.

Several recent studies investigating the transcriptional effects of alterations to nucleoid structure indicate that structural properties may not be merely affecting gene expression, but regulating transcription. In addition to the work described in Chapter 3, we performed additional experiments to determine whether a correlation exists between the physical location of a gene with respect to the remainder of the bacterial nucleoid and transcription of that gene. To do this, we attempted to use electron microscopy *in situ* hybridization (EMISH) techniques to evaluate nucleoid structural changes, specifically to determine whether the average physical position of a gene with respect to the remainder of the compacted nucleoid was relocated due to a change in transcriptional activity.

Although the procedure for EMISH was standardized for eukaryotic metaphase chromosomes (Narayanswami and Hamkalo, 1991; Narayanswami and Hamkalo, 1994), it has never been applied to bacterial chromatin. In this work, we attempted to adapt Narayanswami and Hamkalo's technique to isolated bacterial nucleoids. We obtained grids with adsorbed chromosomal DNA. We were unable to identify experimental conditions that would preserve bacterial nucleoid attachment to the TEM grids while minimizing non-specific adsorption of probe and competitor DNA to the grids. Significantly, the size of the bacterial chromosome (4.6 Mb) is a fraction of the size of the mouse metaphase chromosomes used in previous EMISH studies (~60 – 200 Mb). The EMISH procedure for eukaryotic chromosomes utilized the broadly different sizes of eukaryotic chromosomal and probe DNA molecules to achieve different effects on the DNA molecules during the washes. Due to the small size of the bacterial chromosome, a method to chemically crosslink the chromosomal DNA to the grids may be necessary prior to hybridization of probe DNA. The EMISH procedure contained a glutaraldehyde-fixing step. However, because glutaraldehyde chemically

crosslinks proteins, it may be less effective for bacterial chromosomes where the protein content is significantly lower than eukaryotic chromosomes.

A second obstacle encountered in these studies was the low adsorption density of chromosomes to the TEM grids (approximately 1-2 nucleoids per grid). A carbon layer was deposited on the grid immediately prior to nucleoid attachment to maximize the layer's hydrophilicity. Exposure of carbon layer to water or humidity induced a chemical rearrangement of the carbon atoms resulting in a more hydrophobic layer. Because the nucleoid preparation was in an aqueous solution, this hydrophilic to hydrophobic conversion may be accelerated during adsorption, which may have limited the adsorption of nucleoids to the grid, as a hydrophilic layer is required. The development of a grid coating that can be easily converted from hydrophilic to hydrophobic by a simple but controllable process would enable longer nucleoid adsorption times and therefore could potentially raise the nucleoid adsorption density.

REFERENCES

Bates, D., Epstein, J., Boye, E., Fahrner, K., Berg, H. & Kleckner, N. (2005). The Escherichia coli baby cell column: a novel cell synchronization method provides new insight into the bacterial cell cycle. *Molecular Microbiology* **57**(2), 380-391.

Cunha, S., Woldringh, C. L. & Odijk, T. (2001). Polymer-mediated compaction and internal dynamics of isolated Escherichia coli nucleoids. *Journal of Structural Biology* **136**(1), 53-66.

Humphery-Smith, I. (1999). Replication-induced protein synthesis and its importance to proteomics. *Electrophoresis* **20**(4-5), 653-659.

French, S. (1992). Consequences of replication fork movement through transcription units *in vivo*. *Science* **258**, 1362-1365.

Gauthier, M., Chung, J., Choi, L. & Nguyen, T. T. (1998). Second Virial Coefficient of Arborescent Polystyrenes and Its Temperature Dependence. *Journal of Physical Chemistry B* **102**, 3138-3142.

Johnson, R. C., Johnson, L. M., Schmidt, J. W. & Gardner, J. F. (2005). Major nucleoid proteins in the structure and function of the *Escherichia coli* chromosome. In *The bacterial chromosome* (Higgins, N. P., ed.), pp. 65-132. ASM Press, Washington, D. C.

Kojima, M., Kubo, K. & Yoshikawa, K. (2006). Elongation/compaction of giant DNA caused by depletion interaction with a flexible polymer. *Journal of Chemical Physics* **124**(2).

Narayanswami, S. & Hamkalo, B. (1991). DNA sequence mapping using electron microscopy. *Genetic Analysis--Biomolecular Engineering* **8**(1), 14-23.

Narayanswami, S. & Hamkalo, B. (1994). Electron microscopic localization of *in situ* hybrids. In *Methods in MOlecular Biology Volume 29: Chromosome analysis protocols* (Gosden, J. R., ed.), Vol. 29, pp. 335-351. Humana Press, Inc., Totowa, New Jersey.

Oana, H., Tsumoto, K., Yoshikawa, Y. & Yoshikawa, K. (2002). Folding transition of large DNA completely inhibits the action of a restriction endonuclease as revealed by single-chain observation. *Febs Letters* **530**(1-3), 143-146.

Peter, B. J., Arsuaga, J., Breier, A. M., Khodursky, A. B., Brown, P. O. & Cozzarelli, N. R. (2004). Genomic trascriptional response to loss of chromosomal supercoiling in Escherichia coli. *Genome Biology* **5**, R87.

Pingoud, A., Urbanke, C., Alves, J., Ehbrecht, H.-J., Zabeau, M. & Gualerzig, C.

(1984). Effect of polyamines and basic proteins on cleavage of DNA by restriction endonucleases. *Biochemistry* **23**, 5697-5703.

Postow, L., Hardy, C. D., Arsuaga, J. & Cozzarelli, N. R. (2004). Topological domain structure of the Escherichia coli chromosome. *Genes and Development* **18**, 1766-1779.

Tsumoto, K., Luckel, F. & Yoshikawa, K. (2003). Giant DNA molecules exhibit on/off switching of transcriptional activity through conformational transition. *Biophysical Chemistry* **106**(1), 23-29.

Vasilevskaya, V. V., Khokhlov, A. R., Matsuzawa, Y. & Yoshikawa, K. (1995). Collapse of Single DNA Molecule in Poly(Ethylene Glycol) Solutions. *Journal of Chemical Physics* **102**(16), 6595-6602.

Yoshikawa, K., Takahashi, M., Vasilevskaya, V. V. & Khokhlov, A. R. (1996). Large discrete transition in a single DNA molecule appears continuous in the ensemble. *Physical Review Letters* **76**(16), 3029-3031.

APPENDIX A

STRUCTURAL STUDIES OF THE *ESCHERICHIA COLI* NUCLEOID WITH ELECTRON MICROSCOPY *IN SITU* HYBRIDIZATION

A.1 Abstract

We hypothesize that the physical structure of the bacterial nucleoid (the *in vivo*, compacted chromosome and associated proteins and RNA) serves as a global transcriptional regulator. The goal of this work was to determine whether a correlation exists between the physical location of a gene with respect to the remainder of the bacterial nucleoid and transcription of that gene. To do this, we used electron microscopy *in situ* hybridization (EMISH) and chromosomal restriction mapping techniques to evaluate nucleoid structural changes resulting from alterations in specific and global transcription profiles. We were unable to detect whether transcriptionally-related structural changes to the *Escherichia coli* nucleoid exist due to experimental limitations.

A.2 Introduction

Traditionally, the bacterial nucleoid has been viewed largely as a ball of highly condensed DNA with only local organization (i.e. operons). However, recent studies have shown the bacterial nucleoid is spatially and temporally organized (Niki *et al.*, 2000; Viollier *et al.*, 2004). Because it has been known for some time that transcription is affected by the structural constraints of the nucleoid (Ryter and Chang, 1975; Brewer, 1990; Claverie-Martin and Magasanik, 1991; Rabin *et al.*, 1992; Wang

and Lynch, 1996), results indicating a dynamic nucleoid structure have triggered a renewed interest in the physical structure of the bacterial nucleoid and the possible factors affecting nucleoid structure. Several recent studies investigating the transcriptional effects of alterations to nucleoid structure indicate that structural properties may not be merely affecting gene expression, but regulating transcription. Peter *et al*. found that altering the local supercoiling density of chromosomal regions affected the transcription of several stress-related genes throughout the chromosome (Peter *et al.*, 2004). In another study, Jeong *et al.* identified three levels of spatial correlations of gene expression corresponding to intergenic distances up to 16 kb, over 100-125 kb and over 600-800 kb (Jeong *et al.*, 2004). Kèpés found that regulator-encoding cistrons tended to be periodically spaced from their targets and target genes with the same regulator tended to be distributed periodically (Kèpés, 2004). Similarly, Carpentier *et al.* found that *Bacillus subtilis* and *E. coli* genes were positively or negatively correlated to changes in the expression of other genes positioned at well-defined intervals from the gene, indicating that a structured packing of the nucleoid may be a general property of the prokaryotic nucleoid (Carpentier *et al.*, 2005). Together, these results imply a three-dimensional topological structure that allows clustering of regulators and targets.

In spite of recent evidence that transcription is affected and possibly regulated by nucleoid structure, few studies have been designed to observe the phenomenon directly. Notably, a study that examined the transcriptional effects of a mutant HU protein with increased chromosomal binding affinity found the mutant protein caused a dense condensation of the nucleoid, accompanied by a shift in transcriptional profiles that increased expression of several repressed genes in wild type cells and repressed several constitutive housekeeping genes. These changes resulted in radical changes in cell morphology, physiology and metabolism, providing direct evidence

that nucleoid structure affects global transcription profiles (Kar *et al.*, 2005).

We hypothesize the bacterial nucleoid structure serves as a global transcriptional regulator. More specifically, we suggest that genes are located in the peripheral or compacted regions of the nucleoid at specific times throughout the replication cycle, and a dynamic restructuring of the nucleoid to relocate different portions of the chromatin to the peripheral regions periodically is controlled by the replication cycle. Since it is known that only the peripheral regions of the nucleoid are accessible to the transcription machinery (Ryter and Chang, 1975), we propose that this restructuring would regulate global gene expression. To test this hypothesis, we used electron microscopy *in situ* hybridization (EMISH) to label the physical locale of a target gene (i.e. *lacZ*) on nucleoids isolated from exponential phase *E. coli* cells. In addition, the global transcriptional profile of *E. coli* cells was changed using chloramphenicol and the structure of the chromosome was probed using restriction endonucleases.

A.3 Materials and Methods

A.3.1 Bacterial Strain and Growth Conditions

E. coli B/r A (ATCC 12407) were grown in C-medium (17.2 mM dibasic potassium phosphate, 11.0 mM monobasic potassium phosphate, 9.5 mM ammonium sulfate, 0.41 mM magnesium sulfate, 0.17 mM sodium chloride, 3.6 μM iron II sulfate, 1.0 μM EDTA) containing 0.1% glucose (Roberts *et al.*, 1955) at 37°C, shaking at 350 RPM to OD600 ~0.4. The doubling time for these cultures was 44 min. Where indicated, chloramphenicol was added to a final concentration of 30 μg/mL and cultures were incubated at 37°C, 350 RPM for 30 min. For visual inspection by

fluorescent microscopy, approximately 5 minutes prior to cell harvest 4´, 6-diamidino-2´-phenylindole, dihydrochloride (DAPI) (Pierce Biotechnology, Rockford, IL) was added to cultures to a final concentration of 1 μg/mL. Cells were harvested by centrifugation at 14,000*g*, 4°C for 10 minutes.

A.3.2 Nucleoid Isolations for Electron Microscopy

Two procedures were used to isolate nucleoids from harvested *E. coli* B/r cells. The 'high-salt procedure' developed by Stonington and Pettijohn was employed with some modifications (Stonington and Pettijohn, 1971). Harvested cell pellets were resuspended in 250 μL Solution A and vortexed briefly. After two minutes, 50 μL of Solution B was added and the samples were inverted to mix. After one minute, 250 μL of Solution C (1% Brij 58, 0.4% sodium deoxycholate, 10 mM EDTA pH 8.0, 2 M sodium chloride) was added and the samples were incubated at room temperature for 10 - 20 minutes, until the suspensions began to clear. Nucleoid suspensions were loaded onto 10 - 30% sucrose continuous gradients in 10 mM Tris-HCl pH 8.1, 1 M NaCl, 1 mM EDTA, 1 mM β-mercaptoethanol. Gradients were centrifuged at 28,000*g*, 4°C for 45 minutes in a Beckman SW41 rotor. Acceleration and deceleration were set to 1. Nucleoids were also isolated using a 'low-salt procedure' based on Kornberg *et al.*'s modification of the Stonington and Pettijohn procedure, where the 2 M NaCl in Solution C was replaced with 10 mM spermidine (Kornberg *et al.*, 1974). In addition, cell suspensions were incubated at 37°C for 5 minutes to allow cell lysis. Nucleoid suspensions from low-salt preparations were loaded onto 15 - 30% sucrose continuous gradients in 20 mM sodium diethylmalonate pH 7.1, 5 mM magnesium chloride, 1 mM β-mercaptoethanol. Gradients were centrifuged at 3000*g*, 4°C for 35 minutes in a Beckman SW41 rotor. Acceleration and deceleration were set to 1.

Gradients from both high- and low-salt preparations were fractionated into 0.3 mL aliquots. One hundred microliters of each fraction were combined with 100 µL of a 1/200 dilution of Picogreen in TE. The fluorescence was measured and the DNA concentration of each fraction was calculated. Calf thymus DNA was used as a standard.

A.3.3 Electron Microscopy of Isolated Nucleoids

Nucleoids were attached to butvar-coated nickel grids that were freshly coated with carbon by glow-discharge as described by Postow *et al.* (Postow *et al.*, 2004). Eight microliter aliquots from the fraction containing the peak DNA concentration were adsorbed to the grid for 2 minutes. Grids were rinsed for consecutive 1 minute intervals in 0.1 M ammonium acetate, 0.01 M ammonium acetate and 2% uranyl acetate. Grids were viewed using a Tecnai T12 transmission electron (FEI Co., Hillsboro, Oregon), and imaged with an SIS Megaview III CCD camera. Images were analyzed with ImageJ software (NIH, Bethesda, MD).

A.3.4 Digoxigenin-Labeled Oligonucleotide Probe Synthesis

Oligonucleotide primers with the following sequences were obtained from Integrated DNA Technologies, Inc. (Coralville, IA): *lacZ* forward primer, 5'-ccaacttaatcgccttgcagcaca-3'; *lacZ* reverse primer, 5'-tcggcaaagaccagaccgttcata-3'. The *lacZ* fragment was amplified by polymerase chain reaction from fragmented chromosomal DNA isolated from *E. coli* B/r cell pellets using the FastDNA® Kit and the FastPrep® Instrument (Qbiogene, Inc., CA). Digoxigenin labeled oligonucleotide probe was synthesized from a *lacZ* fragment template using the PCR DIG probe

synthesis kit according to the manufacturer's recommendations (Roche Applied Science, Indianapolis, IN).

A.3.5 Agarose Gel Electrophoresis and Northern Verification

DNA gel electrophoresis was performed using a 1% agarose gel in 0.5x TBE running buffer. Samples were mixed with 6x blue/orange loading dye (Promega Co., Madison, WI) and electrophoresed for 90 minutes at 75 V.

Total RNA was isolated from *E. coli* B/r A cells according to the procedures described in Chapter 2. Two microgram samples of total RNA were mixed with 5x RNA loading dye (0.01% bromophenol blue, 2.5% formaldehyde, 20% glycerol, 30% formamide, 50 mM MOPS pH 7.0, 12.5 mM sodium acetate, 6.5 mM EDTA) and RNA molecules were separated using formaldehyde gel electrophoresis as described previously (Sambrook and Russell, 2001). RNA was transferred to a nylon membrane and Northern blots were performed according to procedures outlined in Appendix B.

A.3.6 Electron Microscopy *In Situ* Hybridization (EMISH)

Electron microscopy *in situ* hybridization techniques were adapted from a protocol designed by Narayanswami and Hamkalo for analysis of eukaryotic chromosomal organization (Narayanswami and Hamkalo, 1994). Briefly, a Carbon/butvar-coated grid with adsorbed nucleoid DNA was placed on a drop of 8% glutaraldehyde and incubated at room temperature for 20 minutes. The grid was then rinsed in Photo-flo solution (Kodak, Rochester, NY), denatured in a drop of freshly prepared 0.12 M sodium hydroxide in 2x SSC for 20 minutes, rinsed in Photo-flo and air dried. Next, the grid was placed in a 50 µL drop of hybridization solution (50%

formamide, 2% Ficoll, 1% dextran sulfate, 0.6 M sodium chloride, 10 mM Tris-HCl pH 7.0, 1 mM EDTA, 2 µg fragmented salmon sperm DNA, 2 µg yeast tRNA) containing approximately 80 ng DIG-labeled probe oligonucleotide. The grid was incubated at 30ºC in a humid chamber for 18 hours. Following the hybridization, the grid was washed three times for 20 minutes each in 2x SSC at room temperature. The grid was placed in a 50 µL drop of primary antibody solution (1x PBS, 0.5 M sodium chloride, 1 mg/mL bovine serum albumin, 0.4 µg/mL mouse anti-DIG IgG (Roche Diagnostics, Indianapolis, IN)) immediately following the washes. Grids were incubated for 4 hours at 37ºC in a humid chamber, then washed three times for 10 minutes each in drops of 1x PBS, 0.5 M sodium chloride at room temperature. The grid was then placed in a 50 µL drop of 1% BSA buffer (20 mM Tris-HCl pH 8.0, 10 mg bovine serum albumin/mL, 154 mM sodium chloride, 1 mg sodium azide/mL) containing a 1/20 dilution of 15 nm gold conjugated-goat anti-mouse IgG (Electron Microscopy Sciences, Hatfield, PA), and incubated in a humid chamber for 18 hours at room temperature. After the incubation, the grid was washed three times for 20 minutes each in drops of 1% BSA buffer. Finally, the grid was re-stained for 2 minutes in 2% uranyl acetate and air dried prior to viewing.

A.3.7 Chromosomal Digestion and Pulsed Field Gel Electrophoresis (PFGE)

Select nucleoid preparations were exposed to EcoRI digestion. Following cell lysis, 50 µL of select nucleoid suspensions were exposed to 10 µg Proteinase K per milliliter of suspension for 1 hour at 0ºC. Phenylmethylsulphonyl fluoride (PMSF) was added to a final concentration of 40 µg/mL and the proteinase K was deactivated for 1 hour at 0ºC. Proteinase K-treated and control samples were each combined with 1.5 µL of 1 M magnesium chloride and 10 Units of EcoRI (New England Biolabs,

Ipswich, MA). The reaction was incubated at 4ºC for 18 hours, then 10 µL of 6x blue/orange loading dye was added to arrest digestion. Thirty microliters of each sample were loaded into an 1% agarose gel in 0.5x TBE prepared for the Bio-rad CHEF Mapper Electrophoresis System (Bio-rad Laboratories, Hercules, CA). Samples were electrophoresed according to the manufacturer's recommendations. Briefly, the auto-algorithm function was employed with the following settings: minimum fragment size = 1 kb, maximum fragment size = 0.5 Mb, temperature = 14ºC. The calculated parameters were: voltage = 6.0 V/cm, run time = 7:53 hr, included angle = 120º, initial switch time = 0.065 s, final switch time = 44.695 s, ramp = linear. After electrophoresis, the fragmented DNA was stained with ethidium bromide and imaged with a Bio-rad Chemidoc XRS system and Quantity One software (Bio-rad Laboratories, Hercules, CA).

Restriction endonuclease assays were repeated with NcoI (New England Biolabs, Ipswitch, MA) in place of EcoRI. Samples were electrophoresed as described previously with the following modifications. The auto-algorithm function utilized the following settings: minimum fragment size = 50 kb, maximum fragment size = 0.5 Mb, temperature = 14ºC. The calculated parameters were: voltage = 6.0 V/cm, run time = 28:28 hr, included angle = 120º, initial switch time = 6.75 s, final switch time = 44.695 s, ramp = linear.

A.4 Results

A.4.1 *E. coli* Nucleoid Isolations

E. coli nucleoids were successfully isolated using both high- and low- salt preparations. To verify cell lysis and nucleoid compaction following isolation, we

viewed nucleoid isolations using fluorescent microscopy (Figure A.1). In addition, nucleoid compaction was verified by density gradient centrifugation. Figure A.2 shows representative gradient profiles for nucleoids isolated using both high- and low-salt preparations. Notably, the efficiency of cell lysis was significantly reduced in stationary phase cells. This behavior has been observed previously (Witholt *et al.*, 1974). Therefore nucleoids were prepared from early exponential phase cells. In addition, to achieve efficient cell lysis, lyophilized lysozyme was dissolved in Solution B immediately prior to use.

A.4.2 Nucleoid Visualization with Transmission Electron Microscopy

We observed and imaged high- and low- salt nucleoids using transmission electron microscopy. These images are included in Chapter 3 of this dissertation. We note that high-salt nucleoids typically consisted of a central, dense mass with several loops emanating from the central mass. Low-salt nucleoids, on the other hand, consisted of a central mass with few loops extended from the central body. In addition, membrane fractions were typically associated with the central nucleoid mass.

The number of nucleoid bodies that attached to each grid was limited, in general 1-2 nucleoids per grid. To increase the number of nucleoids attached to each grid, two procedures were tested. Nucleoids were isolated using the high-salt procedure. Subsequently, isolated nucleoids were diluted 1:1 with 10% sucrose in 10 mM Tris-HCl pH 8.1, 1 M sodium chloride, 1 mM EDTA, 1 mM β-mercaptoethanol to decrease the density of the solution below that of the nucleoids and allow settling. Grids were incubated overnight at 4°C in 100 µL nucleoid solution containing 80 U

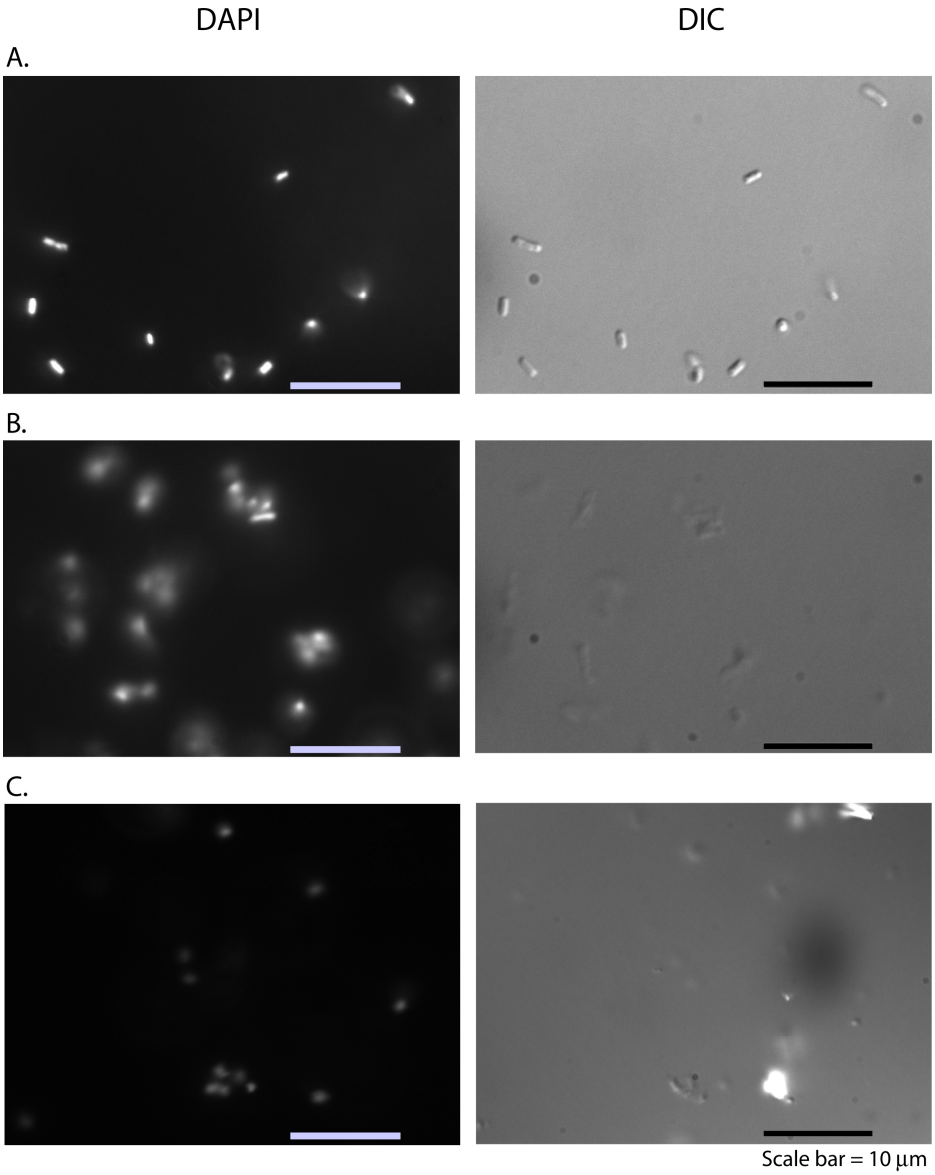

Figure A.1 Fluorescent and differential interference contrast images of DAPI-stained *E. coli* nucleoid preparations. (A) Unlysed *E. coli* cells; (B) *E. coli* high-salt nucleoid preparations; (C) *E. coli* low-salt nucleoid preparations

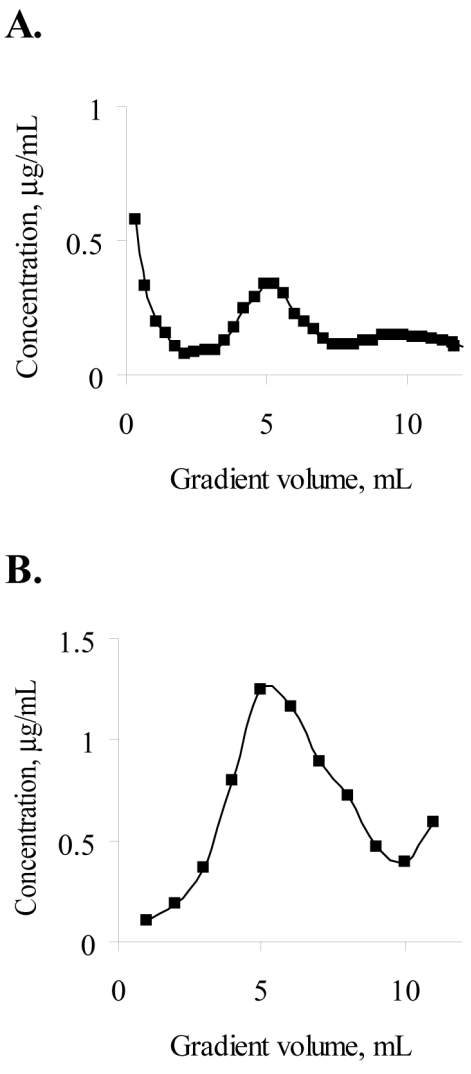

Figure A.2 DNA concentration measured for sucrose density gradient fractions containing nucleoid isolations from high-salt (A) and low-salt (B) preparations. The x-axis represents the volume from the top of the gradient.

RNAsin (Promega Co., Madison, WI). The overnight incubation increased the total amount of DNA attached to the grids. However, the DNA attached to the grids was denatured. In addition, all the grids displayed a high level of background attachment. (Figure A.3). I concluded that overnight chromosome settling resulted in settling of contaminants as well as chromosomal DNA. Therefore, to avoid long incubations, a procedure to increase the nucleoid settling rate by centrifugation was attempted.

The second procedure to increase nucleoid attachment involved centrifuging the nucleoid solution onto grids. Nucleoids were isolated and diluted with 10% sucrose as previously noted. Microcentrifuge tubes were partially filled with poly(dimethysiloxane) and cured. This made it possible to place the grids on a flat surface below the nucleoid solution. Approximately 200 μL of nucleoid suspension was layered into the modified tubes containing 2-3 grids each. The tubes were centrifuged at 500*g* for 1 hour at 4°C in a fixed angle rotor. As seen in Figure A.3, this procedure compromised the carbon/butvar coat of the grid. Based on these results, it is probable that the carbon coat is compromised by the shear forces present during centrifugation.

A.4.3 Verification of DIG-Labeled *lacZ* Oligonucleotide Probe Synthesis

Control experiments were performed to verify the synthesis and activity of a DIG-labeled oligonucleotide probe complementary to *lacZ*. The apparent size of the DIG-labeled fragment as measured by gel electrophoresis was 1904 bp, which agreed well with the predicted size, 1764 bp, accounting for the additional DIG side chains of the probe (data not shown). To verify the activity of probe, total RNA was isolated from exponential *E. coli* cells grown in the presence and absence of isopropyl β-D-1-

A.

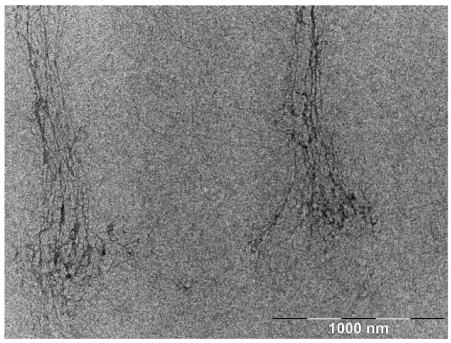

B.

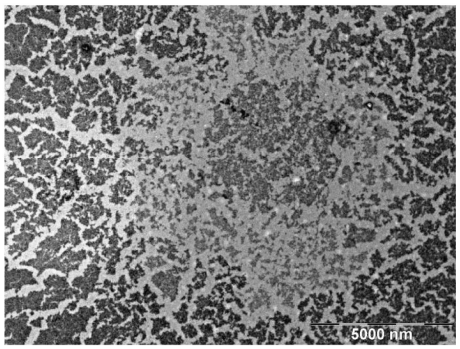

C.

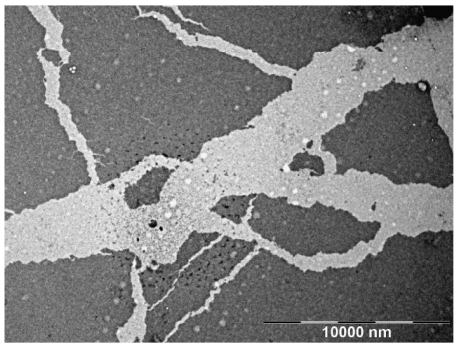

Figure A.3 Consequences of attempts to increase the nucleoid adsorption density on Carbon/butvar-coated Nickel grids. Attempts to increase the adsorption density resulted in nucleoid decompaction (A) and carbon/butvar coat disruption (B, C).

thiogalactopyranoside (IPTG) to induce *lacZ* expression. Results showed the probe reacted to mRNA extracted from cells grown in the presence but not the absence of IPTG (Figure A.4). Together, these results showed the oligonucleotide probe was active and specific.

A.4.4 Electron Microscopy *In Situ* Hybridization

We performed experiments to elucidate the physical location of the *lacZ* gene under active and repressed conditions. We were unable to obtain grids containing adsorbed chromosomal DNA with DIG-labeled *lacZ* oligonucleotide probe hybridized to the DNA. Hybridized grids typically did not have any DNA molecules adsorbed. We adsorbed DIG-labeled *lacZ* oligonucleotide directly to the grid and were able to image short DNA fragments labeled with 15 nm gold particles (Figure A.5), indicating that the hybridization step of the EMISH procedure was the limiting step. We hypothesize that the stringent washes incorporated to reduce non-specific binding between the probe oligonucleotide and the grids also promote desorption of the chromosomal DNA from the grid by the same mechanism.

A.4.5 Protein-free Nucleoids Exhibit Increased Accessibility to Restriction Enzymes Compared to Controls

We hypothesized that the accessibility of the nucleoid could be probed using restriction endonucleases. Preliminary experiments were performed to ensure the restriction enzymes were active in the nucleoid preparation solution. Results showed that the addition of 25 mM magnesium chloride to the reaction solution was necessary to allow endonuclease activity. In addition, to minimize nucleoid decompaction during

Figure A.4 Image of chemiluminescent reaction showing *lacZ*-DIG oligonucleotide probe bound to total RNA sample isolated from *E. coli* cells grown to exponential phase in the presence of 5 mM isopropyl β-D-1-thiogalactopyranoside (IPTG). Lane 1, empty; Lane 2, Total RNA from *E. coli* cells grown in the presence of 5 mM IPTG; Lane 3, Total RNA from *E. coli* cells grown with no IPTG; Lane 4, empty.

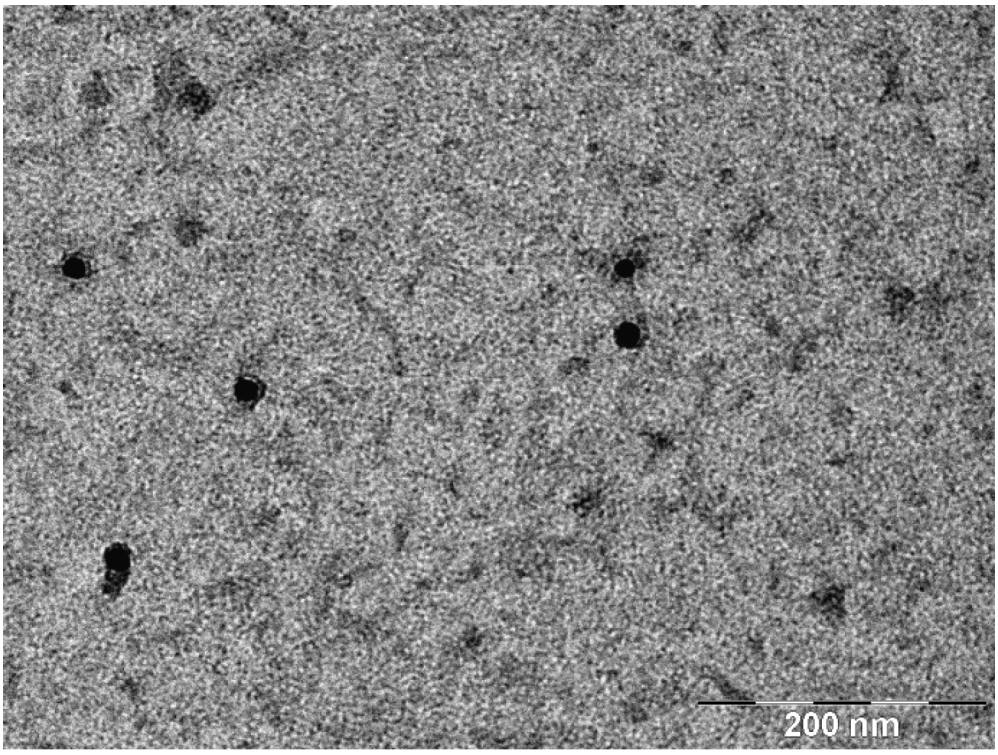

Figure A.5 Electron micrograph with DIG-labeled *lacZ* oligonucleotide probe associated with 15 nm gold particles, demonstrating successful association of the probe with primary and secondary antibodies.

chromosomal digestion, reactions were performed at 4ºC for an extended time (18 hours). To determine structural features introduced in the *E. coli* nucleoid by nucleoid associated proteins (NAPs), nucleoids were prepared from chloramphenicol-treated cultures and/or treated with proteinase K and PMSF. Subsequently, the nucleoid preparations were digested with EcoRI and electrophoresed. Figure A.6(A) shows preliminary evidence that the removal of NAPs may increase chromosomal accessibility to restriction endonuclease activity. Exponential phase cultures that were treated with proteinase K showed increased chromosomal digestion when compared to nucleoids containing NAPs (lane 7 versus lane 6). To distinguish between the effects of NAPs and nascent polypeptides, nucleoids from chloramphenicol-treated cells were exposed to identical treatments. Proteinase K-treated nucleoids again exhibited increased digestion when compared to NAP-containing nucleoids (lane 11 versus lane 10). Together, these preliminary results indicate NAPs may protect certain regions of the chromosome from digestion by restriction endonucleases. Notably, chloramphenicol-treated nucleoid preparations that were not exposed to EcoRI digestion also showed significant degradation (lane 9). Therefore the experiments should be repeated for verification.

An experiment to determine whether this increased endonuclease susceptibility in proteinase K-treated cells is specific to certain restriction sites was performed. The previously described nucleoid preparations were exposed to NcoI in place of EcoRI. We hypothesized the low number of cut sites for NcoI on the *E. coli* chromosome would allow determination of changes in endonuclease activity at each specific restriction site. No chromosomal digestion was observed in any sample (Figure A.6(B)). These results probably reflect a difference in the efficiencies of NcoI and EcoRI in the nucleoid preparation solution.

Figure A.6 EcoRI (A) and NcoI (B) mediated *E. coli* genome fragmentation. Images show PFGE profiles stained with ethidium bromide of nucleoid fragments separated after digestion. (A) 2, CHEF Lambda DNA markers (Bio-rad Laboratories, Hercules, CA); 3, unlysed *E. coli*; 5, undigested nucleoids; 6, EcoRI digested nucleoids; 7, proteinase K-treated EcoRI digested nucleoids; 9, undigested chloramphenicol-treated nucleoids; 10, EcoRI digested chloramphenicol-treated nucleoids; 11, proteinase K-treated chloramphenicol-treated nucleoids; 12, CHEF Lambda DNA markers. (B) 1, CHEF Lambda DNA markers; 2, undigested nucleoids; 3, proteinase K-treated undigested nucleoids; 4, RNase A-treated undigested nucleoids; 5, chloramphenicol-treated undigested nucleoids; 6, proteinase K-treated chloramphenicol-treated undigested nucleoids; 7, RNase A-treated chloramphenicol-treated undigested nucleoids; 8, NcoI digested nucleoids; 9, proteinase K-treated digested nucleoids; 10, RNase A-treated digested nucleoids; 11, chloramphenicol-treated digested nucleoids; 12, proteinase K-treated chloramphenicol-treated digested nucleoids; 13, RNase A-treated chloramphenicol-treated digested nucleoids; 14, CHEF Lambda DNA markers; 15, unlysed *E. coli*.

A.

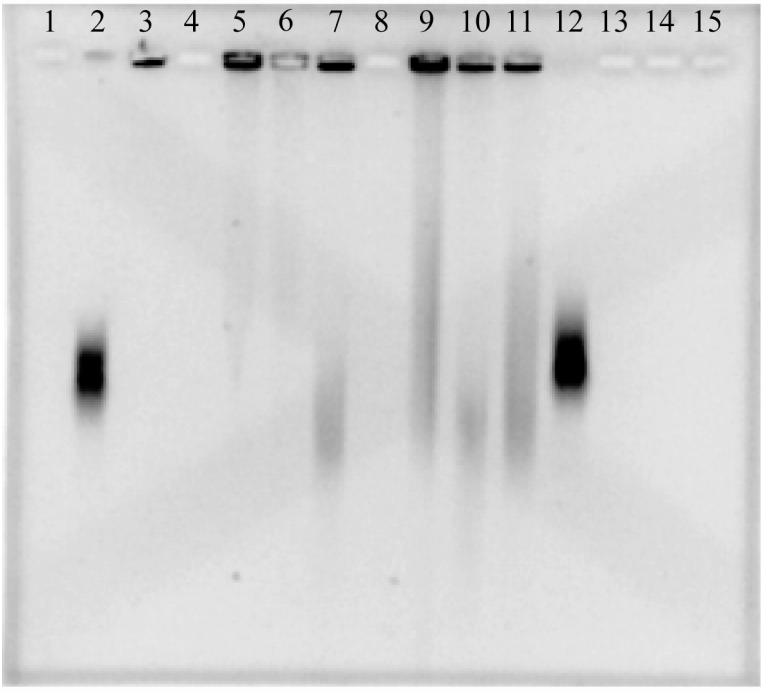

B.

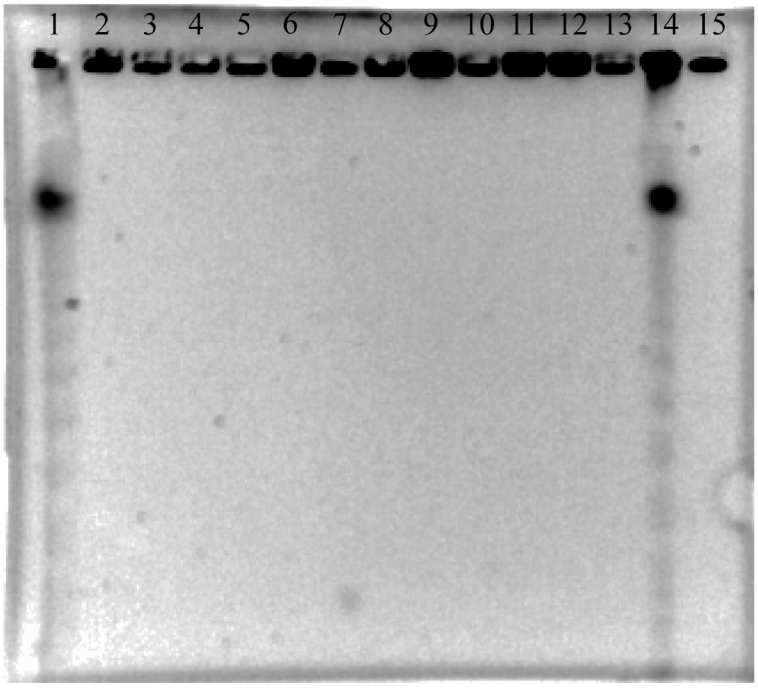

A.5 Discussion

Due to the difficulty of manipulating bacterial nucleoids while maintaining a compact structure, few techniques have been developed to directly investigate physical changes within the nucleoid. Although fluorescent *in situ* hybridization (FISH) procedures have provided extensive information regarding bacterial flora and interspecies relations in recent years, it does not provide the resolution required to examine the structural features of bacterial nucleoids. Scientists working to map locations on mammalian metaphase chromosomes in the late 1980s encountered a similar problem. In response, Narayanswami and Hamkalo adapted *in situ* hybridization techniques for use with electron microscopy (Narayanswami and Hamkalo, 1991; Narayanswami and Hamkalo, 1994).

Although the procedure for EMISH was standardized for eukaryotic metaphase chromosomes, it has never been applied to bacterial chromatin. In this work, we attempted to adapt Narayanswami and Hamkalo's technique to isolated bacterial nucleoids. We obtained grids with adsorbed chromosomal DNA. We note that the staining solution, 2% uranyl acetate plays a role in fixing the DNA to the grids as the removal of this step immediately following DNA adsorption resulted in grids lacking adsorbed DNA. We were unable to identify experimental conditions that would preserve bacterial nucleoid attachment to the TEM grids while minimizing non-specific adsorption of probe and competitor DNA to the grids. Significantly, the size of the bacterial chromosome (4.6 Mb) is a fraction of the size of the mouse metaphase chromosomes used in previous EMISH studies (~60 – 200 Mb). Therefore, the total number of binding sites between the bacterial chromosome and the TEM grid is most likely a great deal smaller than for attached eukaryotic chromosomes. The EMISH procedure for eukaryotic chromosomes utilized the broadly different sizes of

eukaryotic chromosomal and probe DNA molecules to achieve different effects on the DNA molecules during the washes. This size difference is greatly reduced for bacterial chromosomes versus probe DNA. Therefore it may be necessary to determine some chemical means to immobilize the bacterial nucleoid DNA prior to hybridization of the oligonucleotide probe to the grids before EMISH procedures can be successfully applied to bacterial chromosomes.

REFERENCES

Brewer, B. J. (1990). Replication and the transcriptional organization of the *Escherichia coli* chromosome. In *The Bacterial Chromosome* (Drlica, K. & Riley, M., eds.), pp. 61-83. American Society for Microbiology Press, Washington D. C.

Carpentier, A.-S., Torresani, B., Grossmann, A. & Henaut, A. (2005). Decoding the nucleoid organisation of Bacillus subtilis and Escherichia coli through gene expression data. *BMC Genomics* **6**, article 84.

Claverie-Martin, F. & Magasanik, B. (1991). Role of Integration Host Factor in the regulation of the *glnHp2* promoter of *Escherichia coli*. *Proceedings of the National Academy of Sciences* **88**(5), 1631-1635.

Jeong, K. S., Ahn, J. & Khodursky, A. B. (2004). Spatial patterns of transcriptional activity in the chromosome of *Escherichia coli*. *Genome Biology* **5**, R86.

Kar, S., Edgar, R. & Adhya, S. (2005). Nucleoid remodeling by an altered HU protein: reorganization of the transcriptional program. *Proceedings of the National Academy of Sciences* **102**(45), 16397-16402.

Kèpés, F. (2004). Periodic transcriptional organization of the E. coli genome. *Journal of Molecular Biology* **340**, 957-964.

Kornberg, T., Lockwood, A. & Worcel, A. (1974). Replication of the *Escherichia coli* chromosome with a soluble enzyme system. *Proceedings of the National Academy of Sciences* **71**(8), 3189-3193.

Narayanswami, S. & Hamkalo, B. (1991). DNA sequence mapping using electron microscopy. *Genetic Analysis--Biomolecular Engineering* **8**(1), 14-23.

Narayanswami, S. & Hamkalo, B. (1994). Electron microscopic localization of *in situ* hybrids. In *Methods in MOlecular Biology Volume 29: Chromosome analysis protocols* (Gosden, J. R., ed.), Vol. 29, pp. 335-351. Humana Press, Inc., Totowa, New Jersey.

Niki, H., Yamaichi, Y. & Hiraga, S. (2000). Dynamic organization of chromosomal DNA in Escherichia coli. *Genes and Development* **14**, 212-223.

Peter, B. J., Arsuaga, J., Breier, A. M., Khodursky, A. B., Brown, P. O. & Cozzarelli, N. R. (2004). Genomic trascriptional response to loss of chromosomal supercoiling in Escherichia coli. *Genome Biology* **5**, R87.

Postow, L., Hardy, C. D., Arsuaga, J. & Cozzarelli, N. R. (2004). Topological domain structure of the *Escherichia coli* chromosome. *Genes and Development* **18**, 1766-1779.

Rabin, R. S., Collins, L. A. & Stewart, V. (1992). In vivo requirement of Integration Host Factor for *nar* (Nitrate reductase) operon expression in *Escherichia coli* K-12. *Proceedings of the National Academy of Sciences* **89**(18), 8701-8705.

Roberts, R. B., Abelson, P. H., Cowie, D. B., Boulton, E. T. & Britten, R. J. (1955). *Studies of Biosynthesis in Escherichia coli*, Carnegie Institute of Washington, Washington, D. C.

Ryter, A. & Chang, A. (1975). Localization of transcribing genes in the bacterial cell by means of high resolution autoradiography. *Journal of Molecular Biology* **98**, 797-810.

Sambrook, J. & Russell, D. W. (2001). *Molecular Cloning: a Laboratory Manual*. 3rd edit, Cold Spring Harbor Laboratory Press, Cold Spring Harbor, NY.

Stonington, O. G. & Pettijohn, D. E. (1971). Folded Genome of Escherichia-Coli Isolated in a Protein-DNA-Rna Complex. *Proceedings of the National Academy of Sciences of the United States of America* **68**(1), 6-&.

Viollier, P. H., Thanbichler, M., McGrath, P. T., West, L., Meewan, M., *et al.* (2004). Rapid and sequential movement of individual chromosomal loci to specific subcellular locations during bacterial DNA replication. *Proceedings of the National Academy of Sciences* **101**(25), 9257-9262.

Wang, J. C. & Lynch, A. S. (1996). Effects of DNA supercoiling on gene expression. In *Regulation of gene expression in Escherichia coli* (Lin, E. C. C. & Lynch, A. S., eds.), pp. 127-147. R. G. Landes Company, Austin, TX.

Witholt, B., Boekhout, M., Brock, M., Kingma, J., Heerikhuizen, H. v. & Leij, L. d. (1974). An Efficient and Reproducible Procedure for the Formation of Spheroplasts from Variously Grown *Escherichia coli*. *Analytical Biochemistry* **74**, 160-170.

APPENDIX B

NORTHERN BLOT ANALYSIS OF *ESCHERICHIA COLI* TRANSCRIPTS DURING THE CELL DIVISION CYCLE

B.1 Introduction

In Chapter 2, transcript levels were measured at several times during the *E. coli* division cycle using two-color DNA oligonucleotide microarrays. The data collected was based on the relative intensity of a fluorescently-labeled test cDNA sample to a fluorescently-labeled control cDNA sample, which is expressed on a Log_2 scale. Therefore, small changes in transcript levels, which are expected for cell cycle-related transcript regulation, may be difficult to detect. To verify that transcript changes that were detected using microarray technology could also be detected by an alternative experiment approach, we performed Northern blot verification experiments for selected genes.

B.2 Materials and Methods

B.2.1 *E. coli* Cell Synchronization and RNA Isolation

E. coli B/r A (ATCC 12407) cells were grown and synchronized as described in Chapter 2. Total RNA was isolated as previously described (Chapter 2), and kept at -80ºC until use.

B.2.2 Digoxigenin-labeled Oligonucleotide Probe Synthesis

Oligonucleotide primers with the following sequences were obtained from Integrated DNA Technologies, Inc. (Coralville, IA): *rpoA* forward primer 5'-tcctggaaatcctgctcaacctga-3'; *rpoA* reverse primer 5'-agcggacagtcaattccagatcgt-3'; *rpoN* forward primer 5'-cgaaacgcaagacagtgaaacgct-3'; *rpoN* reverse primer 5'-cttgctcaaagaaggcttgctgct-3'; *nrdA* forward primer 5'-ctgctttcaacctgggcgcaatta-3'; *nrdA* reverse primer 5'-accagatcgtcttgtgcgtcttca-3'. Gene fragments were amplified by polymerase chain reaction from fragmented chromosomal DNA isolated from *E. coli* B/r cell pellets using the FastDNA® Kit and the FastPrep® Instrument (Qbiogene, Inc., CA). Each reaction contained 0.5 µg template DNA, 2 µM forward and reverse primers and PCR SuperMix (Invitrogen, Carlsbad, CA). The final reaction volume was 55 µL. Thirty five cycles with a 30 second denaturing step at 95°C, a 30 second annealing step at 55°C and a two minute elongation step at 72°C were performed. Digoxigenin (DIG) labeled oligonucleotide probes were synthesized from the gene fragments using the PCR DIG probe synthesis kit according to the manufacturer's recommendations (Roche Applied Science, Indianapolis, IN).

B.2.3 Formaldehyde Agarose Gel Electrophoresis and Transfer to Nylon Membrane

Isolated RNA was separated on formaldehyde agarose gel electrophoresis, transferred to positively charged nylon membranes by capillary elution and immobilized by baking the membrane (Sambrook and Russell, 2001). The membrane was prehybridized at 55ºC for 2 hours in 1x Hybridization solution (50% formamide, 0.25 M sodium phosphate pH 7.2, 0.25 M sodium chloride, 7% SDS, 100 µg/mL fragmented salmon sperm DNA and 5 µg/mL yeast tRNA). Then, approximately 40 ng of DIG-labeled oligonucleotide probe was hybridized to the membrane under

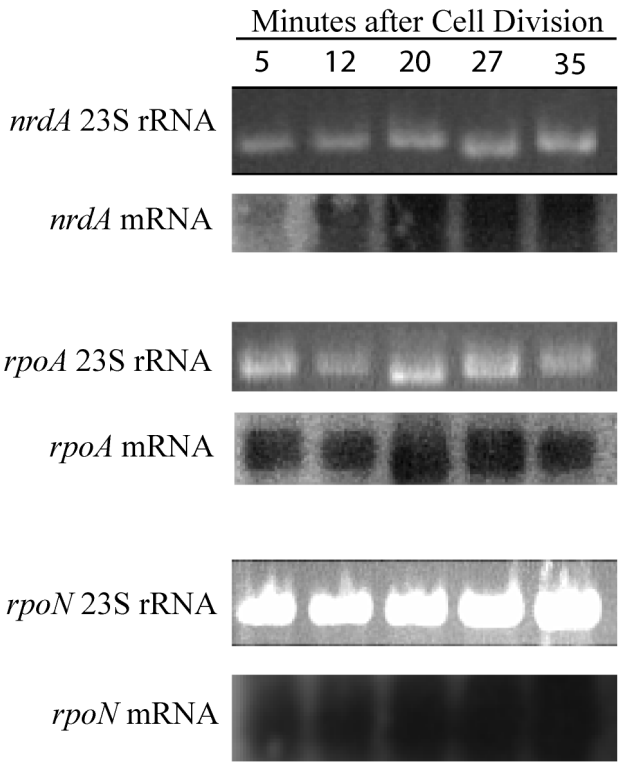

Figure B.1 Images of 23S rRNA and Northern hybridization of *nrdA*, *rpoA* and *rpoN* transcripts during the *E. coli* cell division cycle.

stringent conditions for 16 hours (55°C in 50% formamide, 0.25 M sodium phosphate pH 7.2, 0.25 M sodium chloride, 7% SDS, 100 µg/mL fragmented salmon sperm DNA and 5 µg/mL yeast tRNA). Membranes were washed consecutively with 2x SSC, 0.1% sodium lauryl sulfate at room temperature and 0.1x SSC, 0.1% sodium lauryl sulfate at 55ºC, and exposed to a 1:20,000 dilution of alkaline phosphotase conjugated, anti-DIG Fab fragments in 1x Blocking Reagent (both from Roche Applied Sciences, Indianapolis, IN). Reactions were detected with the CDP-Star substrate according to manufacturer's recommendations (Roche Applied Sciences, Indianapolis, IN). Specific reactions were detected using x-ray film (Kodak Co., Rochester, NY) and quantified using Quantity One software (Biorad Laboratories, Hercules, CA). Transcript sizes were determined by comparison with Roche RNA-DIG standards I (Roche Applied Sciences, Indianapolis, IN), and were consistent with predicted transcript sizes.

B.3 Results

The transcript levels for the genes *rpoA*, *nrdA* and *rpoN* were examined at several points throughout the *E. coli* division cycle. These genes were chosen due to their relatively high level of expression. However, the background level was still high for these experiments, rendering image analysis difficult (Figure B.1). Qualitatively, *rpoA* appeared to show no change in the level of expression (as expected), while transcript levels for both *nrdA* and *rpoN* appeared to increase slightly as the cell cycle progressed. No concrete conclusions could be drawn from these data.

REFERENCES

Sambrook, J. & Russell, D. W. (2001). *Molecular Cloning: a Laboratory Manual*. 3rd edit, Cold Spring Harbor Laboratory Press, Cold Spring Harbor, NY.

APPENDIX C

DETAILED EXPERIMENTAL TECHNIQUES

C.1 C-Medium Preparation

1. Add 3 g dibasic potassium phosphate, 1.5 g monobasic potassium phosphate, 1.25 g ammonium sulfate, 100 µL 10% sodium chloride and 2 µL of 0.5 mM EDTA were added to 18 MΩ water, and the final volume was brought to 1 L.

2. Sterilize by autoclaving in 500 mL bottles for 32 minutes.

3. Sterilize magenesium sulfate (1 M) by autoclaving; and filter-sterilize glucose (20 w/v %) and 100 mM ferrous sulfate with 0.2 µm pore diameter nylon filters. Prepare all ferrous sulfate solutions fresh.

4. To each 500 mL bottle of autoclaved solution, add 2.5 mL of filter-sterilized 20% glucose, 206 µL of 1 M magnesium sulfate, and 18 µL of 100 mM ferrous sulfate. Medium was stored for no more than one week.

C.2 Bacterial Growth Rate Assay

1. Inoculate culture medium (warmed to growth temperature) with 1:1000 volume of stationary state cell suspension (50 µL into 50 mL).

2. Incubate at growth temperature and 375 RPM until OD600 reaches approximately 0.1.

3. Measure OD600 of suspension every 15 minutes by removing 0.75 mL cell suspension and placing in 1 mL plastic cuvette. Use water as a blank for the spectrophotometer. Continue these measurements until OD600 ~ 1.2. *Note*: The spectrophotometer cannot accurately read OD600 > 0.3, so for higher concentrations dilute the cell suspension prior to measuring the OD600.

4. Plot LN(OD600) vs. Time and calculate the slope of the line and the R^2 value. The slope is equal to the growth rate (μ). The doubling time (τ_d) is equal to Ln(2)/μ.

Explanation of Mathematics:

In the exponential growth phase,

$\frac{dX}{dt} = \mu X$ where X = cell concentration, μ = growth rate and $X = X_o$ at $t = 0$.

Integrating the equation:

$$\ln\left(\frac{X}{X_o}\right) = \mu t \quad \text{OR} \quad \ln(X) = \mu t + \ln(X_o)$$

To calculate μ, plot ln(X) vs. t. The slope will be μ and the y-intercept will be ln(X_o). To calculate the doubling time of the cell concentration, use the same equation:

$$\ln\left(\frac{X}{X_o}\right) = \mu t \text{ , where } X = 2X_o \text{ when } t = \tau_d.$$

$$\ln(2) = \mu \tau_d \text{ OR } \tau_d = \frac{\ln(2)}{\mu}$$

Reference: Shuler M.L. and F. Kargi (1992). *Bioprocess Engineering*. Englewood Cliffs, New Jersey: Prentice-Hall, Inc. pg.154-161.

C.3 Coulter Counter Operation

Attaching Aperture

1. Power: off; Reset/Count: Count; Fill/Close: Close
2. Add stopcock grease to both aperture tube and glass fitting in sampling stand
3. Add 2-3 mL of Isoton II gently to aperture tube
4. Carefully attach the aperture tube, ensuring no grease gets inside tube. Revolve 2-3 times to seal tube onto fitting. Attach rubber band.
5. Place Isoton II in sample vial on beaker platform and immerse aperture in solution.
6. Power: on; Fill/Close: Fill. Slowly turn Reset/Count to Reset. Aperture tube should fill with Isoton II.
7. When full, Fill/Close: Close; Reset/Count: Count. Repeat to remove air bubbles from inside of tube.

8. Set dial on sampling stand to appropriate volume for aperture (for 30 μm, 50 μL).

To Count Particles
1. Begin with sample on sampling platform.

2. Fill/Close: Close; Reset/Count: Reset, Door must be closed. Ensure the mercury level is above the coalescence bulb and below the Start Contact, and there are no breaks in the mercury column. Repeat steps 1 & 2 if this is not the case. When the mercury has reached the appropriate level, a light will illuminate the sample and the counter will reset to 88888, then 00000.

3. Reset/Count: Count. Wait for beep. Record count displayed on counter.

4. Repeat at least 2 times per sample.

Changing Samples
1. Start with Reset/Count: Count, Fill/Close: Close.

2. Turn Fill/Close to Fill. Wait 2 seconds.

3. Turn Fill/Close to Close. Lower beaker platform and allow extra drops of solution from aperture tube to drop into sample vial.

4. Rinse aperture tube with Isoton II if desired.

5. Place new sample on stand and lift until the tube is approximately 0.2 cm from the bottom of the vial.

6. Ensure aperture is clear by viewing in screen (with door open for illumination).

Emptying USED ISOTON II flask
1. Start with Reset/Count: Count, Fill/Close: Close. Turn power on sampling stand off.

2. Release vacuum by lifting stopper on USED ISOTON II flask.

3. Empty flask into sink and return flask. Ensure the stopper is sealed into flask.

4. Turn power on.

Removing Aperture Tube
1. Start with Reset/Count: Count, Fill/Close: Close

2. Set Fill/Close to Fill, Reset/Count to Reset, and allow Isoton II to drain into waste flask for 5 seconds. Set Reset/Count to Count, Fill/Close to Close.

3. Turn off power. Release vacuum by lifting stopper from USED ISOTON II Erlenmeyer flask.

4. Set Reset/Count: Reset, Fill/Close: Fill. Liquid in tube with drain into electrolyte solution bottle.

5. Remove rubber bands and carefully remove aperture tube. Remove stopcock grease from aperture tube with Kimwipe.

6. Rinse tube gently with ddH_20 and store.

To clear blocks

1. Start with Reset/Count: Count, Fill/Close: Close

2. Set Fill/Close to Fill, Reset/Count to Reset.

3. Abruptly turn Reset/Count to Reset. Repeat 4 – 6 times until blocking particle is removed.

4. If particle is still blocking aperture, boil aperture as follows:
   a. Set current to 4.5 mA (dial = 450, knob = 10 mA).
   b. Set Fill/Close to Close, Reset/Count to Reset. When mercury is below the start contact, close door for 2-3 seconds. Repeat 2 -3 times if needed.
   c. Reset current to correct settings for counting.

C.4 *E. coli* Population Synchronization by Membrane Elution

1. Prewarm synchronization device and at least 2 L C-medium to 37˚C overnight.

2. Inoculate 3 x 50 mL C-medium with 1 mL overnight culture. Grow cells to an OD600 = ~0.1.

3. Wet the synchronization device membrane with 50 mL sterile C-medium.

4. Pour cells on top of membrane and allow them to attach for 10 minutes.

5. Draw the medium through the membrane with vacuum filtration. Leave a small amount of culture on top of membrane to prevent drying of cells.

6. Pour off remaining fluid and invert membrane holder.

7. Add approximately 125 mL C-medium to top of membrane and connect to peristaltic pump.

8. Pump media through membrane at 15 mL/min (70% of maximum) for 2 min to wash unattached cells away from membrane.

9. Reduce pump speed to 4 mL/min (25% of maximum).

10. After 40 min, collect eluate cultures. Analyze for synchrony using the Coulter Counter.

Reference: Helmstetter, C. E. (1969). Methods for studying the microbial division cycle. In *Methods in Microbiology* (Norris, J. R. & Ribbons, D. W., eds.), Vol. 1, pp. 327-363. 34 vols. Academic Press, London, New York.

C.5 *E. coli* RNA Stabilization and Isolation

Stabilization

1. Pre-cool centrifuge to 4˚C. For 15 mL conical tubes: 8000 RPM, 2 min, 4˚C, acceleration 9, deceleration 5. For 50 mL round bottom tubes: 10,000 RPM.

2. Remove 2 equal volume cultures from 37˚C incubator and swirl in ice bath for 60 seconds.

3. Centrifuge immediately for 2 min in pre-cooled rotor.

4. When centrifuge stops, remove medium from tube by pipetting or by inverting the tube. Immediately add 1 mL Qiagen RNAprotect bacterial reagent. (Note: if remaining culture volume exceeds 0.5 mL, add RNAprotect reagent in a 1:2 medium:RNAprotect ratio.

5. Incubate at room temperature for at least 5 minutes. Centrifuge at 14,000rpm for 10 min.

6. Remove supernatant and keep pellet at -20˚C until ready for RNA isolation.

Total RNA Isolation

1. Warm cell pellet to room temperature.

2. Remove supernatant and resuspend cells in 100 µL 1 mg/mL lysozyme in TE. Combine pellets as needed.Incubate at room temperature for 10 minutes.

3. Prepare DNAse I. For each sample mix 10 µL DNAse I stock with 70 µL buffer.

4. Add 350 µL RLT buffer to each sample. Vortex.

5. Add 250 µL 100% Ethanol to each sample. Mix by pipetting (Do not vortex).

6. Add samples to RNeasy columns and spin at max speed in a microfuge for 15 sec.

7. Discard flow-through. Add 350 µL RW1 buffer to the column. Centrifuge for 15 sec. Discard flow-through.

8. Add 80 µL DNAse I solution to each sample. Incubate at room temperature for 15 minutes.

9. Add 350 µL RW1 buffer to each sample. Centrifuge for 15 sec. Discard flow-through.

10. Transfer column to a fresh collection tube. Add 500 µL RPE to each sample. Centrifuge for 15 sec and discard flow-through.

11. Add an additional 500 µL RPE to each column. Centrifuge for 2 minutes. Be careful not to wet column with flow-through. Discard flow-through.

12. Transfer column to a 1.5 mL collection tube. Add 30 µL RNAse-free water. Centrifuge for 1 min.

13. Add 30 µL RNAse-free water. Centrifuge for 1 min to elute.

14. Discard column and measure concentration of RNA using RNAse-free cuvette. (1:10 dilution for async, no dilution for sync cultures).

C.6 High-salt Nucleoid Isolation

Reagents:
Solution A: 20% sucrose, 10 mM Tris-HCl pH 8.1, 0.1 M NaCl
Solution B: 4 mg/mL lysozyme, 120 mM Tris-HCl pH 8.1, 50 mM EDTA pH 8.0
Solution C: 1% Brij 58, 0.4% Sodium deoxycholate, 10 mM EDTA pH 7.0, 2 M NaCl
Gradient Mix: 1 M NaCl, 10 mM Tris-HCl pH 8.1, 1 mM EDTA pH 8.0, 1 mM β-mercaptoethanol

Procedure:
1. Prepare 2-12 mL 10-30% sucrose gradients in gradient mix.

2. Chill cell suspension in ice bath for 60 sec. ($<5x10^8$ cells/sample)

3. Centrifuge cells at 10,000*g*, 4˚C for 2 minutes.

4. Remove supernatant and resuspend in 250 µL Solution A. Vortex briefly. Incubate on ice for 2 minutes.

5. Add 50 µL Solution B. Incubate on ice for 1 minute.

6. Add 250 µL Solution C. Mix gently and incubate at 10˚C for 10 minutes. Solution should clear. Chill on ice.

7. Load each sample onto a 12 mL 10-30% sucrose gradient in gradient mix. Spin gradients at 27,000*g*, 4˚C for 45 minutes, Acceleration =1 Deceleration = 1.

8. After centrifugation, fractionate gradients into ~200 mL fractions in a 96-well plate. Measure fluorescence to locate folded nucleoids.

Reference: Postow, L., Hardy, C. D., Arsuaga, J. & Cozzarelli, N. R. (2004). Topological domain structure of the Escherichia coli chromosome. *Genes and Development* **18**, 1766-1779.

C.7 Low-salt Nucleoid Isolation

Reagents:
Resuspension buffer (High-salt Solution A): 20% sucrose, 10 mM Tris-HCl pH 8.1, 0.1 M NaCl
'Lysozyme' (Solution B): 4 mg/mL lysozyme, 120 mM Tris-HCl pH 8.1, 50 mM EDTA pH 7.0
BDES (or Solution C*): 1% Brij 58, 0.4% Sodium deoxycholate, 10 mM EDTA pH 7.0, 10 mM spermidine
4x Solution A (Gradient Buffer): 80 mM Sodium diethylmalonate, 20 mM $MgCl_2$ (To prepare 1x, add β-mercaptoethanol to 1 mM concentration.)
40% Sucrose

Procedure:
1. Prepare 2-12 mL 15-30% sucrose gradients in Gradient Buffer.

2. Chill cell suspension in ice bath for 60 sec. ($<5x10^8$ cells/sample)

3. Centrifuge cells to pellet.

4. Remove supernatant and resuspend in 200 µL Resuspension buffer. Incubate on ice for 2 minutes.

5. Add 50 µL 'Lysozyme'. Incubate on ice for 1 minute.

6. Add 250 µL BDES. Mix gently and incubate at 37˚C for 5 minutes. Solution

should clear. Chill on ice.

7. Load each sample onto a 12 mL 15-30% sucrose gradient in 1x Solution A. Spin gradients at 3000*g*, 4˚C for 30 minutes. Acceleration = 1, Deceleration = 1.

8. After centrifugation, fractionate gradients into 0.3 mL fractions. Measure [DNA] to locate folded nucleoids.

Reference: Murphy, L. D. & Zimmerman, S. B. (1997). Isolation and characterization of spermidine nucleoids from Escherichia coli. *Journal of Structural Biology* **119**(3), 321-335.

C.8 Picogreen-DNA Assay

Reagents:
1 mg/mL Calf thymus DNA in TE
1x TE pH 8.0
Picogreen stock reagent (Invitrogen Cat #P7589)

Procedure:
1. Prepare DNA Standards: Prepare 1:10 dilution of 1 mg/mL DNA (100 ug/mL final concentration) in 1xTE. Prepare the following standards:

DNA concentration, ug/mL	µL 100 ug/mL DNA	µL dilution buffer
0	0	500
0.5	2.5	497.5
1	5	495
2	10	490
3	15	485

2. Prepare Picogreen Working Reagent: Dilute Picogreen stock into 1x TE at a ratio of 1:200. Add 50 µL stock Picogreen per 10 mL Assay buffer. Protect from light. Do not prepare more than 1 hr prior to assay.

3. Assay concentration of DNA samples: In a 96 well, black plate mix 100 µL of each sample and three replicates of each standard in separate wells. Add 100 µL Picogreen working reagent to each well and cover. Incubate at room temperature for 10 minutes.

4. Measure the fluorescence of the wells using the microplate fluorometer in Dave Putnam's lab (Room 305). λ_{ex} = 480 nm, λ_{em} = 520 nm.

C.9 Transmission Electron Microscopy Grid Preparation

Materials:
-300 hex mesh Ni grids
-Formvar solution in ethylene dichloride
-ethylene dichloride wash
-burette with stopcock
-glass slides
-razor blade
-glass bowl filled to brim with ultrapure water

Procedure (perform in Duffield prep lab):

FORMVAR COATING:

1. Remove filter paper from around stopcock. Close stopcock and fill burette with ethylene dichloride wash.

2. Open stopcock completely and drain ethylene dichloride back into same bottle.

3. Close stopcock and place a clean glass slide in the burette. Fill burette with formvar/ethylene dichloride solution.

4. Open stopcock completely and allow solution to drain back into same container. This creates a film <40nm on the slide. If a thicker film is desired, open stopcock only partially.

5. Remove slide from burette. Repeat for 2 additional slides. Close stopcock and fill burette with ethylene dichloride to wash. Open stopcock completely to drain. Remove stopcock, wrap with filter paper and replace stopcock.

6. Run razor blade down 3 edges of one of the slides (2 long, one short) on both sides of the slide. Cut plastic coating at the top of both sides of the slide.

7. Heat both sides of the slide with breath. Holding the slide vertically with the cut edge down, slowly dip slide into water in glass bowl. Films should separate from slide and float away from slide.

8. Place grids on the plastic film, dull side down.

9. Use 2 additional slides to pick up grids from water bath by dipping at a 30° angle on top of the formvar sheet and immersing both in the waterbath.

10. Dry grids in oven for >1 hr.

CARBON COATING (perform <1 day prior to use):

11. Sharpen carbon rods on machine. Polish the ends of the rods.

12. Replace rods into machine, making sure to depress the spring in the holder. Turn guard to direct evaporated carbon downwards.

13. Place slides containing grids and a piece of polished brass directly below the carbon rods.

14. Pull a vacuum to at least $5x10^{-5}$ torr.

15. Turn Off knob to 'LT' and allow rods to heat and begin to evaporate. When brass turns orange (~5-10 sec), turn knob back to off and release vacuum.

16. Remove grids and brass from machine. Pull vacuum and turn machine off.

C.10 Attachment of DNA to TEM grids

Materials:
10nm carbon/butvar-coated Ni-hex grids
0.1 M Ammonium acetate, filtered
0.01 M Ammonium acetate, filtered
Uranyl acetate (2%)
Wide bore 200 µL pipette tips

Procedure:

1. Hold grid carbon-side up with reverse forceps. Place 8 µL nucleoid suspension on the grid. Incubate for 2 minutes at room temperature.

2. Remove solution by touching a torn piece of filter paper to the edge of the grid. Place grid carbon-side down on a drop of 0.1 M ammonium acetate. Incubate for 1 minute.

3. Transfer grid to a drop of 0.01 M ammonium acetate. Incubate for 1 minute.

4. Transfer grid to a drop of uranyl acetate to stain DNA. Incubate for 1 minute.

5. Pick up grid with reverse forceps. Slide a piece of filter paper between the forceps and use it to push the grid out of the forceps and into a grid box.

C.11 Electron Microscopy *In Situ* Hybridization

Materials:
20xSSC
BSA, 50 mg/mL
Salmon sperm DNA, 10 mg/mL
Formamide
Hybridization Buffer (1 mL): 100 mg dextran sulfate, 0.5 mL formamide, 2 µL 0.5M EDTA, 10 µL 1 M Tris-HCl pH 7, 10 µL 2% Ficoll, 20 µL 50 mg/mL BSA, 4 µL 10 mg/mL salmon sperm DNA, 120 µL 5 M NaCl
PBS
PBS/NaCl: Dilute 5M NaCl 1:10 in PBS, and filter through a 0.22um filter
1% BSA buffer: 20 mM 1 M Tris-HCl pH 8.0, 1% BSA frac V, 154 mM NaCl, 0.1% Sodium azide. Filter through 0.22 um filter.

Prepare fresh:
0.5 mL 8% glutaraldehyde: 160 µL 25% glutaraldehyde, 340 µL ultrapure water
1 mL Photoflo solution: 5 µL Photoflo 200, 1 mL ultrapure water
0.5 mL Denaturing solution: 60 µL 1 M NaOH, 50 µL 20x SSC, 390 µL ultrapure water

Procedure:
1. Attach chromosomes to gold EM grids coated with formvar and carbon support films. Wash sequentially with 0.1 M ammonium acetate and 0.01 M ammonium acetate.

2. *Fixation*: Immerse grid in 8% glutaraldehyde solution. Fix for 20 minutes at 25°C. Rinse grid in Kodak Photoflo 200 solution (drying aid)

3. *Denaturation:* Prepare 0.12 M NaOH in 2x SSC fresh. Immerse grid in solution for 20 min at 25°C. Remove grid and rinse with Photoflo solution to remove alkali and air-dry.

4. *Hybridization*:
   a. Make 100 µL hybridization solution: mix 79 µL Hyb Buffer, 7 µL yeast tRNA (1 mg/mL) and ~80 ng probe DNA. Mix well.
   b. Denature probe by boiling for 5 mins. Chill rapidly on ice.
   c. Place the grids in the hyb solution and incubate at 30°C overnight.
   d. After hyb, rinse grids 3x20min in 2xSSC at 25°C. DO NOT dry grids before next step.

5. *Detection:*
   a. Primary ab (anti-DIG, mouse). Dilute primary ab in PBS with NaCl and BSA. (100 µL PBS/NaCl, 2 µL 50 mg/mL BSA, 0.4 µL 0.1 mg/mL mouse anti-DIG). Place grids specimen side up in 50 µL droplets of solution and

incubate in moist atmosphere for 4 hrs at 37°C. After incubation, rinse grids 3x10 min at 25°C with PBS/NaCl to remove unbound ab.

b. Secondary ab (anti-mouse gold conjugate). Dilute secondary ab in 1% BSA solution. (100 µL 1% BSA buffer, 5 µL gold conjugated anti-mouse ab). Place grid in 50 µL of solution and incubate in moist chamber at 25°C overnight. Rinse grids 3x20 min in 1% BSA buffer to remove gold. Rinse in Photoflo.
c. Staining: Rinse grid 1x5 min in ultrapure water. Stain with 2% uranyl acetate in water for 10 mins. Rinse grids 3x2 min in ultrapure water. Dry grids and view.

Reference: Narayanswami, S. and B. Hamkalo (1994). Electron microscopic localization of *in situ* hybrids. Methods in Molecular Biology Volume 29: Chromosome analysis protocols. J. R. Gosden. Totowa, New Jersey, Humana Press, Inc. **29:** 335-351.